# PRELIMINARY STUDY OF RIETI EARTHQUAKE GROUND MOTION DATA V2

**Technical Report** · August 2016

CITATIONS
0

READS
19

**10 authors**, including:

Iunio Iervolino
University of Naples Federico II
**178** PUBLICATIONS **1,800** CITATIONS

SEE PROFILE

Cite as: ReLUIS-INGV Workgroup (2016), *Preliminary study of Rieti earthquake ground motion records V2*, available at http://www.reluis.it.

# PRELIMINARY STUDY OF RIETI EARTHQUAKE GROUND MOTION DATA V2

**INGV:** ITACA-ESM Working Group.[1]

**ReLUIS:** Iunio Iervolino (iunio.iervolino@unina.it),[2] Georgios Baltzopoulos,[3] Eugenio Chioccarelli.[3]

**Warning: This report may be subjected to editing and revisions, check www.reluis.it, esm.mi.ingv.it and www.itc.cnr.it for updates.**

## INDEX



[1] The ITACA-ESM Working Group is: Lucia Luzi (lucia.luzi@ingv.it); Francesca Pacor; Rodolfo Puglia; Maria D'Amico; Emiliano Russo; Chiara Felicetta; Giovanni Lanzano. INGV-Milano, Italy
[2] Dipartimento di Strutture per l'Ingegneria e l'Architettura, Università degli Studi di Napoli Federico II, Italy.
[3] Istituto per le Tecnologie della Costruzione ITC-CNR, URT Università degli Studi di Napoli Federico II, Italy.

# 1. What's New

New elements of this version are:

- data from nine station not included in the previous version of the report are here analyzed;
- Housner intensity is computed among the other integral parameters;
- response spectra associated to the four station with lowest epicentral distance are compared with elastic spectra provided by the Italian seismic code considering four different return periods.

# 2. Introduction

The Italian Accelerometric Network (RAN), managed by the Department of Civil Protection (DPC), and the Italian seismic network (RSN), managed by the Istituto Nazionale di Geofisica e Vulcanologia (INGV) have made available the records of the recent earthquake with epicenter located in the vicinity of Amatrice, central Italy (date 24/08/2016 1.36:32 AM – UTC; Mw 6.0, ref. Bollettino Sismico INGV).

About 200 accelerometric signals, manually processed using the procedure by Paolucci et al (2011), are used to evaluate the peak ground motion, acceleration and displacement spectral ordinates, integral parameters and measures of duration. **Corrected records and details of correction are available on the Engineering Strong-Motion database website (http://esm.mi.ingv.it). The unprocessed records are available at http://ran.protezionecivile.it/IT/index.php?evid=340867 for the RAN network and at the European Integrated Data Archive (http://www.orfeus-eu.org/data/eida/) for the RSN, that includes local networks (University of Genova, University of Trieste, AMRA, among others).**

In order to analyze peak values and spectral acceleration (Sa or PSA), data have been processed and compared to the Ground Motion Prediction Equation (GMPE) by Bindi et al (2011) for rock and soil. The geometric mean of the horizontal components are used in the analysis. As a function of epicentral distance and for fixed spectral ordinate, the average attenuation law (and its standard deviation) have been compared with the points corresponding to the values recorded at the various stations.

Moreover *Peak Ground Acceleration* (PGA), *Peak Ground Velocity* (PGV) and *Peak Ground Displacement* (PGD) are calculated for the three components and they are reported in Tables 1. *Arias Intensity* ($I_A$) and Housner Intensity are the integral parameters computed for each record. Durations is computed for each record as *Significant Duration* (Sd) estimated between 5% and 95% and between 5% and 75% of the $I_A$. In Tables 2 are reported integral parameters and duration for the three directions of each record.

# 3. Geographic Information

An earthquake of Mw 6.0 struck central Italy on 2016-08-24 at 01:36:32 GMT (Bollettino sismico INGV), in the vicinity of Amatrice, causing diffuse building collapse and about 250 casualties. The causative fault is normal, the prevalent style of faulting in the area. The location of the epicentre and the distribution of strong-motion stations are reported in Figure 1. Figure 2 reports the shakamp of the event.

The Amatrice seismic sequence struck an area where several large earthquakes occurred in the past. According to the recent historical catalog CPTI15 (Rovida et al., 2016 [http://emidius.mi.ingv.it/CPTI15-DBMI15/](http://emidius.mi.ingv.it/CPTI15-DBMI15/), updated to 2015) the strongest earthquake occurred on 1639 (Amatrice, Io 9-10 MCS, Mw 6.2) and destroyed the Amatrice village and its neighbourhood (Figure 2).

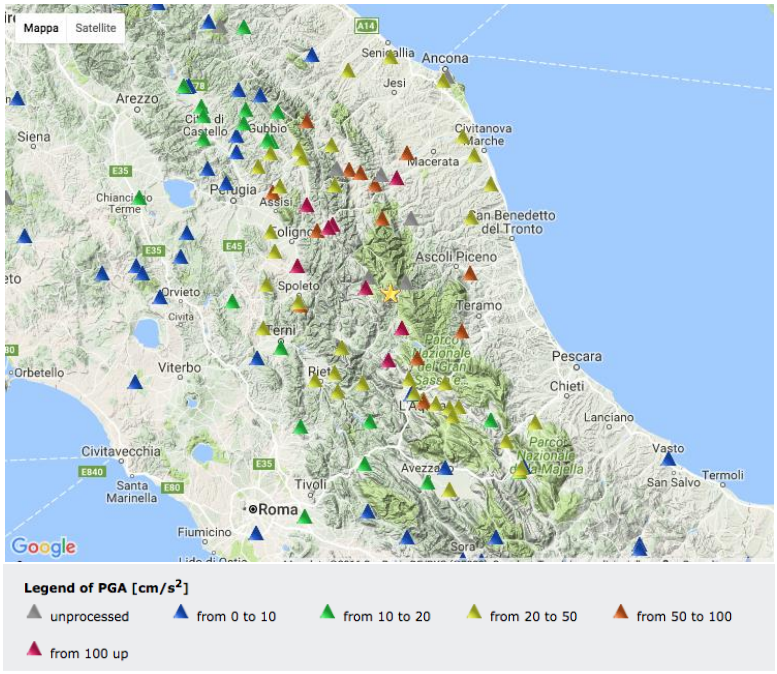


Figure 1: location of the epicentre (yellow star) and strong motion stations within 200 km from the epicentre. The square indicate strong-motion stations and the colours correspond to the PGA values (gal).

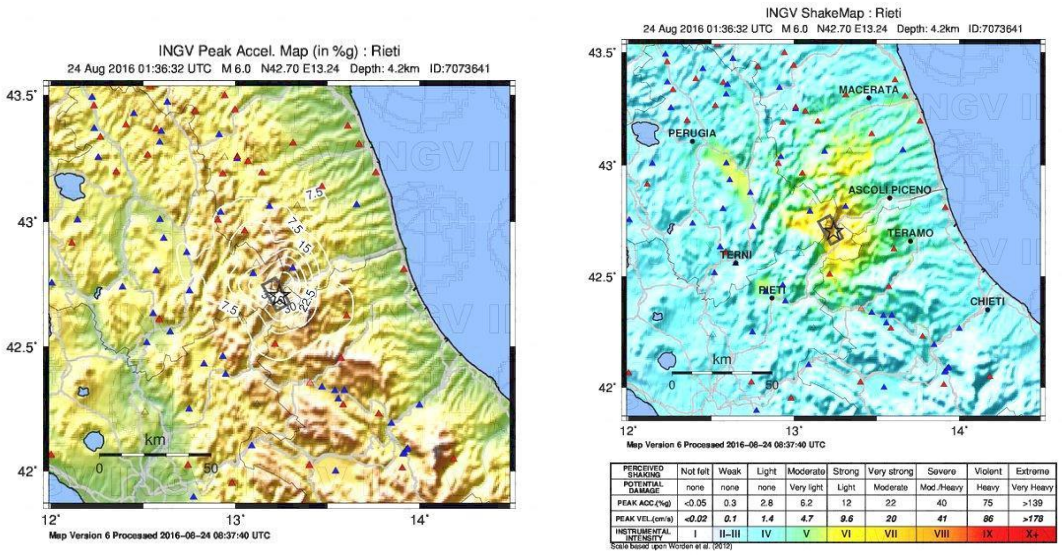


Figure 2: Shakemap of the mainshock (from http://shakemap.rm.ingv.it/shake/)

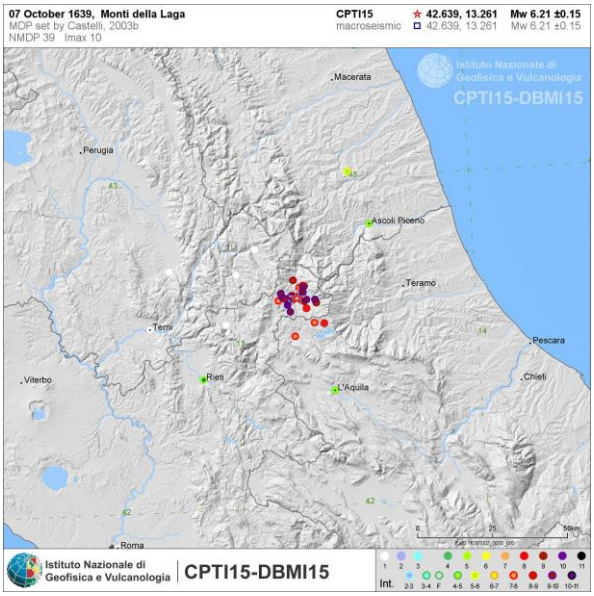


Figure 3: macroseismic field of the 1639 Mw 6.2 Amatrice earthquake (from http://emidius.mi.ingv.it/CPTI15-DBMI15/)

# 4. Strong Motion Data

The Italian Accelerometric Network (RAN), managed by the Department of Civil Protection (DPC), and the Italian seismic network, managed by the Istituto Nazionale di Geofisica e Vulcanologia (INGV) have made available the records of about 200 accelerometric stations. Appendix 1 lists networks id, station id, geographic coordinates of the station and soil type, where available. These data are also available at the Engineering Strong-motion database (esm.mi.ingv.it).

The largest Peak Ground Acceleration (PGA) have been recorded at short epicentral distances (< 15 km) at the stations Amatrice (AMT, 452.60 gal, uncorrected value, E-W component), Norcia (NRC, 376.96, N-S component) and Arquata del Tronto (RQT, 447.87 gal, E-W component, N-S component not available). The peak parameters of the available records are reported in the following table:

Table 1. Peak parameters recorded during the earthquake. For each recording station, the following is provided: station code, direction of record, distance from the epicentre (R_epi), peak ground acceleration (PGA), peak ground velocity (PGV), peak ground displacement (PGD).

| Station Code | Direction | R_epi (km) | PGA (cm/s/s) | PGV (cm/s) | PGD (cm) |
|---|---|---|---|---|---|
| AMT | E-W | 8.90 | 424.98 | 21.52 | 1.54 |
| AMT | N-S | 8.90 | 183.48 | 20.48 | 4.26 |
| AMT | Vertical | 8.90 | 194.04 | 16.72 | 4.46 |
| NRC | E-W | 13.70 | 352.65 | 29.67 | 5.71 |
| NRC | N-S | 13.70 | 366.32 | 23.77 | 6.96 |
| NRC | Vertical | 13.70 | 211.48 | 11.68 | 3.26 |
| RM33 | E-W | 22.30 | 100.36 | 9.30 | 2.39 |
| RM33 | N-S | 22.30 | 99.03 | 6.24 | 2.01 |
| RM33 | Vertical | 22.30 | 35.18 | 4.99 | 1.76 |
| SPD | E-W | 23.70 | 51.91 | 4.98 | 0.95 |
| SPD | N-S | 23.70 | 99.85 | 7.63 | 1.78 |
| SPD | Vertical | 23.70 | 53.69 | 6.29 | 1.90 |
| TERO | E-W | 32.90 | 55.54 | 3.16 | 1.27 |
| TERO | N-S | 32.90 | 83.55 | 4.31 | 1.52 |
| TERO | Vertical | 32.90 | 35.03 | 2.84 | 0.98 |
| ASP | E-W | 37.20 | 84.91 | 3.19 | 0.54 |
| ASP | N-S | 37.20 | 81.77 | 2.75 | 0.54 |
| ASP | Vertical | 37.20 | 37.82 | 1.95 | 0.57 |
| AQV | E-W | 37.30 | 59.60 | 3.93 | 0.83 |
| AQV | N-S | 37.30 | 45.27 | 4.40 | 0.90 |
| AQV | Vertical | 37.30 | 22.75 | 2.69 | 0.84 |
| SPM | E-W | 38.40 | 65.95 | 2.39 | 0.73 |
| SPM | N-S | 38.40 | 63.55 | 3.04 | 1.46 |
| SPM | Vertical | 38.40 | 20.57 | 1.39 | 0.61 |
| MNF | E-W | 38.90 | 71.66 | 4.77 | 1.31 |
| MNF | N-S | 38.90 | 43.46 | 2.90 | 1.43 |
| MNF | Vertical | 38.90 | 59.66 | 4.65 | 1.97 |
| TRE | E-W | 43.70 | 62.96 | 6.11 | 1.10 |
| TRE | N-S | 43.70 | 108.50 | 7.81 | 2.09 |
| TRE | Vertical | 43.70 | 44.71 | 3.40 | 0.79 |
| CLF | E-W | 43.80 | 122.98 | 8.70 | 1.56 |
| CLF | N-S | 43.80 | 128.78 | 11.64 | 2.02 |
| CLF | Vertical | 43.80 | 103.06 | 9.38 | 2.10 |
| FOC | E-W | 44.00 | 256.20 | 8.10 | 0.83 |
| FOC | N-S | 44.00 | 322.54 | 10.18 | 1.34 |
| FOC | Vertical | 44.00 | 125.61 | 5.75 | 1.56 |
| FOS | E-W | 47.70 | 58.70 | 5.26 | 1.16 |

| | | | | | |
|---|---|---|---|---|---|
| FOS | N-S | 47.70 | 74.99 | 4.83 | 1.54 |
| FOS | Vertical | 47.70 | 40.15 | 2.84 | 1.11 |
| MDAR | E-W | 54.00 | 38.94 | 3.44 | 0.90 |
| MDAR | N-S | 54.00 | 54.61 | 3.71 | 1.38 |
| MDAR | Vertical | 54.00 | 29.01 | 2.82 | 1.20 |
| TLN | E-W | 56.90 | 114.77 | 6.95 | 1.28 |
| TLN | N-S | 56.90 | 74.35 | 5.83 | 1.77 |
| TLN | Vertical | 56.90 | 46.14 | 2.83 | 1.24 |
| NCR | E-W | 57.00 | 217.65 | 7.06 | 0.64 |
| NCR | N-S | 57.00 | 149.01 | 4.92 | 1.18 |
| NCR | Vertical | 57.00 | 39.40 | 2.40 | 1.14 |
| SSM1 | E-W | 57.70 | 22.14 | 1.36 | 0.41 |
| SSM1 | N-S | 57.70 | 58.15 | 3.63 | 1.00 |
| SSM1 | Vertical | 57.70 | 39.19 | 4.00 | 1.93 |
| GAG1 | E-W | 60.00 | 75.89 | 6.48 | 1.08 |
| GAG1 | N-S | 60.00 | 89.47 | 7.27 | 1.82 |
| GAG1 | Vertical | 60.00 | 57.11 | 4.00 | 1.64 |
| MTL | E-W | 62.40 | 69.95 | 3.72 | 1.05 |
| MTL | N-S | 62.40 | 66.71 | 6.47 | 1.32 |
| MTL | Vertical | 62.40 | 31.02 | 4.61 | 1.25 |
| TRE1 | E-W | 67.20 | 62.08 | 6.08 | 2.23 |
| TRE1 | N-S | 67.20 | 71.31 | 4.35 | 1.71 |
| TRE1 | Vertical | 67.20 | 30.88 | 2.75 | 1.14 |
| VAL | E-W | 72.50 | 58.27 | 1.95 | 0.46 |
| VAL | N-S | 72.50 | 35.82 | 1.84 | 0.71 |
| VAL | Vertical | 72.50 | 13.61 | 1.28 | 0.70 |
| PP3 | E-W | 80.70 | 49.56 | 4.16 | 3.06 |
| PP3 | N-S | 80.70 | 40.42 | 2.88 | 2.15 |
| PP3 | Vertical | 80.70 | 14.31 | 2.85 | 1.66 |
| MURB | E-W | 83.60 | 45.60 | 3.10 | 0.55 |
| MURB | N-S | 83.60 | 40.57 | 3.26 | 1.00 |
| MURB | Vertical | 83.60 | 13.94 | 2.00 | 0.95 |
| SSFR | E-W | 88.20 | 57.11 | 2.44 | 0.37 |
| SSFR | N-S | 88.20 | 49.56 | 1.83 | 0.67 |
| SSFR | Vertical | 88.20 | 20.42 | 1.21 | 0.63 |

Table 2 reports some integral measures reported for the same records.

Table 2. Integral measures recorded during the earthquake. For each recording station, the following is provided: station code, direction of record, Arias Intensity ($I_A$), Significant duration estimated between 5% and 95% of the IA ($S_{D\ 5\text{-}95}$), Significant duration estimated between 5% and 75% of the IA ($S_{D\ 5\text{-}75}$), spectral intensity (Housner intensity) between 0.10 and 2.5 s (SI).

| Station Code | Direction | $I_A$ (cm/s) | $S_{D\ 5\text{-}95}$ (s) | $S_{D\ 5\text{-}75}$ (s) | SI (cm) |
|---|---|---|---|---|---|
| AMT | E-W | 46.22 | 3.75 | 0.97 | 37.06 |
| AMT | N-S | 17.78 | 3.18 | 0.83 | 55.95 |
| AMT | Vertical | 13.95 | 4.86 | 1.71 | 42.94 |
| NRC | E-W | 104.55 | 6.03 | 1.74 | 107.11 |

| | | | | | |
|---|---|---|---|---|---|
| NRC | N-S | 82.67 | 6.33 | 1.60 | 80.20 |
| NRC | Vertical | 37.89 | 5.56 | 2.38 | 34.96 |
| RM33 | E-W | 8.72 | 9.47 | 2.96 | 35.93 |
| RM33 | N-S | 6.13 | 10.07 | 3.83 | 23.99 |
| RM33 | Vertical | 1.80 | 14.34 | 8.16 | 16.88 |
| SPD | E-W | 3.95 | 10.39 | 4.62 | 22.06 |
| SPD | N-S | 7.16 | 8.62 | 2.44 | 28.43 |
| SPD | Vertical | 3.57 | 10.09 | 3.77 | 25.74 |
| TERO | E-W | 4.78 | 12.79 | 5.92 | 11.48 |
| TERO | N-S | 7.65 | 11.33 | 4.61 | 16.84 |
| TERO | Vertical | 1.74 | 14.68 | 7.48 | 8.83 |
| ASP | E-W | 10.35 | 11.35 | 5.24 | 9.75 |
| ASP | N-S | 7.41 | 12.05 | 4.65 | 9.92 |
| ASP | Vertical | 2.24 | 16.27 | 8.60 | 7.24 |
| AQV | E-W | 3.00 | 14.23 | 5.42 | 13.81 |
| AQV | N-S | 2.82 | 15.89 | 6.19 | 13.56 |
| AQV | Vertical | 0.70 | 18.28 | 8.26 | 10.64 |
| SPM | E-W | 4.93 | 14.43 | 7.03 | 8.98 |
| SPM | N-S | 4.99 | 12.48 | 8.34 | 8.01 |
| SPM | Vertical | 0.90 | 16.21 | 9.15 | 4.95 |
| MNF | E-W | 3.03 | 6.86 | 1.67 | 18.18 |
| MNF | N-S | 1.48 | 10.91 | 5.18 | 8.26 |
| MNF | Vertical | 2.17 | 6.59 | 2.28 | 15.03 |
| TRE | E-W | 5.10 | 14.62 | 6.19 | 15.19 |
| TRE | N-S | 10.62 | 14.52 | 3.36 | 26.17 |
| TRE | Vertical | 2.13 | 15.16 | 8.15 | 10.08 |
| CLF | E-W | 18.13 | 9.03 | 2.96 | 35.24 |
| CLF | N-S | 14.11 | 10.80 | 2.65 | 36.16 |
| CLF | Vertical | 13.98 | 5.31 | 2.89 | 24.35 |
| FOC | E-W | 36.24 | 5.60 | 1.83 | 17.56 |
| FOC | N-S | 38.48 | 4.22 | 1.85 | 19.62 |
| FOC | Vertical | 10.41 | 8.57 | 5.78 | 15.55 |
| FOS | E-W | 4.64 | 9.02 | 2.80 | 16.58 |
| FOS | N-S | 5.94 | 8.81 | 3.11 | 13.80 |
| FOS | Vertical | 1.52 | 13.19 | 7.58 | 10.17 |
| MDAR | E-W | 1.29 | 11.31 | 3.70 | 12.21 |
| MDAR | N-S | 1.97 | 10.01 | 2.62 | 12.43 |
| MDAR | Vertical | 0.67 | 14.89 | 7.78 | 7.95 |
| TLN | E-W | 11.20 | 11.46 | 5.17 | 30.04 |
| TLN | N-S | 6.15 | 12.55 | 5.53 | 19.77 |
| TLN | Vertical | 2.35 | 20.40 | 9.33 | 10.06 |
| NCR | E-W | 31.66 | 4.84 | 1.24 | 11.00 |
| NCR | N-S | 19.01 | 7.20 | 2.98 | 11.85 |
| NCR | Vertical | 1.76 | 13.60 | 7.51 | 9.39 |
| SSM1 | E-W | 1.08 | 143.56 | 86.40 | 4.76 |
| SSM1 | N-S | 2.99 | 11.88 | 4.38 | 10.57 |

| | | | | | |
|---|---|---|---|---|---|
| SSM1 | Vertical | 1.62 | 17.46 | 10.45 | 13.38 |
| GAG1 | E-W | 9.84 | 12.13 | 5.80 | 22.03 |
| GAG1 | N-S | 10.90 | 11.95 | 4.79 | 23.57 |
| GAG1 | Vertical | 5.60 | 15.00 | 7.46 | 16.35 |
| MTL | E-W | 4.72 | 15.40 | 6.51 | 19.36 |
| MTL | N-S | 5.25 | 13.12 | 6.20 | 18.18 |
| MTL | Vertical | 1.89 | 19.34 | 9.18 | 15.88 |
| TRE1 | E-W | 5.28 | 18.34 | 5.23 | 22.65 |
| TRE1 | N-S | 4.69 | 15.60 | 6.06 | 17.26 |
| TRE1 | Vertical | 1.47 | 19.16 | 10.95 | 10.65 |
| VAL | E-W | 2.49 | 11.35 | 3.22 | 6.58 |
| VAL | N-S | 2.00 | 12.65 | 4.88 | 6.06 |
| VAL | Vertical | 0.39 | 20.79 | 12.53 | 3.32 |
| PP3 | E-W | 3.02 | 35.05 | 13.75 | 19.72 |
| PP3 | N-S | 2.19 | 43.13 | 15.30 | 13.16 |
| PP3 | Vertical | 0.73 | 54.20 | 36.62 | 8.56 |
| MURB | E-W | 2.48 | 19.61 | 8.49 | 8.37 |
| MURB | N-S | 2.30 | 19.72 | 7.07 | 9.07 |
| MURB | Vertical | 0.38 | 25.87 | 13.17 | 5.81 |
| SSFR | E-W | 2.76 | 17.67 | 9.35 | 5.74 |
| SSFR | N-S | 2.52 | 21.78 | 13.47 | 5.13 |
| SSFR | Vertical | 0.43 | 18.18 | 9.06 | 4.65 |

# 5. Data comparison with GMPE

Some GM parameters (PGA, PGV and acceleration spectral ordinates at 0.3, 1 and 3 seconds, period used to calculate shakemaps) are compared to the predictions by Bindi et al (2011). These results can be considered as preliminary since:

- the distance is the epicentral distance, whilst Bindi et al. adopts the Joyner-Boore distance; the latter could not be estimated because the fault geometry is still not available.
- the comparison at 3s is outside the range of validity of this GMPE, that can be used until 2s.

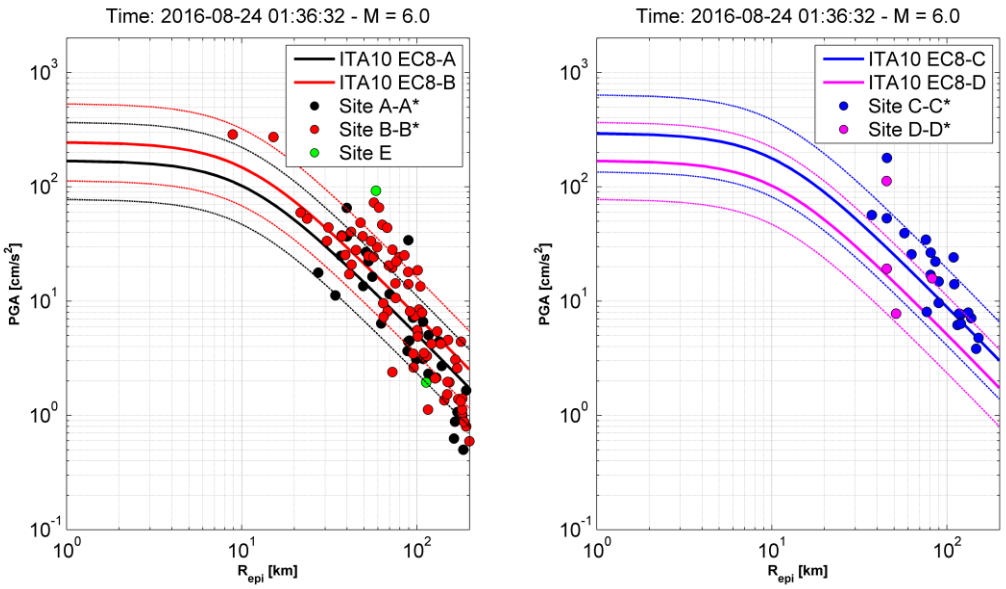


Figure 4: Observed horizontal PGA against Bindi et al (2011): left EC8 A and B sites; right EC8 C and D sites

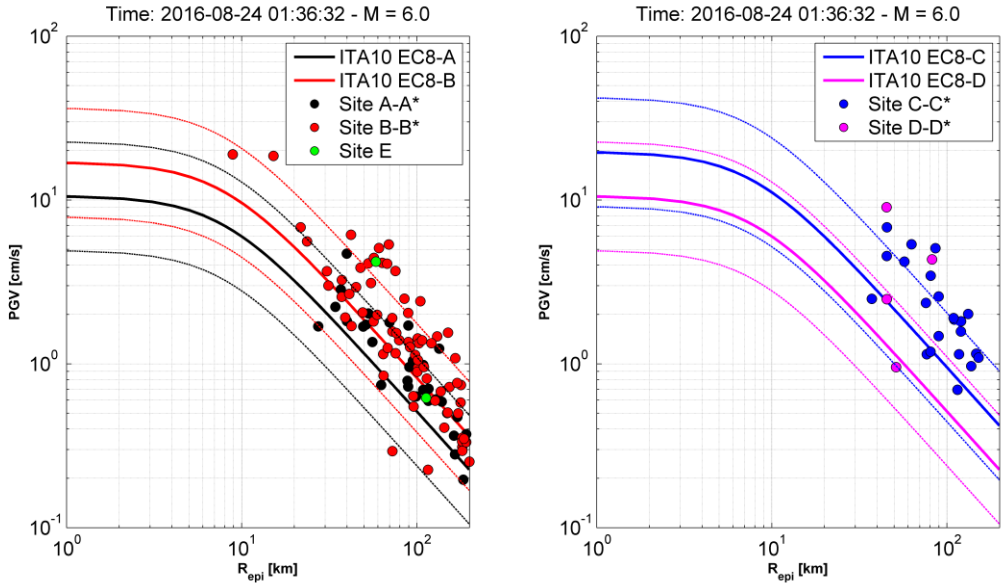


Figure 5: Observed horizontal PGV against Bindi et al (2011): left EC8 A and B sites; right EC8 C and D sites

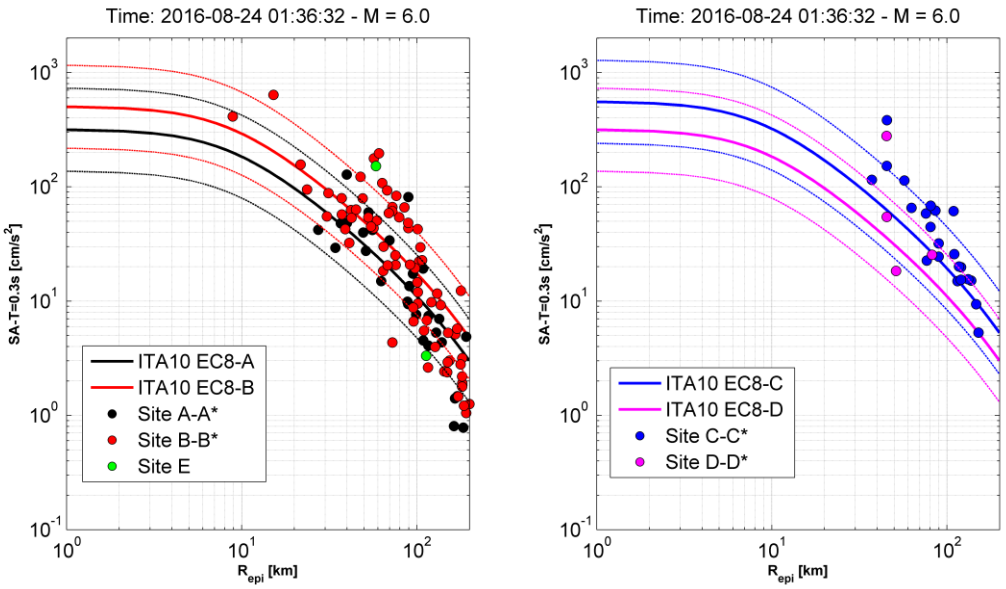


Figure 6: Observed horizontal SA (0.3s) against Bindi et al (2011): left EC8 A and B sites; right EC8 C and D sites

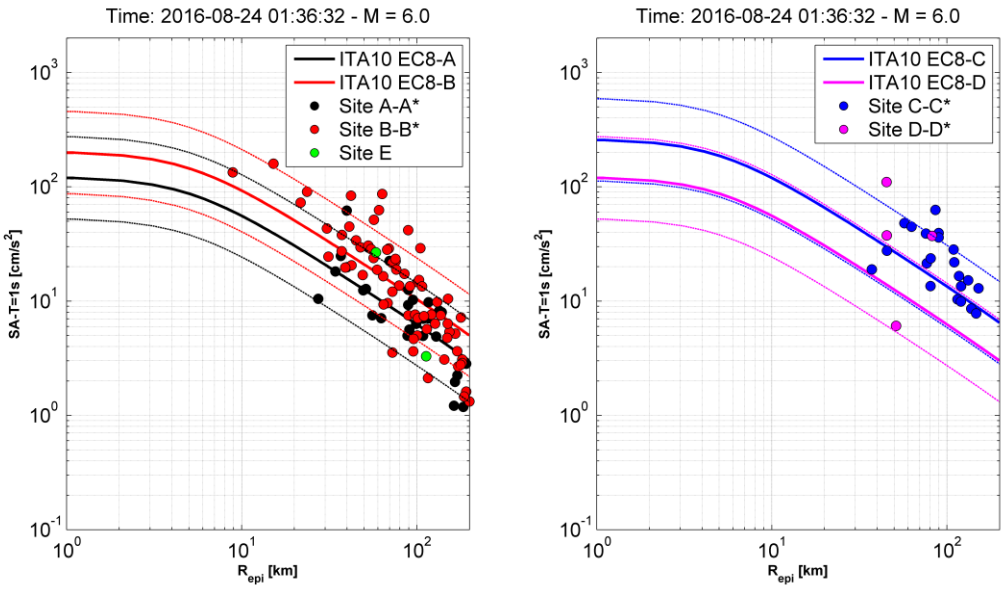


Figure 7: Observed horizontal SA (1s) against Bindi et al (2011): left EC8 A and B sites; right EC8 C and D sites

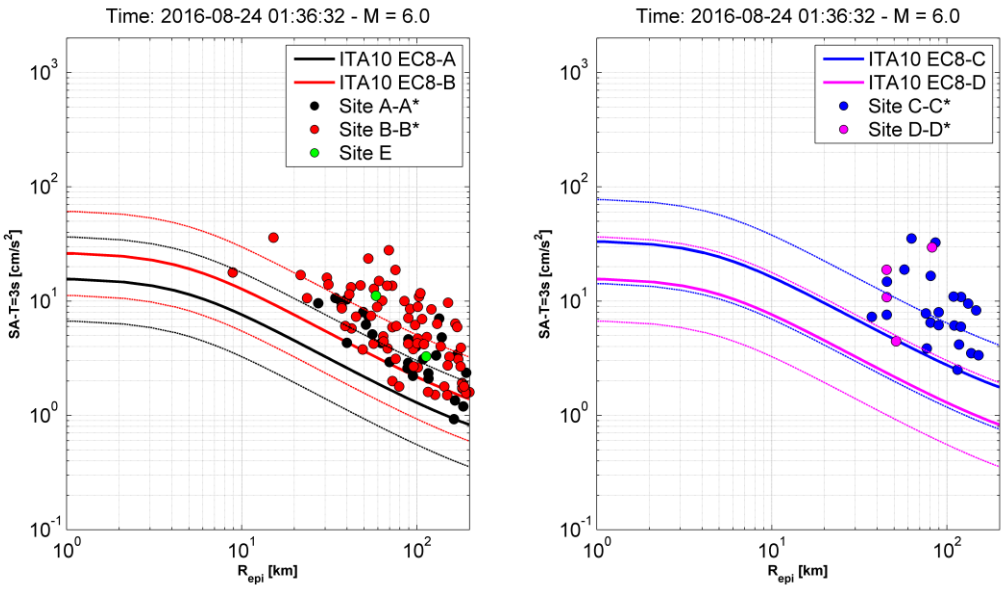


Figure 8: Observed horizontal SA (3s) against Bindi et al (2011): left EC8 A and B sites; right EC8 C and D sites

# 6. Response Spectra

In this section, the pseudo-spectral acceleration (PSA), pseudo-spectral velocity (PSV) and spectral displacement (SD) are reported for all the available records for three different values of damping ratio, (z), that is 2%, 5% and 10%.

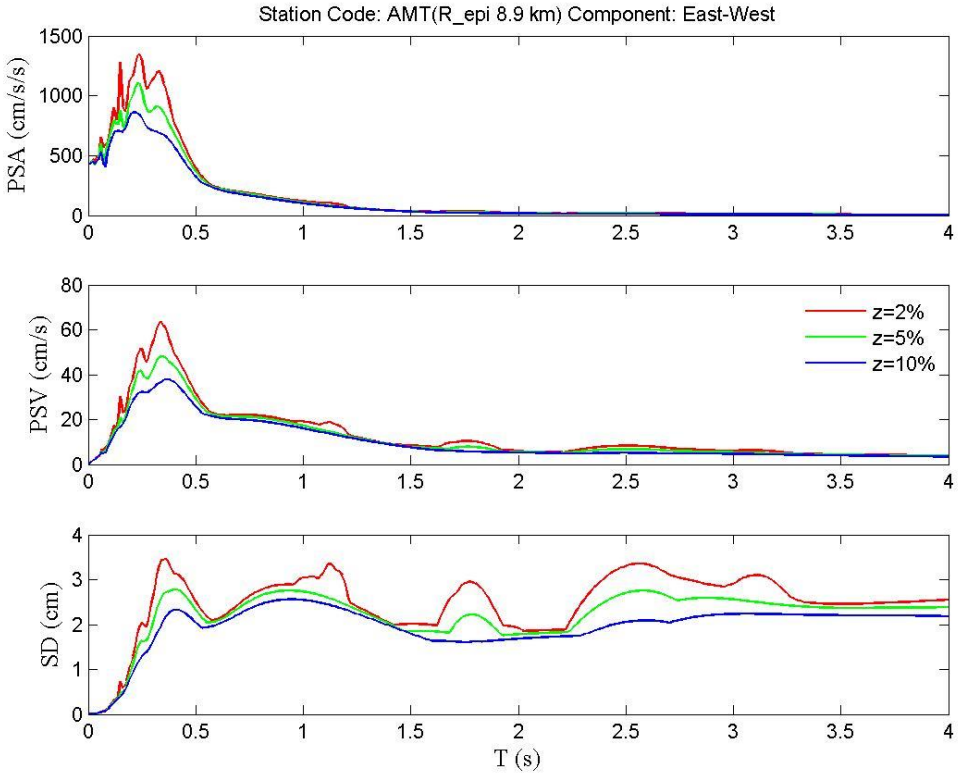

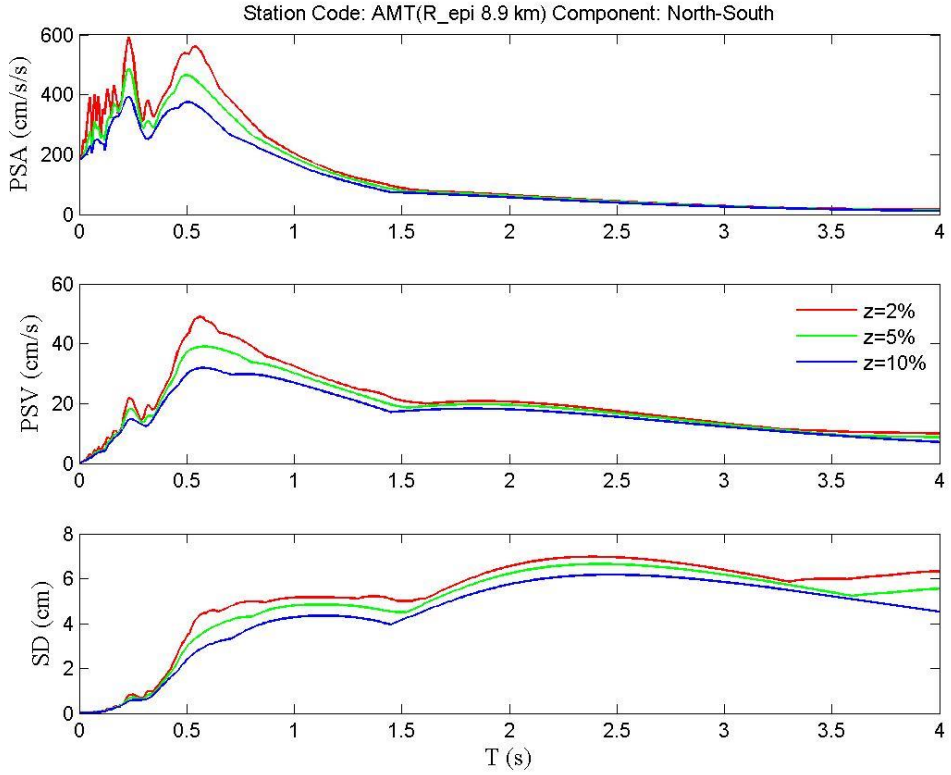
Station Code: AMT(R_epi 8.9 km) Component: North-South
PSA (cm/s/s)
PSV (cm/s)
SD (cm)
T (s)
z=2%
z=5%
z=10%

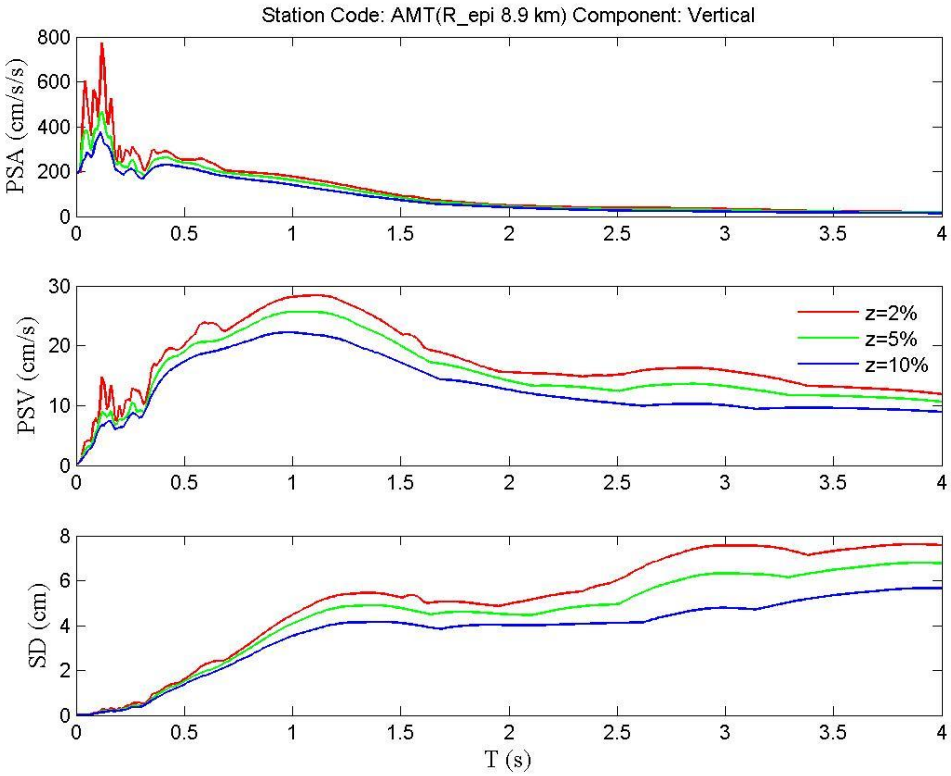
Station Code: AMT(R_epi 8.9 km) Component: Vertical
PSA (cm/s/s)
PSV (cm/s)
SD (cm)
T (s)
z=2%
z=5%
z=10%

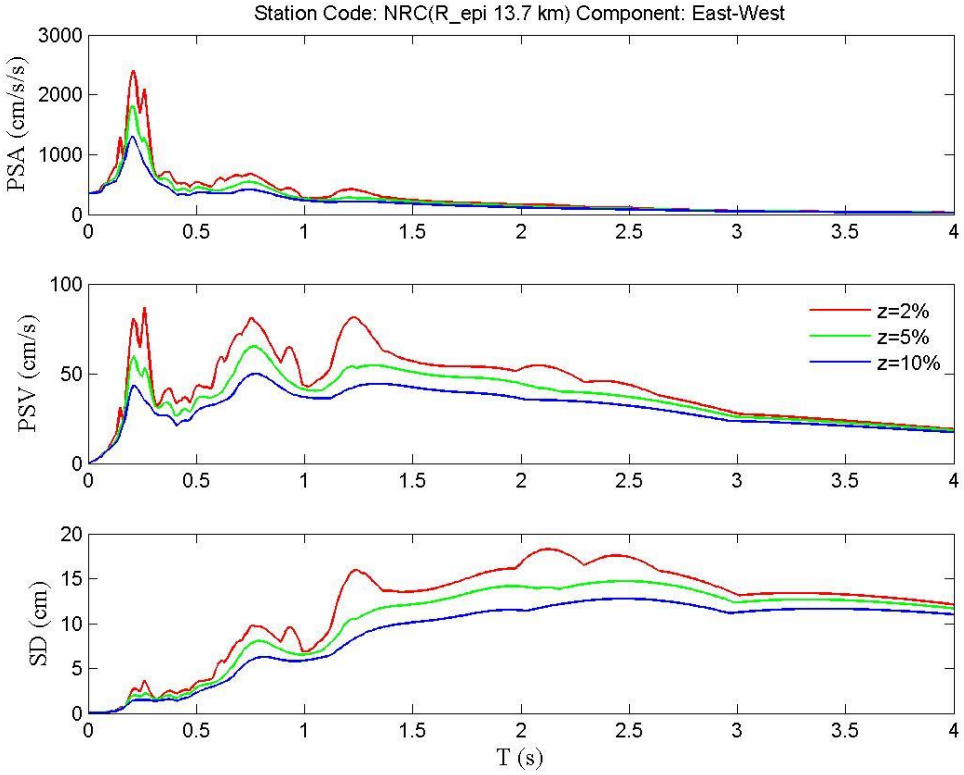
Station Code: NRC(R_epi 13.7 km) Component: East-West
PSA (cm/s/s)
PSV (cm/s)
SD (cm)
z=2%
z=5%
z=10%
T (s)

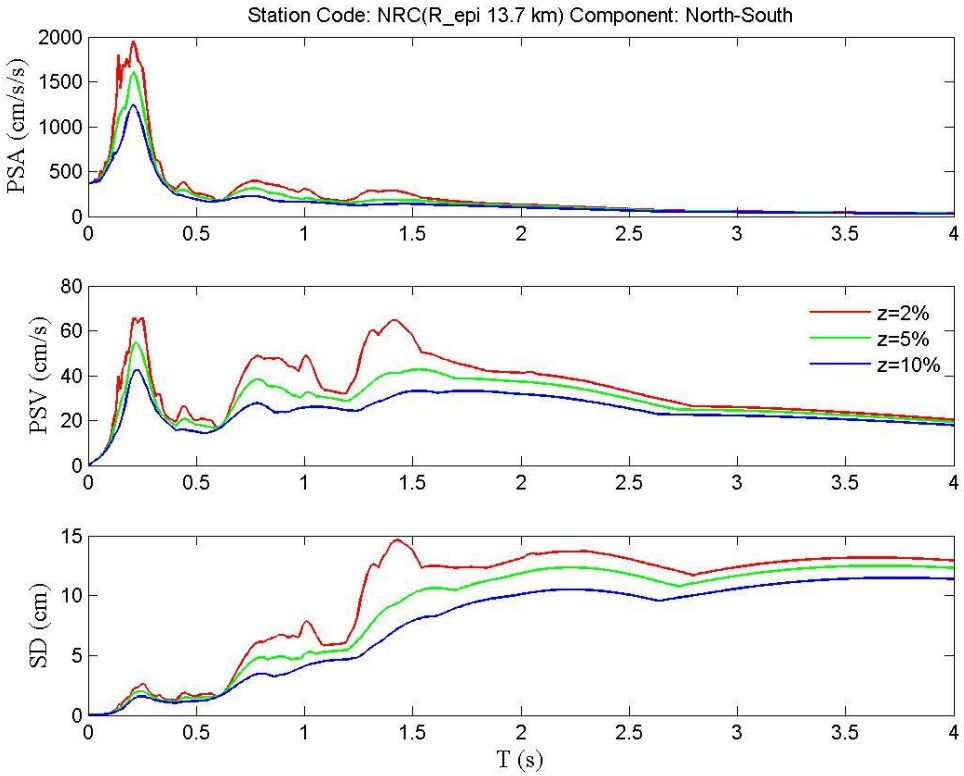
Station Code: NRC(R_epi 13.7 km) Component: North-South
PSA (cm/s/s)
PSV (cm/s)
SD (cm)
z=2%
z=5%
z=10%
T (s)

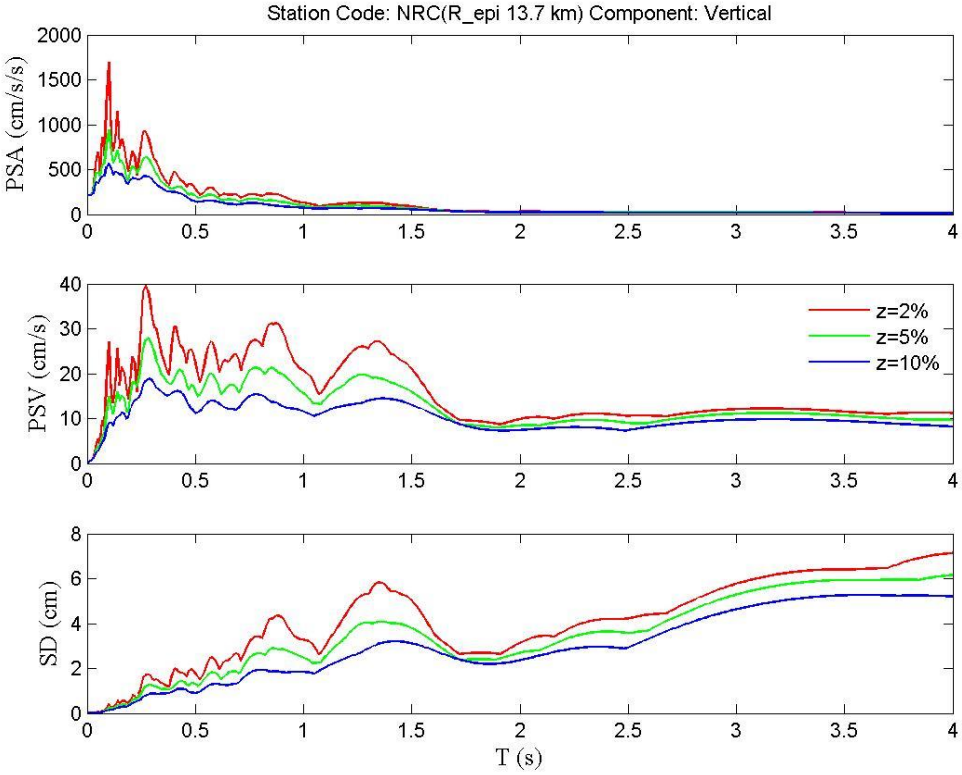
Station Code: NRC(R_epi 13.7 km) Component: Vertical
PSA (cm/s/s)
PSV (cm/s)
SD (cm)
z=2%
z=5%
z=10%
T (s)

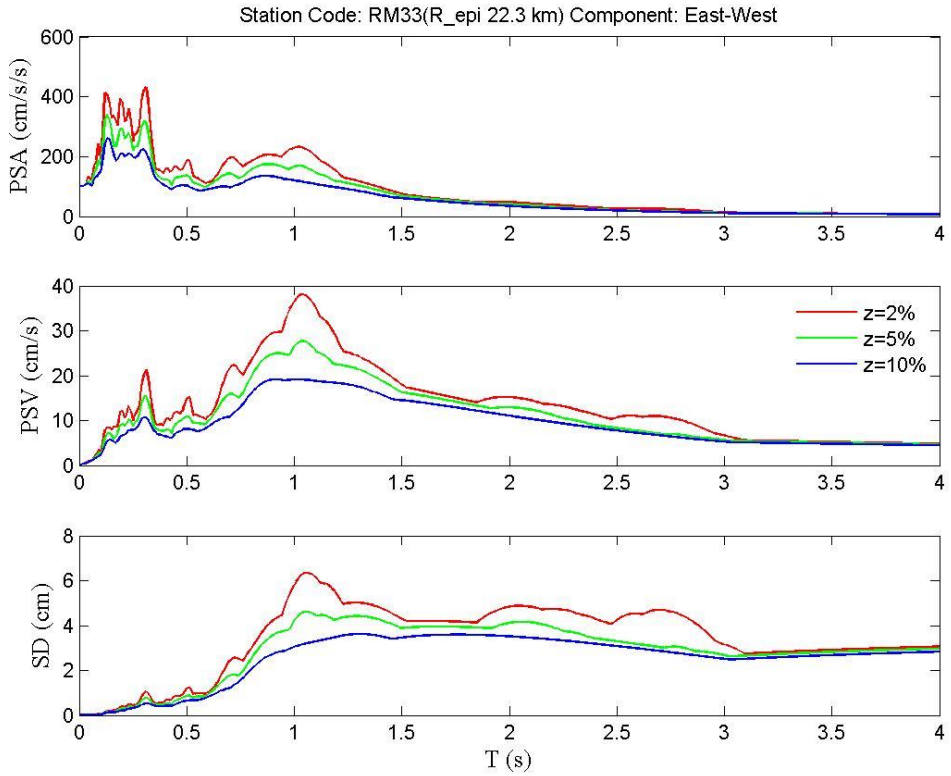
Station Code: RM33(R_epi 22.3 km) Component: East-West
PSA (cm/s/s)
PSV (cm/s)
SD (cm)
z=2%
z=5%
z=10%
T (s)

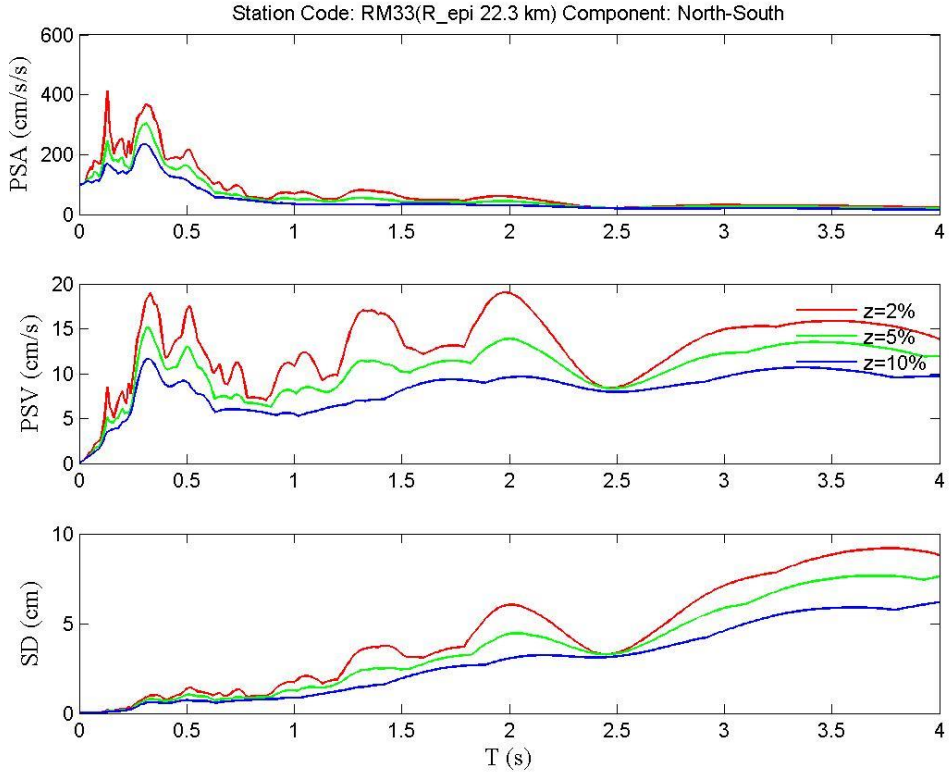
Station Code: RM33(R_epi 22.3 km) Component: North-South
PSA (cm/s/s)
PSV (cm/s)
SD (cm)
z=2%
z=5%
z=10%
T (s)

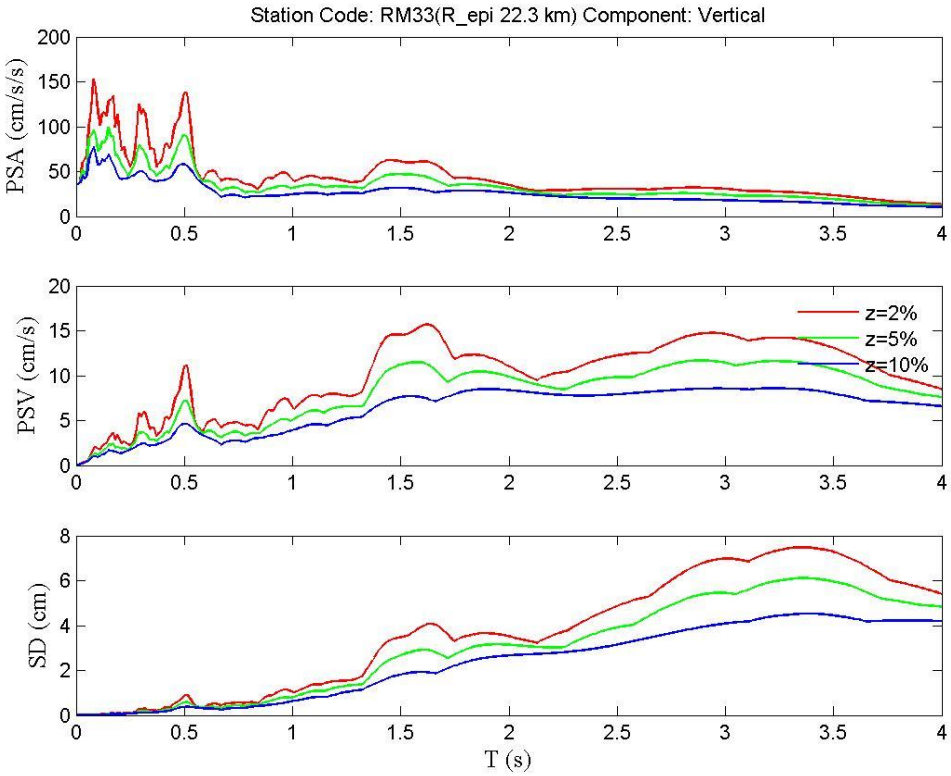
Station Code: RM33(R_epi 22.3 km) Component: Vertical
PSA (cm/s/s)
PSV (cm/s)
SD (cm)
z=2%
z=5%
z=10%
T (s)

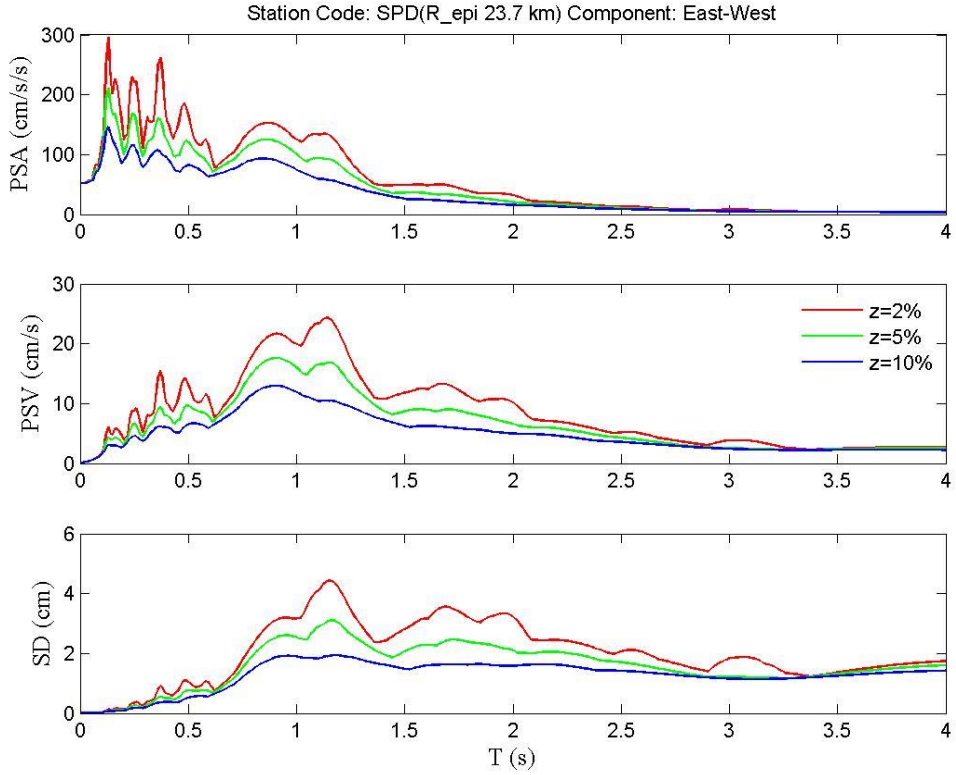
Station Code: SPD(R_epi 23.7 km) Component: East-West
PSA (cm/s/s)
PSV (cm/s)
SD (cm)
z=2%
z=5%
z=10%
T (s)

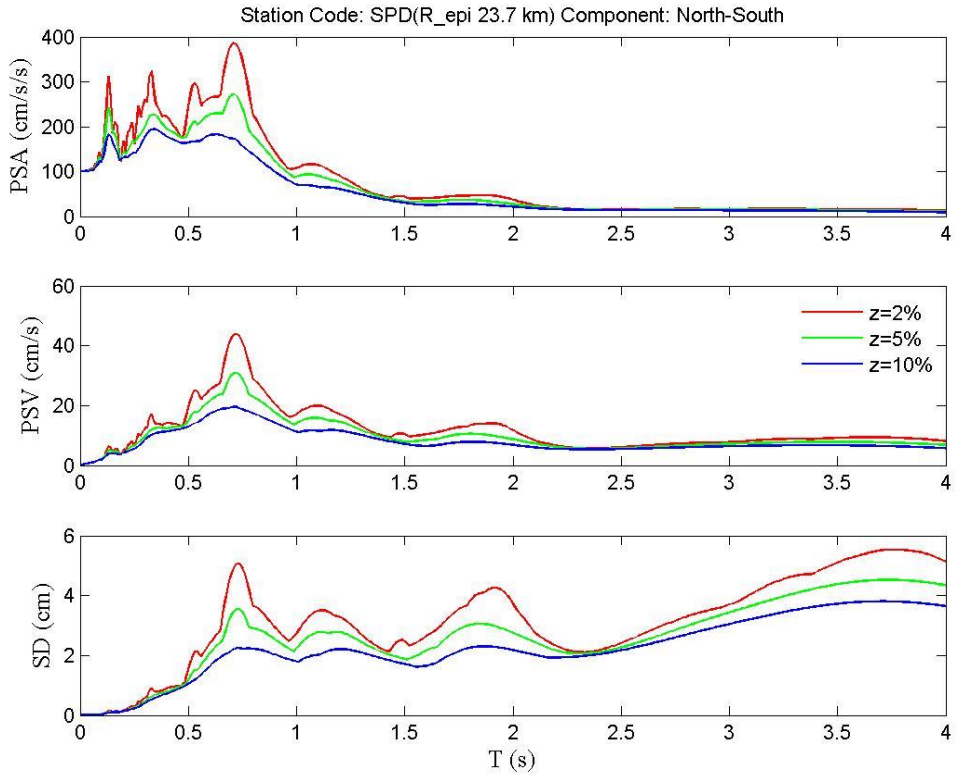
Station Code: SPD(R_epi 23.7 km) Component: North-South
PSA (cm/s/s)
PSV (cm/s)
SD (cm)
z=2%
z=5%
z=10%
T (s)

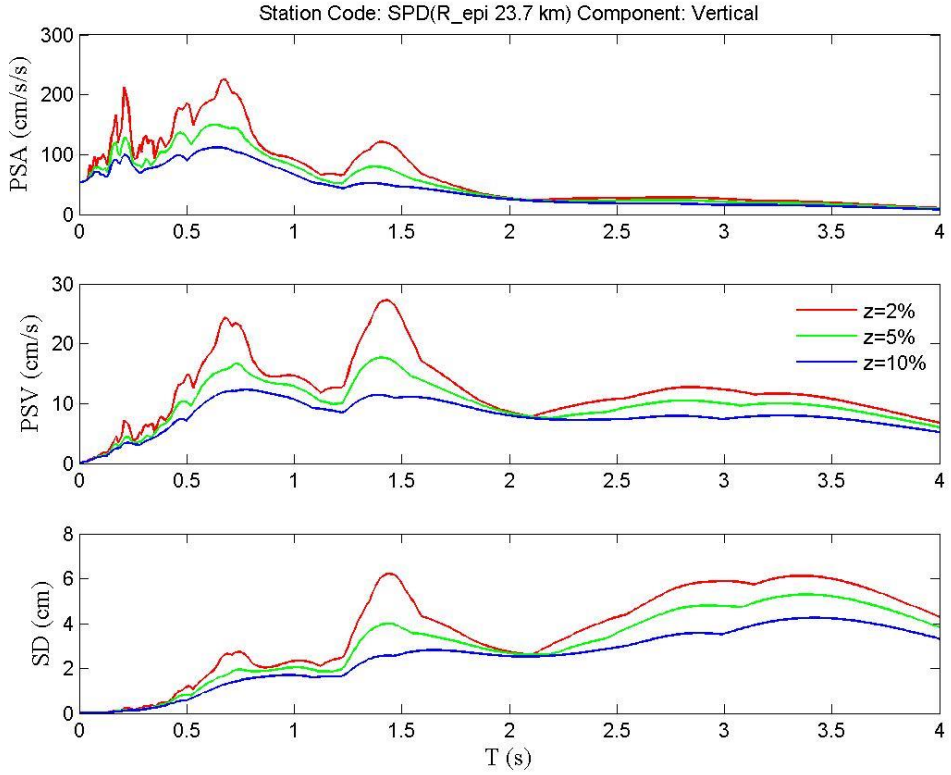
Station Code: SPD(R_epi 23.7 km) Component: Vertical
PSA (cm/s/s)
PSV (cm/s)
SD (cm)
z=2%
z=5%
z=10%
T (s)

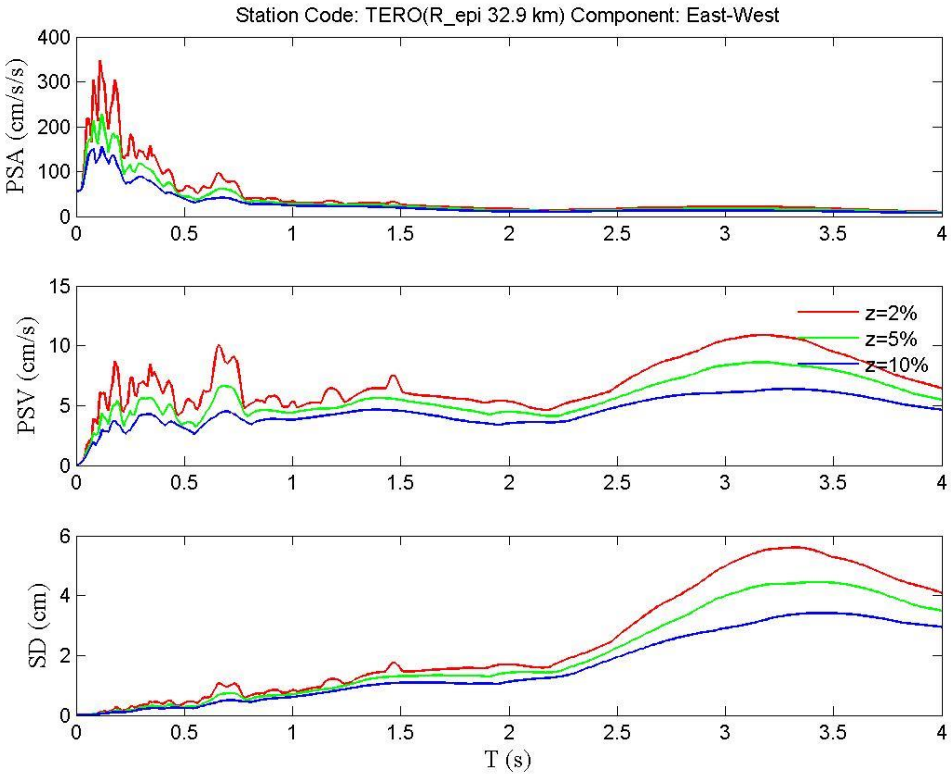
Station Code: TERO(R_epi 32.9 km) Component: East-West
PSA (cm/s/s)
PSV (cm/s)
SD (cm)
z=2%
z=5%
z=10%
T (s)

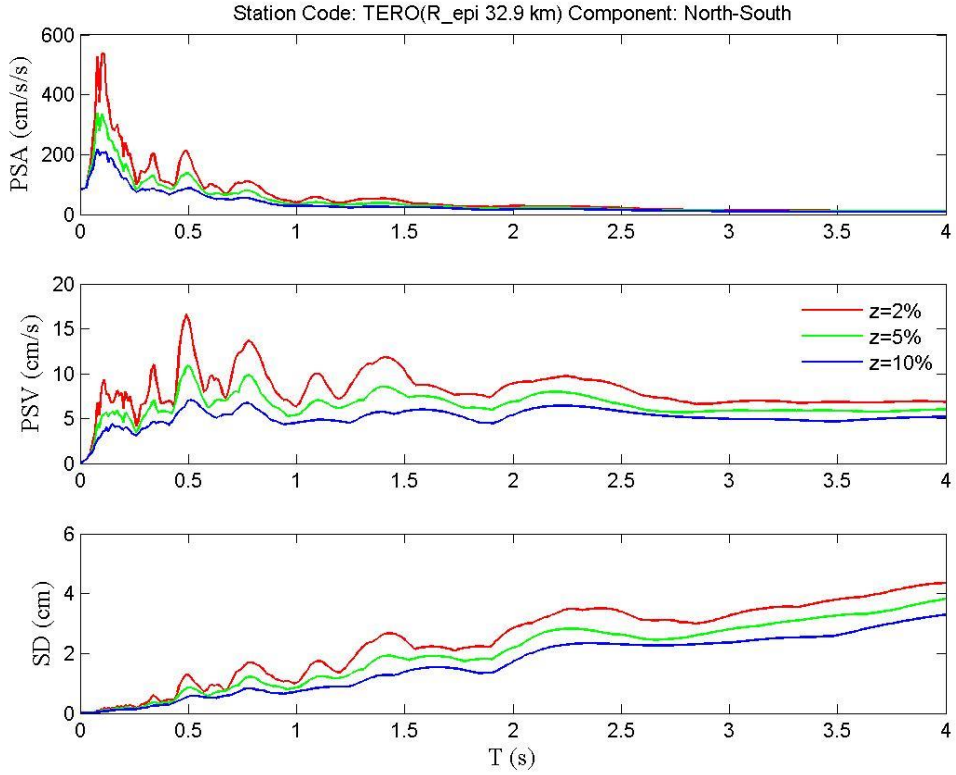
Station Code: TERO(R_epi 32.9 km) Component: North-South
PSA (cm/s/s)
PSV (cm/s)
SD (cm)
z=2%
z=5%
z=10%
T (s)

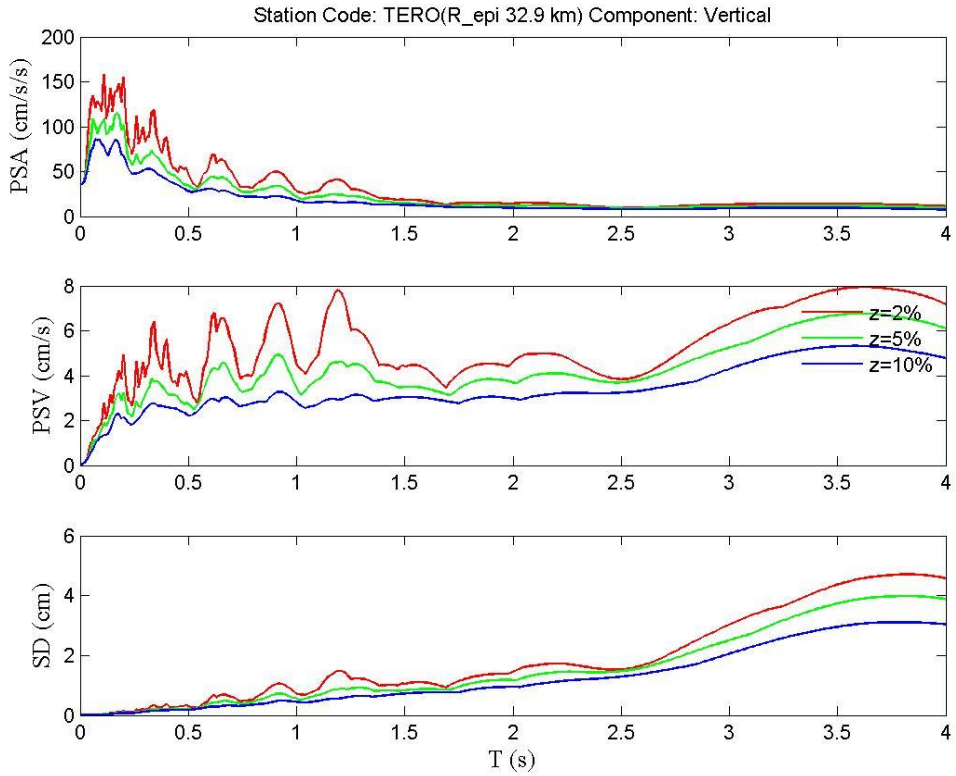
Station Code: TERO(R_epi 32.9 km) Component: Vertical
PSA (cm/s/s)
PSV (cm/s)
SD (cm)
z=2%
z=5%
z=10%
T (s)

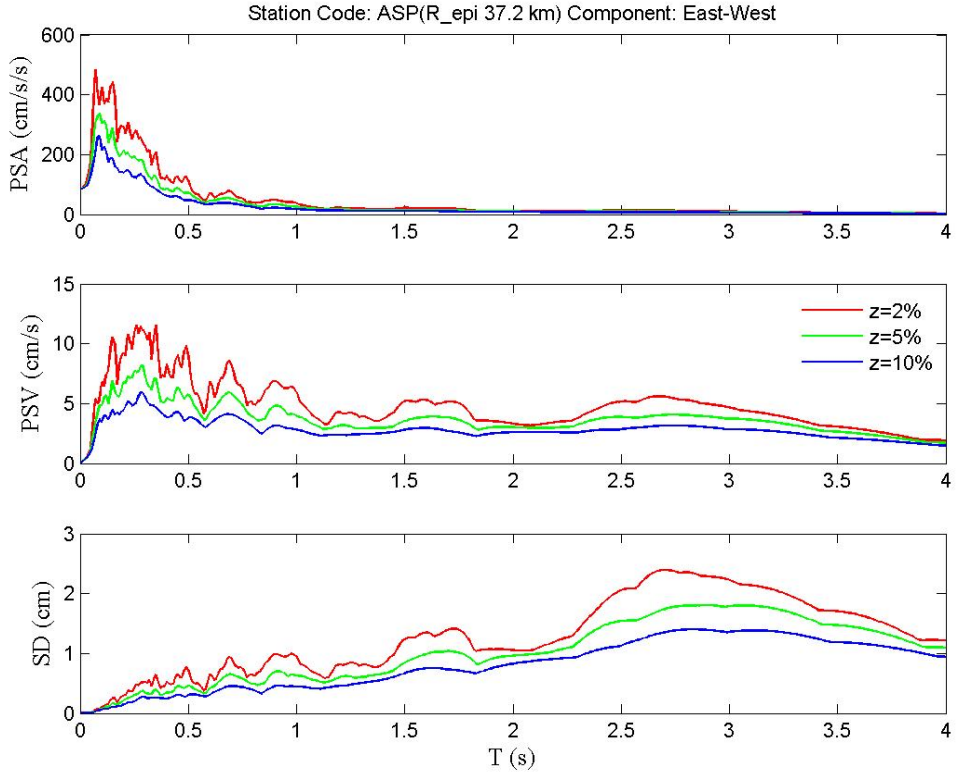
Station Code: ASP(R_epi 37.2 km) Component: East-West
PSA (cm/s/s)
PSV (cm/s)
SD (cm)
z=2%
z=5%
z=10%
T (s)

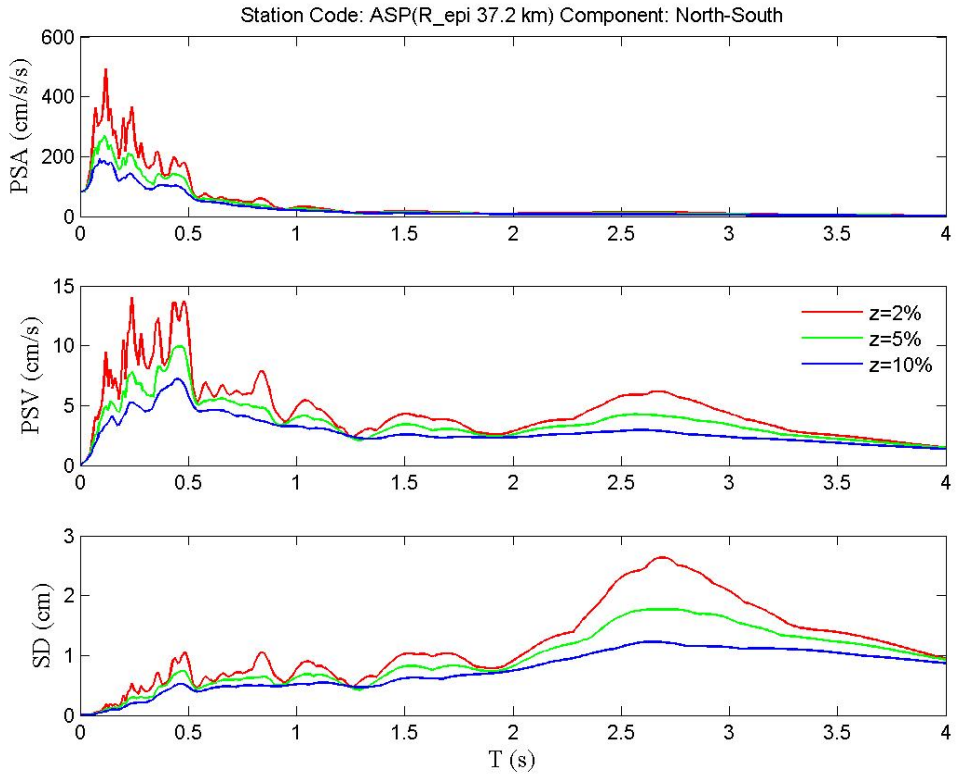
Station Code: ASP(R_epi 37.2 km) Component: North-South
PSA (cm/s/s)
PSV (cm/s)
SD (cm)
z=2%
z=5%
z=10%
T (s)

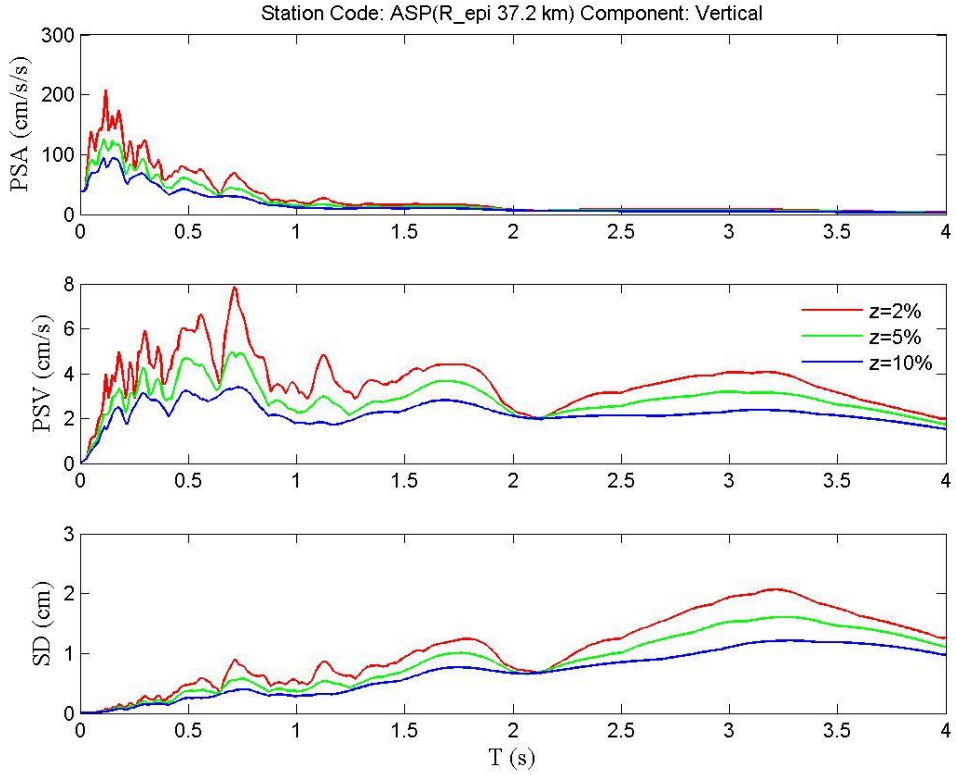
Station Code: ASP(R_epi 37.2 km) Component: Vertical
PSA (cm/s/s)
PSV (cm/s)
SD (cm)
z=2%
z=5%
z=10%
T (s)

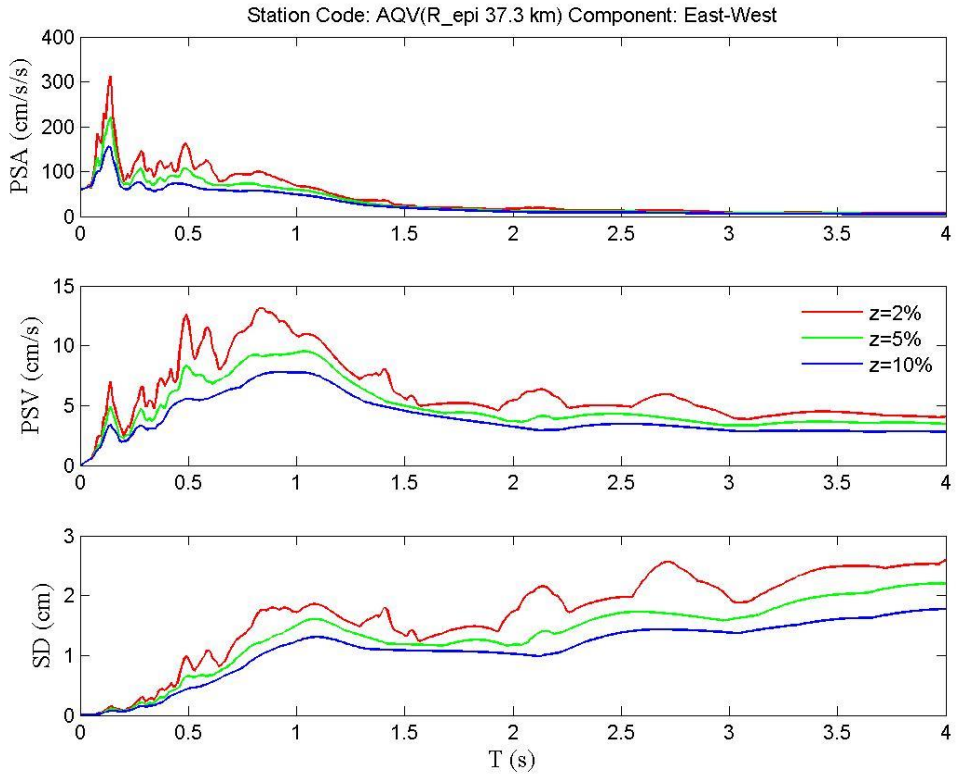
Station Code: AQV(R_epi 37.3 km) Component: East-West
PSA (cm/s/s)
PSV (cm/s)
SD (cm)
z=2%
z=5%
z=10%
T (s)

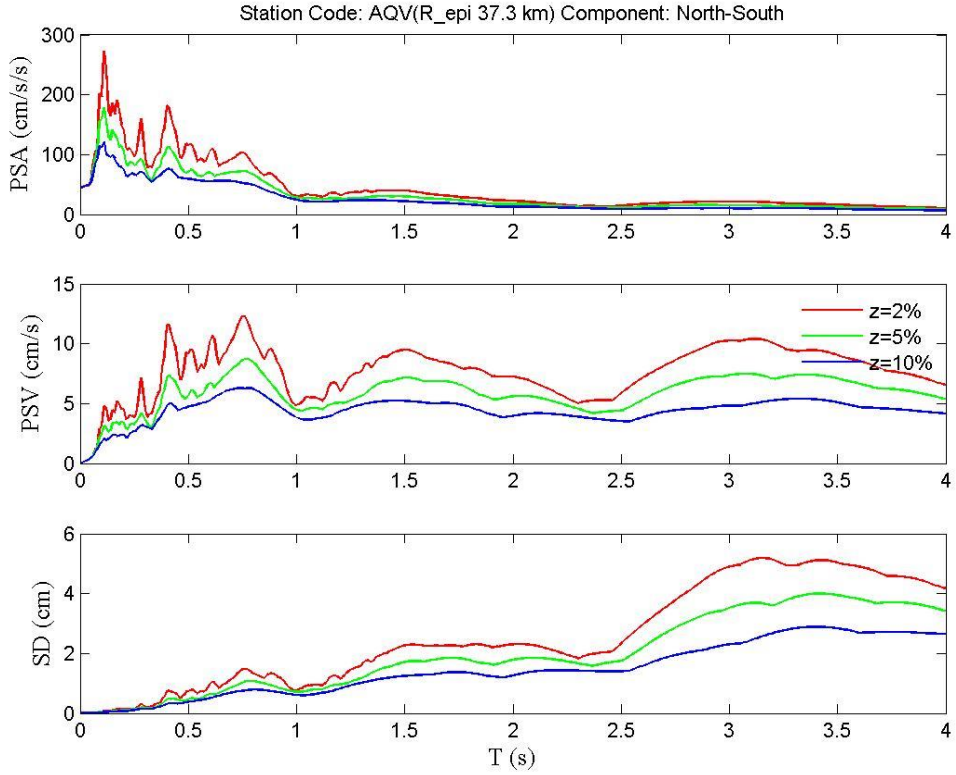
Station Code: AQV(R_epi 37.3 km) Component: North-South
PSA (cm/s/s)
PSV (cm/s)
SD (cm)
T (s)
z=2%
z=5%
z=10%

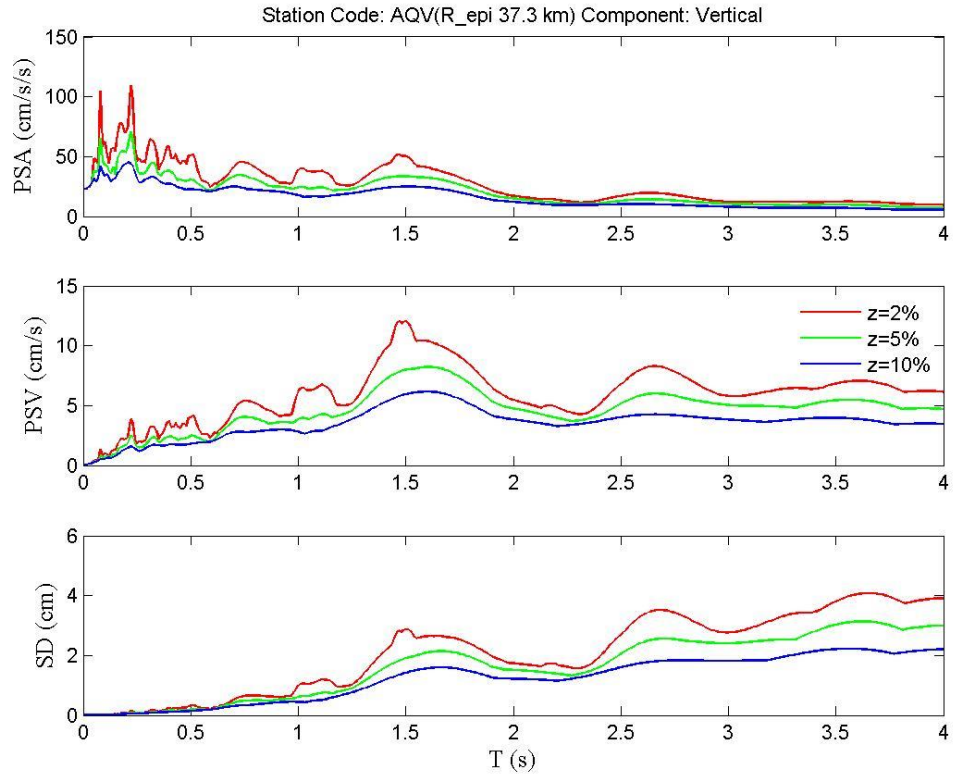
Station Code: AQV(R_epi 37.3 km) Component: Vertical
PSA (cm/s/s)
PSV (cm/s)
SD (cm)
T (s)
z=2%
z=5%
z=10%

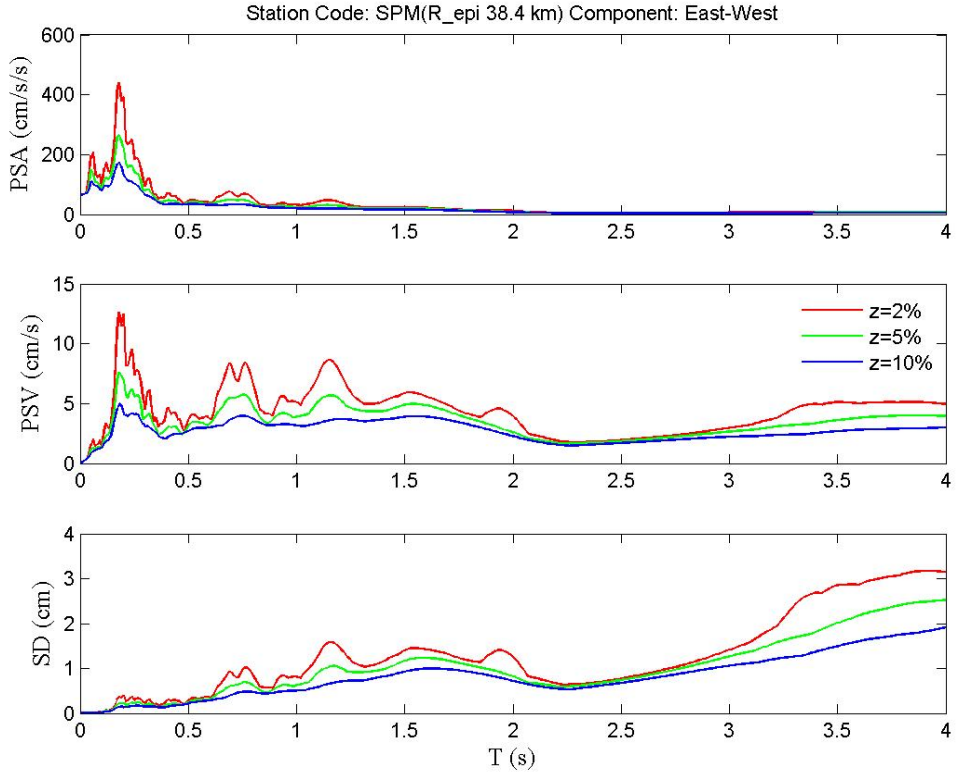
Station Code: SPM(R_epi 38.4 km) Component: East-West
PSA (cm/s/s)
PSV (cm/s)
SD (cm)
z=2%
z=5%
z=10%
T (s)

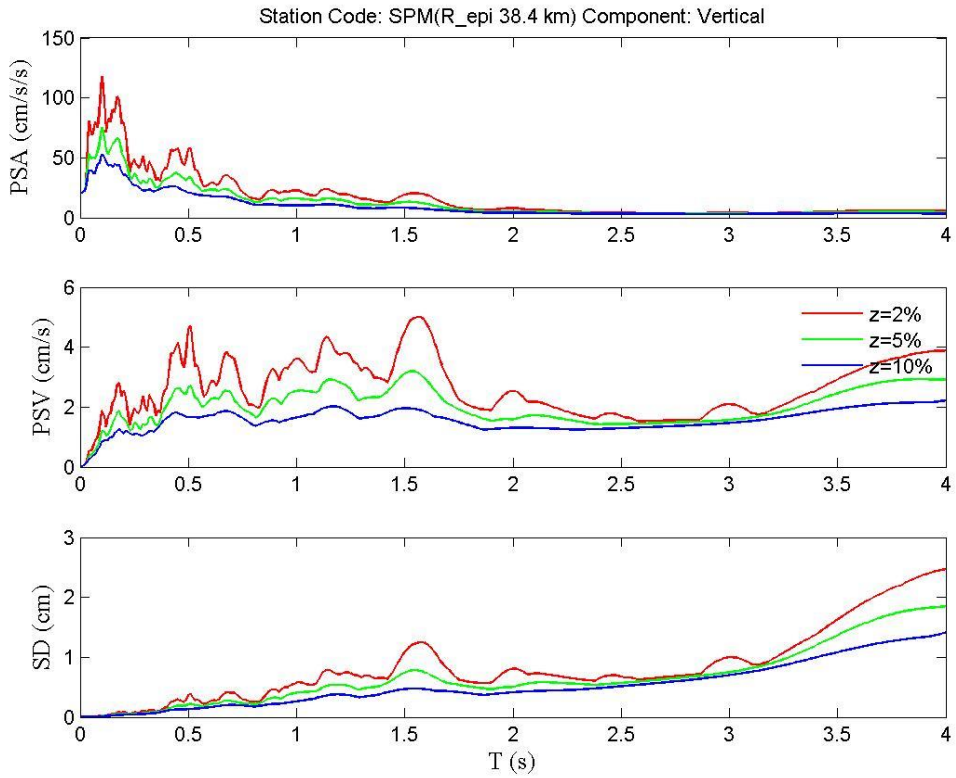
Station Code: SPM(R_epi 38.4 km) Component: Vertical
PSA (cm/s/s)
PSV (cm/s)
SD (cm)
z=2%
z=5%
z=10%
T (s)

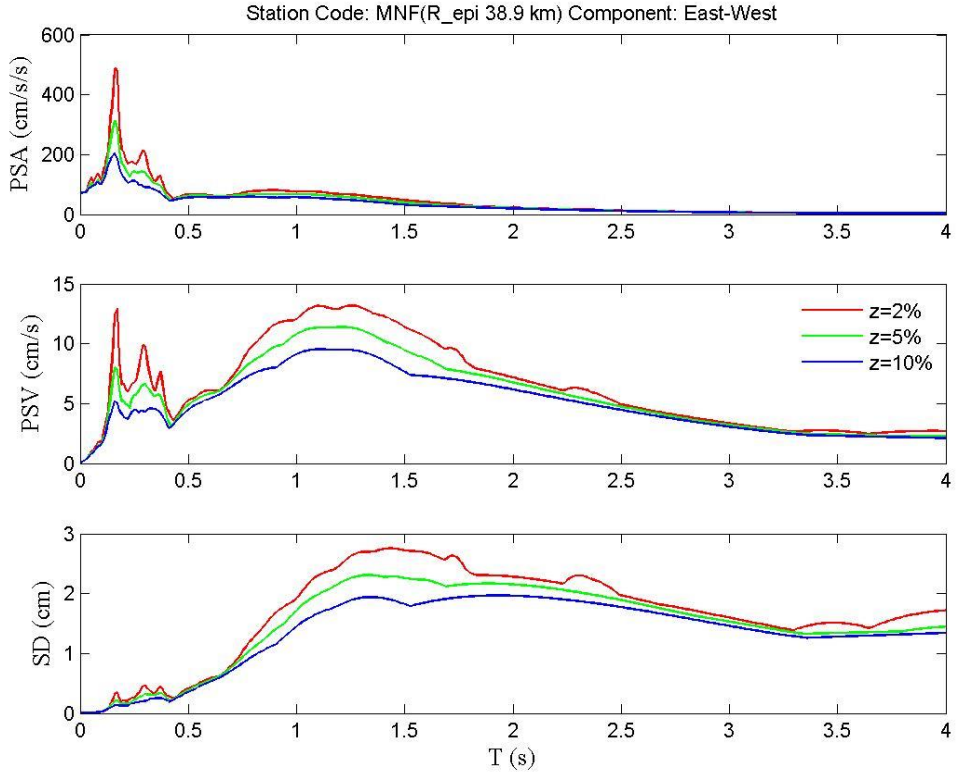
Station Code: MNF(R_epi 38.9 km) Component: East-West
PSA (cm/s/s)
PSV (cm/s)
SD (cm)
z=2%
z=5%
z=10%
T (s)

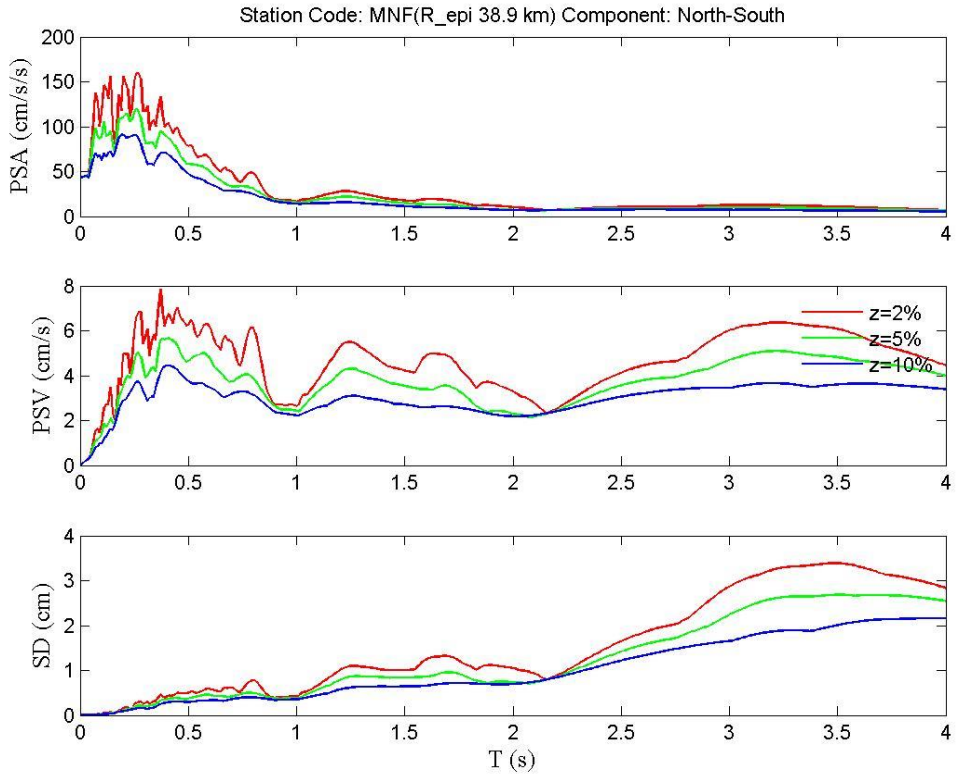
Station Code: MNF(R_epi 38.9 km) Component: North-South
PSA (cm/s/s)
PSV (cm/s)
SD (cm)
z=2%
z=5%
z=10%
T (s)

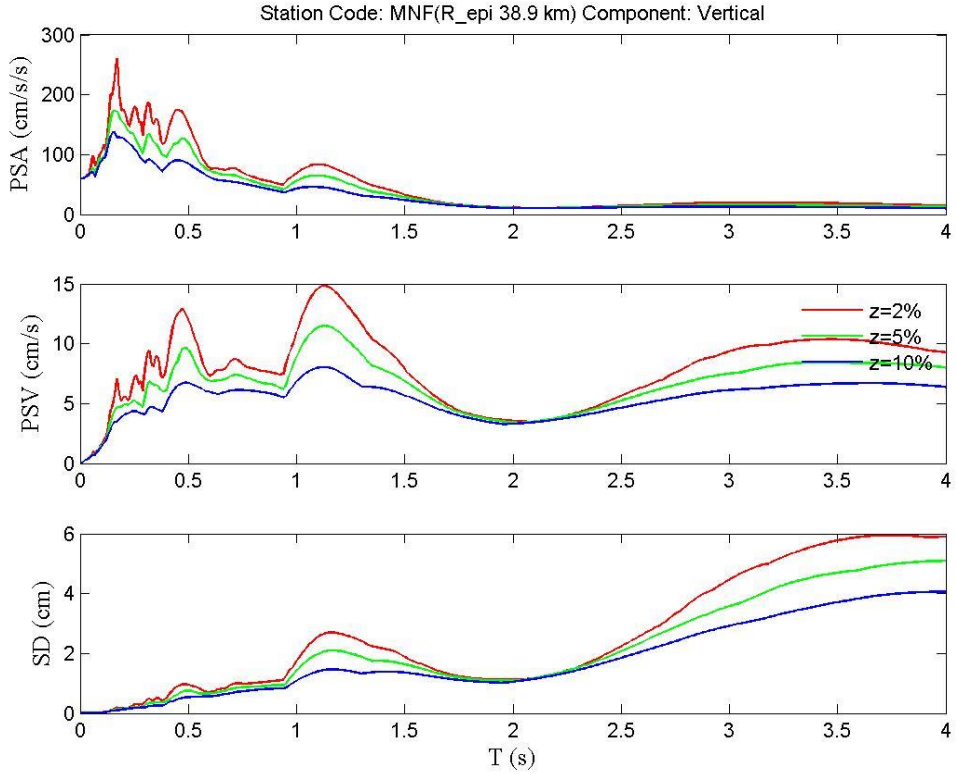
Station Code: MNF(R_epi 38.9 km) Component: Vertical
PSA (cm/s/s)
PSV (cm/s)
SD (cm)
z=2%
z=5%
z=10%
T (s)

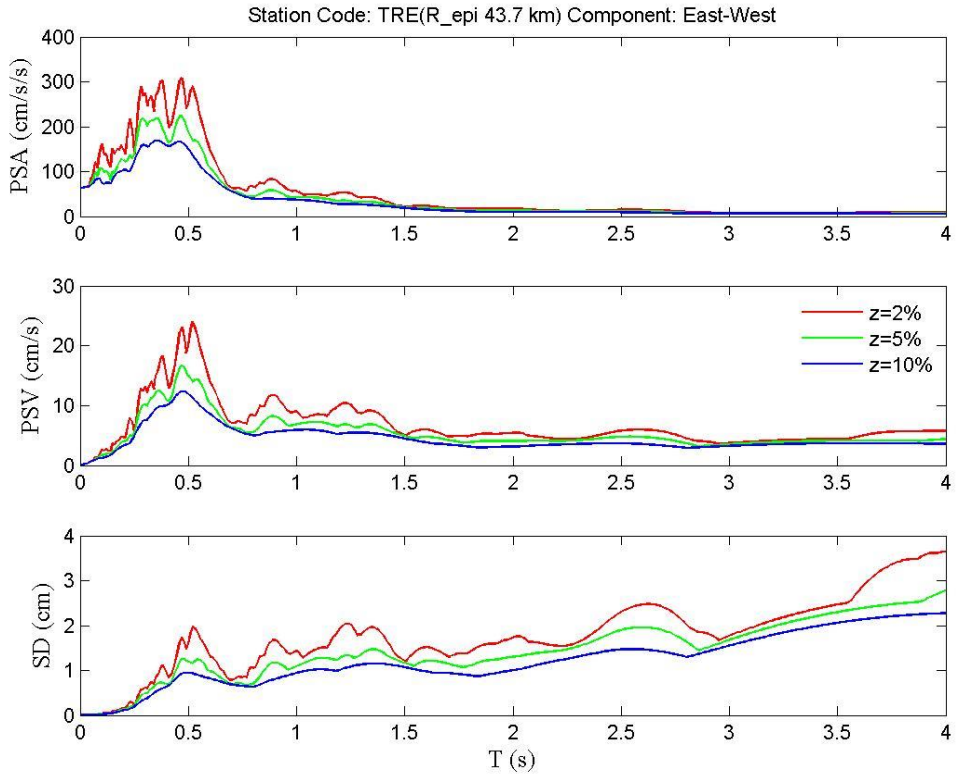
Station Code: TRE(R_epi 43.7 km) Component: East-West
PSA (cm/s/s)
PSV (cm/s)
SD (cm)
z=2%
z=5%
z=10%
T (s)

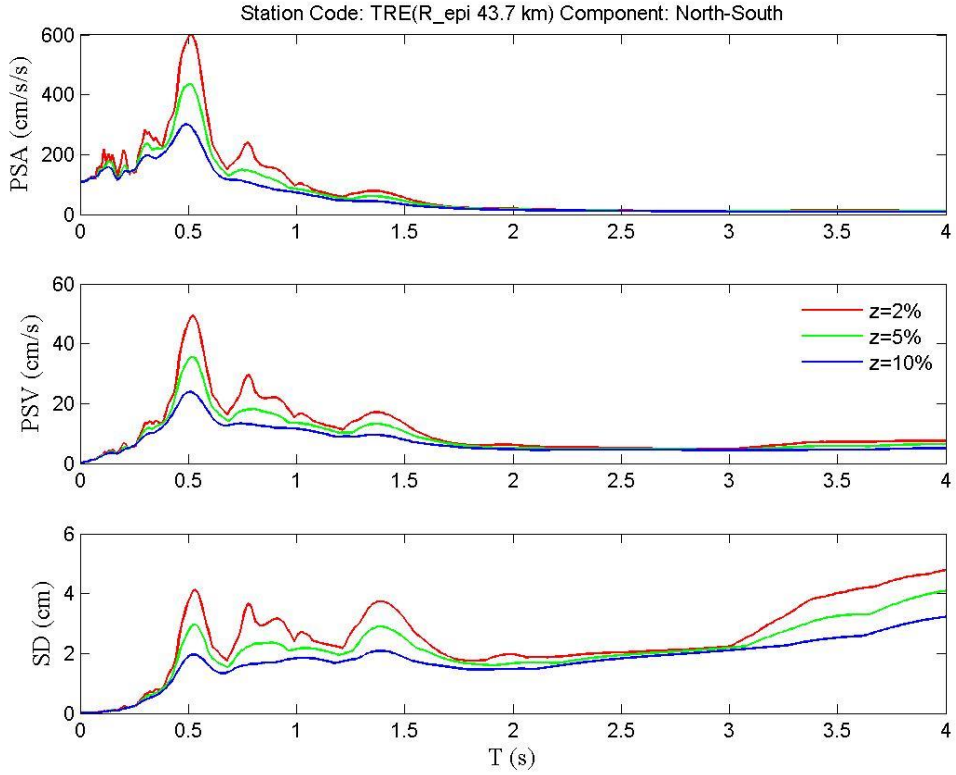
Station Code: TRE(R_epi 43.7 km) Component: North-South
PSA (cm/s/s)
PSV (cm/s)
SD (cm)
z=2%
z=5%
z=10%
T (s)

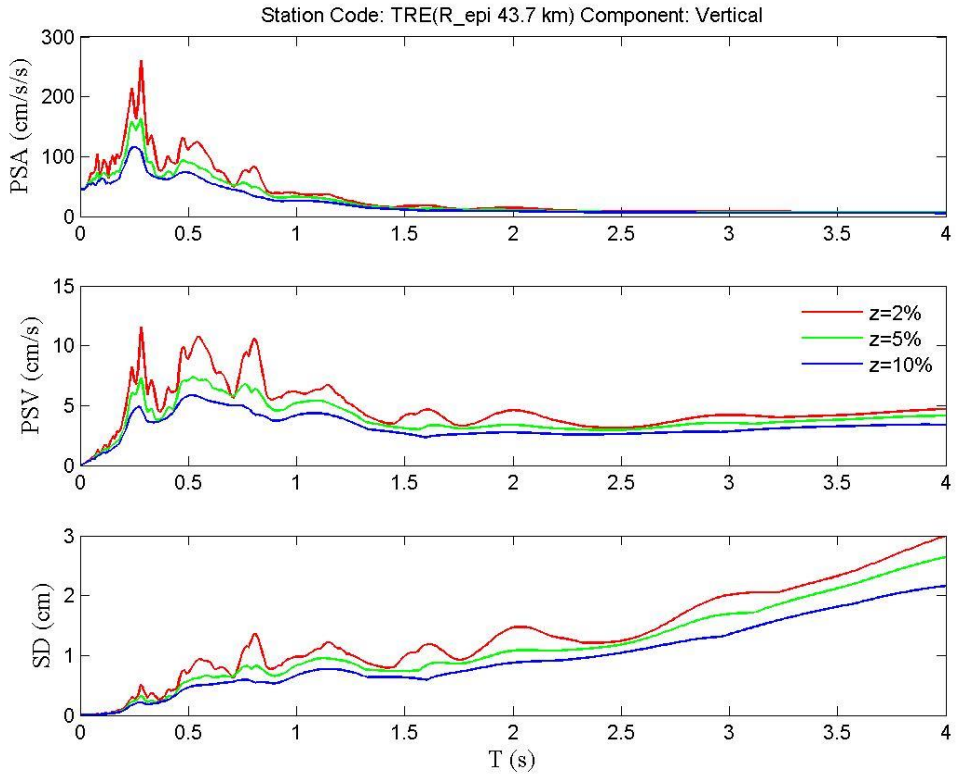
Station Code: TRE(R_epi 43.7 km) Component: Vertical
PSA (cm/s/s)
PSV (cm/s)
SD (cm)
z=2%
z=5%
z=10%
T (s)

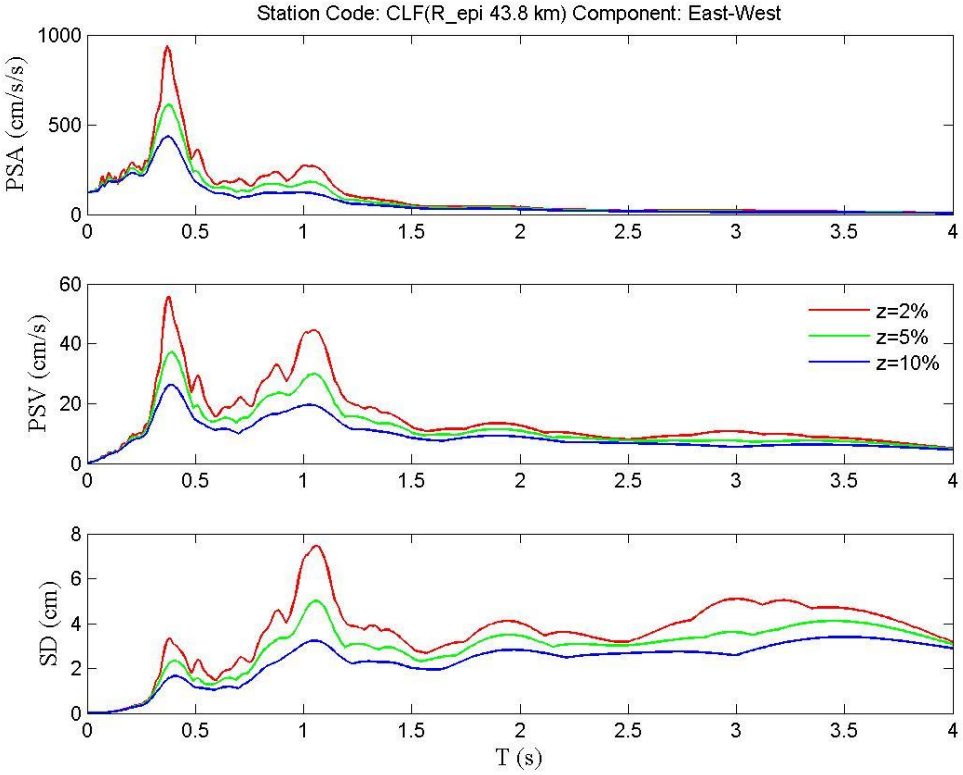
Station Code: CLF(R_epi 43.8 km) Component: East-West
PSA (cm/s/s)
PSV (cm/s)
SD (cm)
z=2%
z=5%
z=10%
T (s)

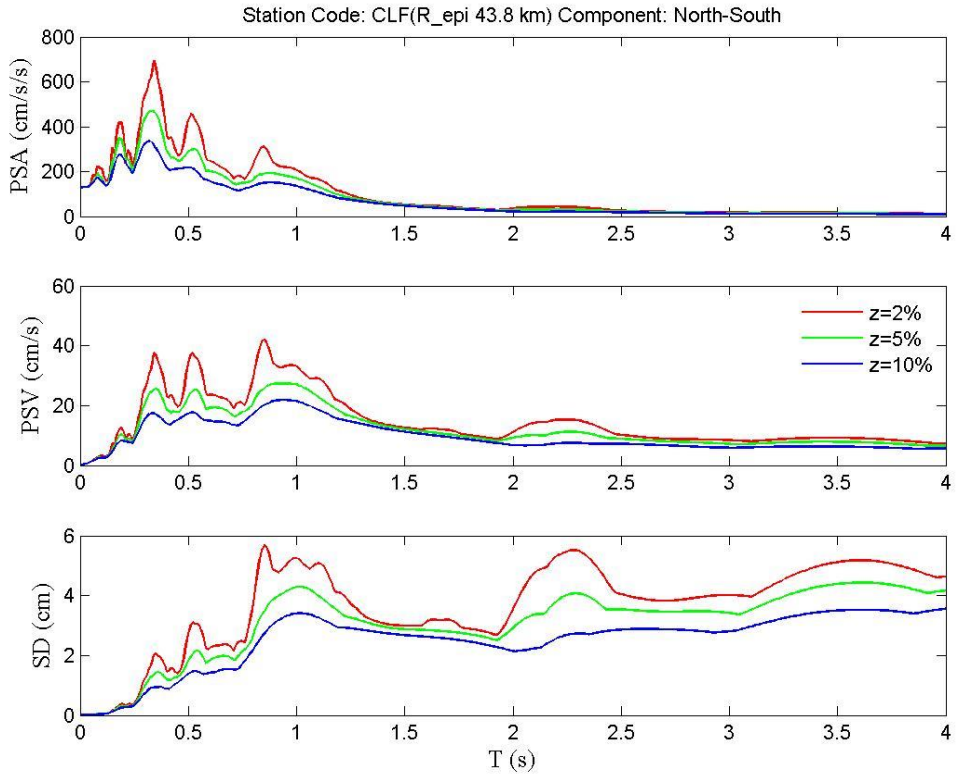
Station Code: CLF(R_epi 43.8 km) Component: North-South
PSA (cm/s/s)
PSV (cm/s)
SD (cm)
z=2%
z=5%
z=10%
T (s)

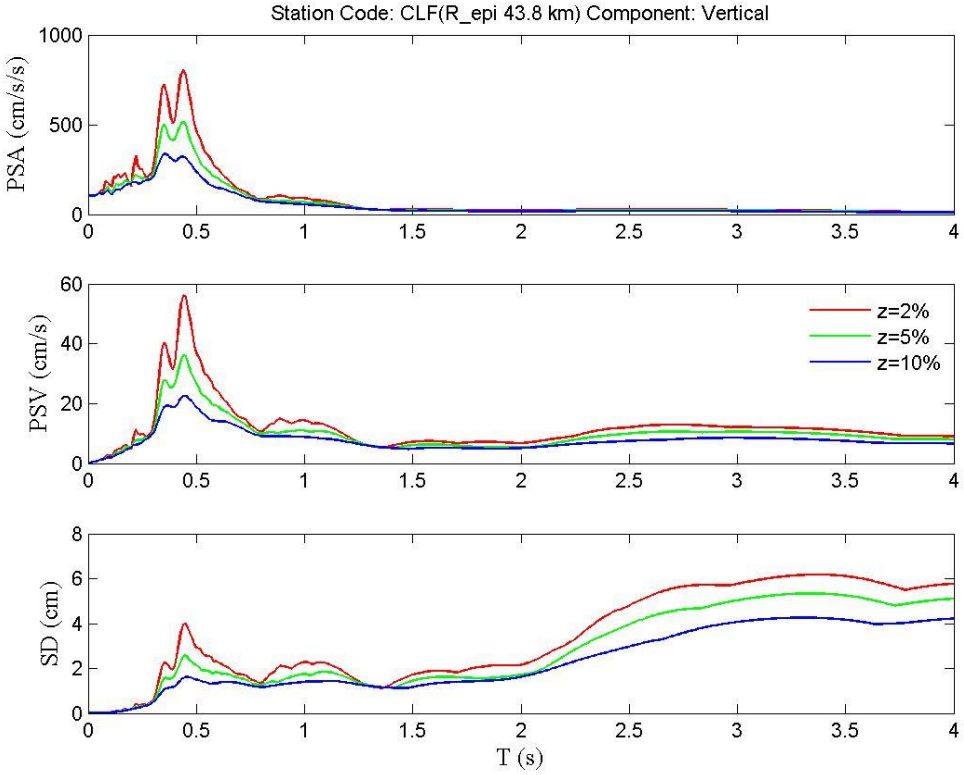
Station Code: CLF(R_epi 43.8 km) Component: Vertical
PSA (cm/s/s)
PSV (cm/s)
SD (cm)
z=2%
z=5%
z=10%
T (s)

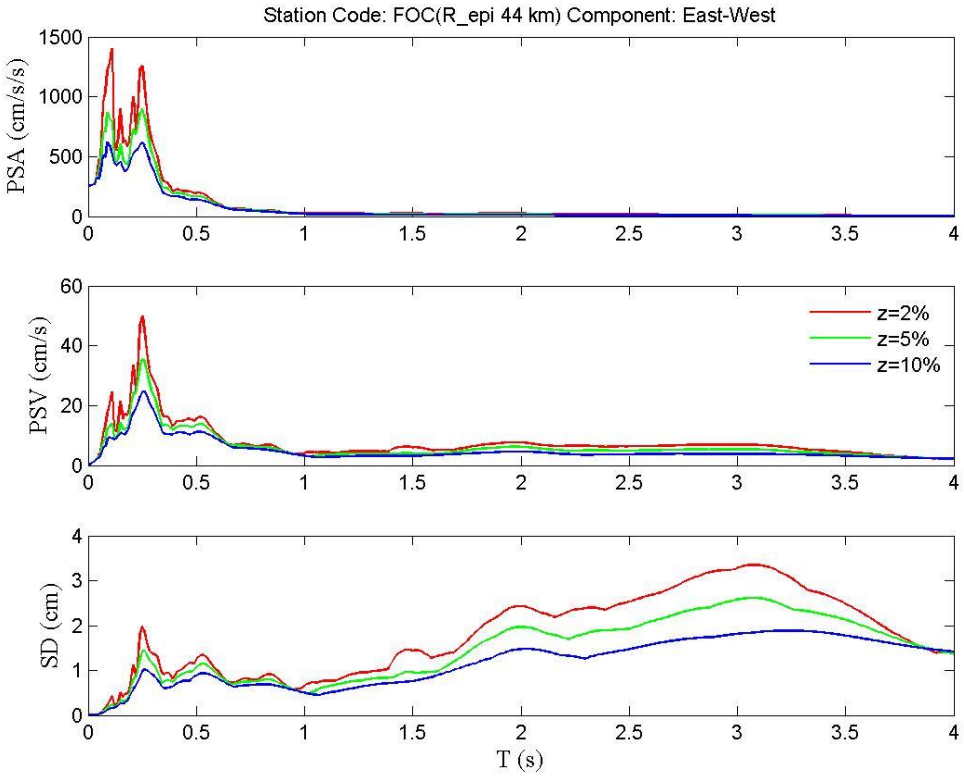
Station Code: FOC(R_epi 44 km) Component: East-West
PSA (cm/s/s)
PSV (cm/s)
SD (cm)
z=2%
z=5%
z=10%
T (s)

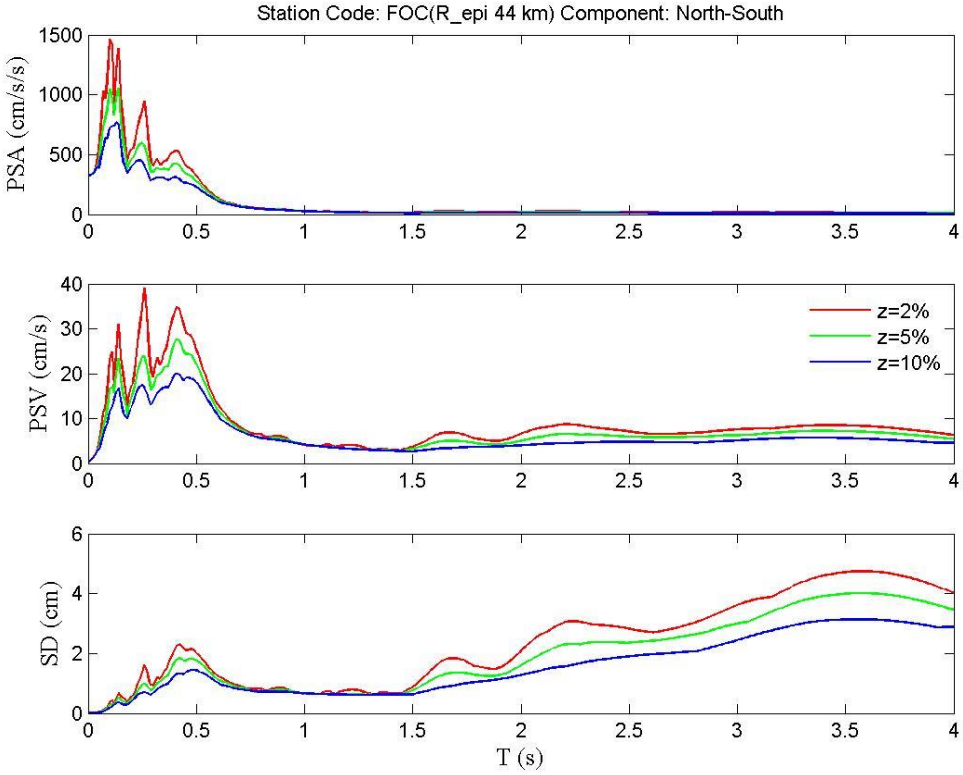
Station Code: FOC(R_epi 44 km) Component: North-South
PSA (cm/s/s)
PSV (cm/s)
SD (cm)
T (s)
z=2%
z=5%
z=10%

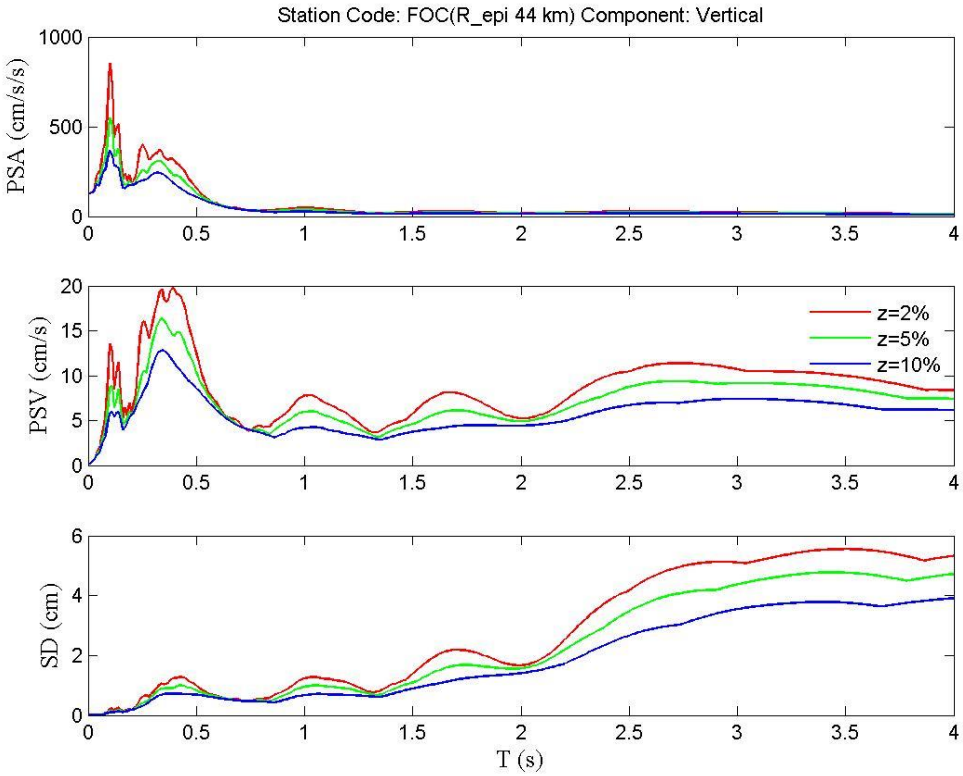
Station Code: FOC(R_epi 44 km) Component: Vertical
PSA (cm/s/s)
PSV (cm/s)
SD (cm)
T (s)
z=2%
z=5%
z=10%

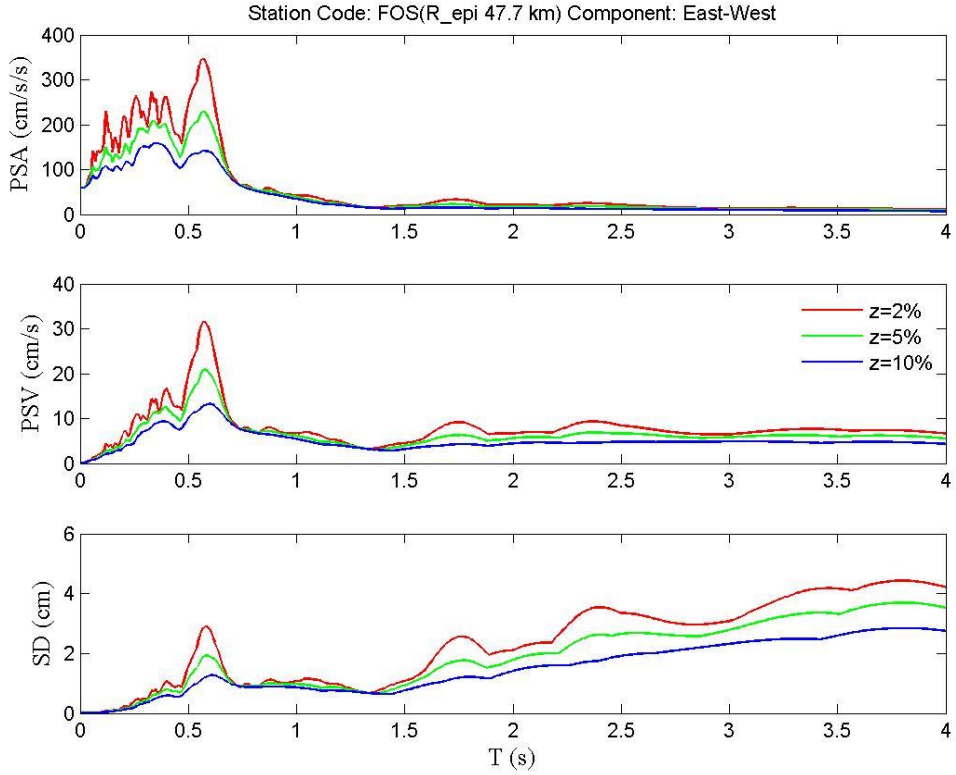
Station Code: FOS(R_epi 47.7 km) Component: East-West
PSA (cm/s/s)
PSV (cm/s)
SD (cm)
z=2%
z=5%
z=10%
T (s)

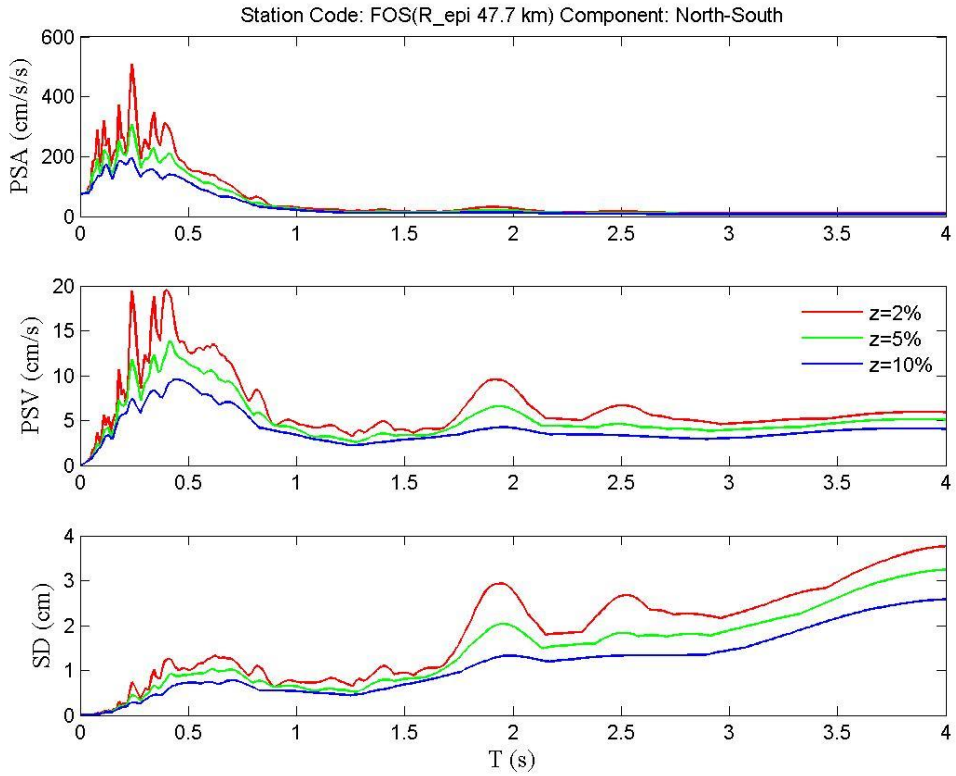
Station Code: FOS(R_epi 47.7 km) Component: North-South
PSA (cm/s/s)
PSV (cm/s)
SD (cm)
z=2%
z=5%
z=10%
T (s)

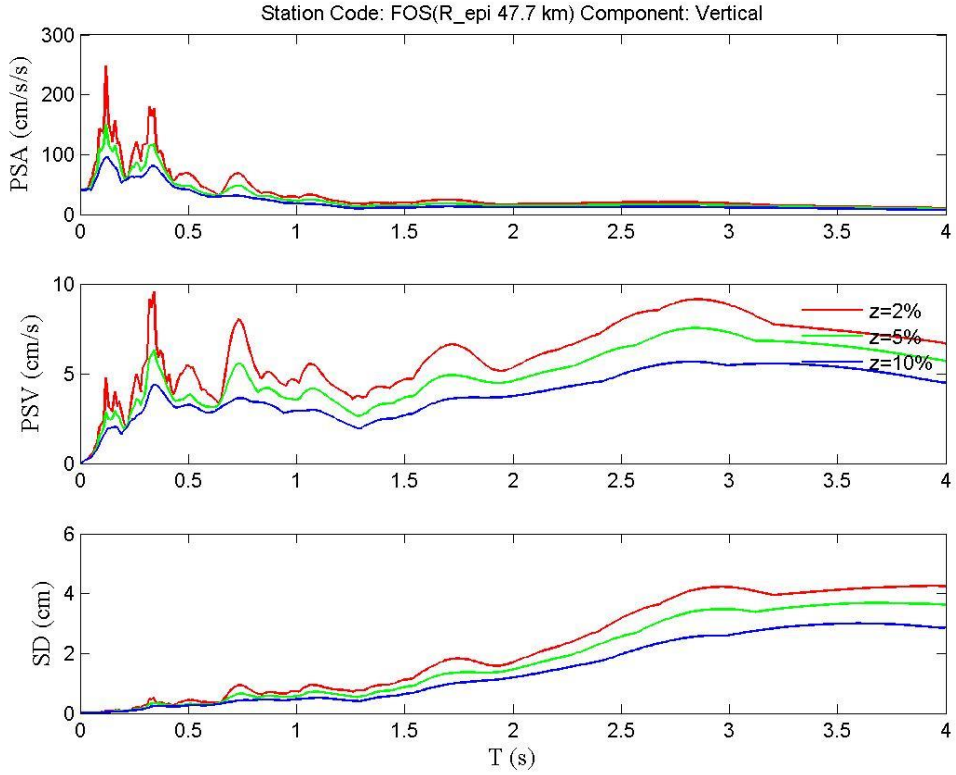
Station Code: FOS(R_epi 47.7 km) Component: Vertical
PSA (cm/s/s)
PSV (cm/s)
SD (cm)
z=2%
z=5%
z=10%
T (s)

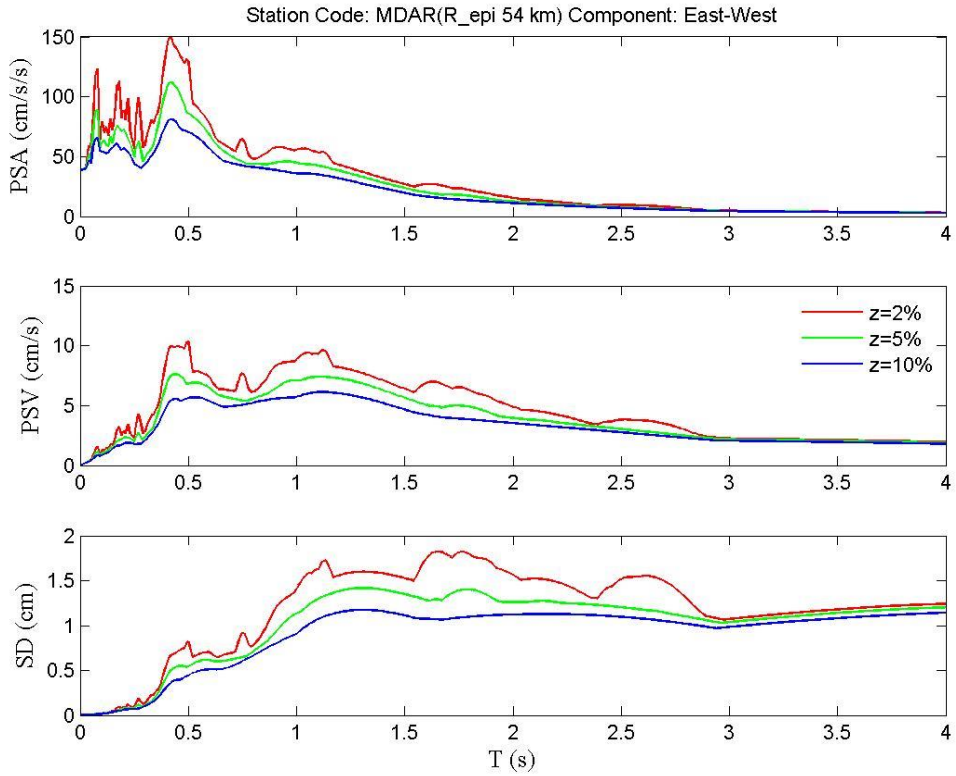
Station Code: MDAR(R_epi 54 km) Component: East-West
PSA (cm/s/s)
PSV (cm/s)
SD (cm)
z=2%
z=5%
z=10%
T (s)

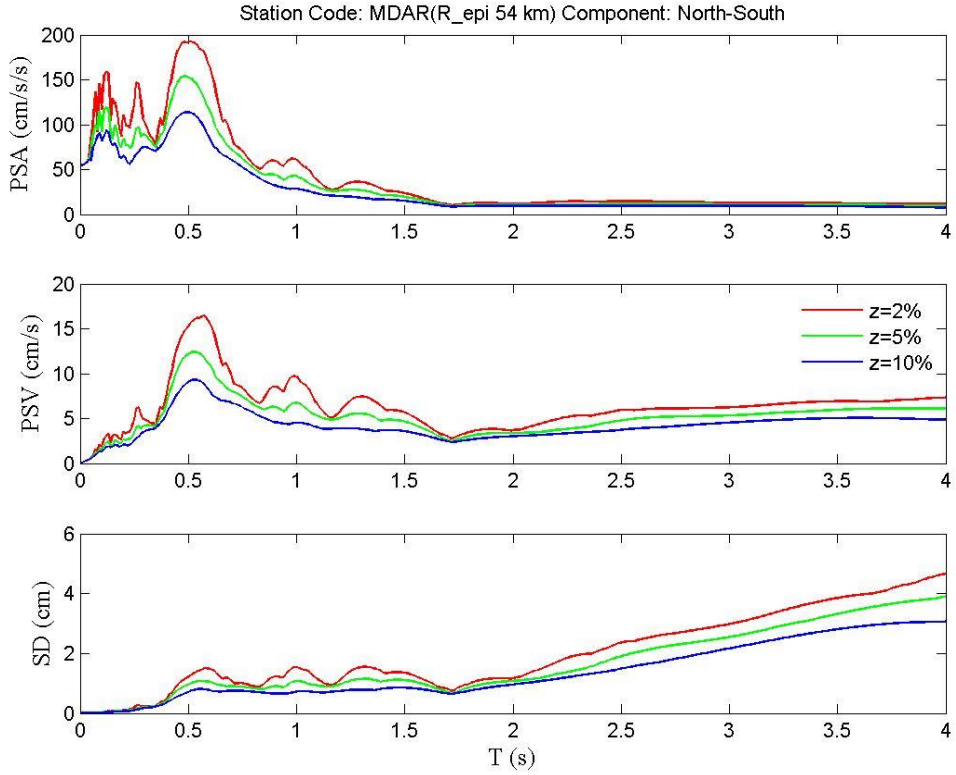
Station Code: MDAR(R_epi 54 km) Component: North-South
PSA (cm/s/s)
PSV (cm/s)
SD (cm)
z=2%
z=5%
z=10%
T (s)

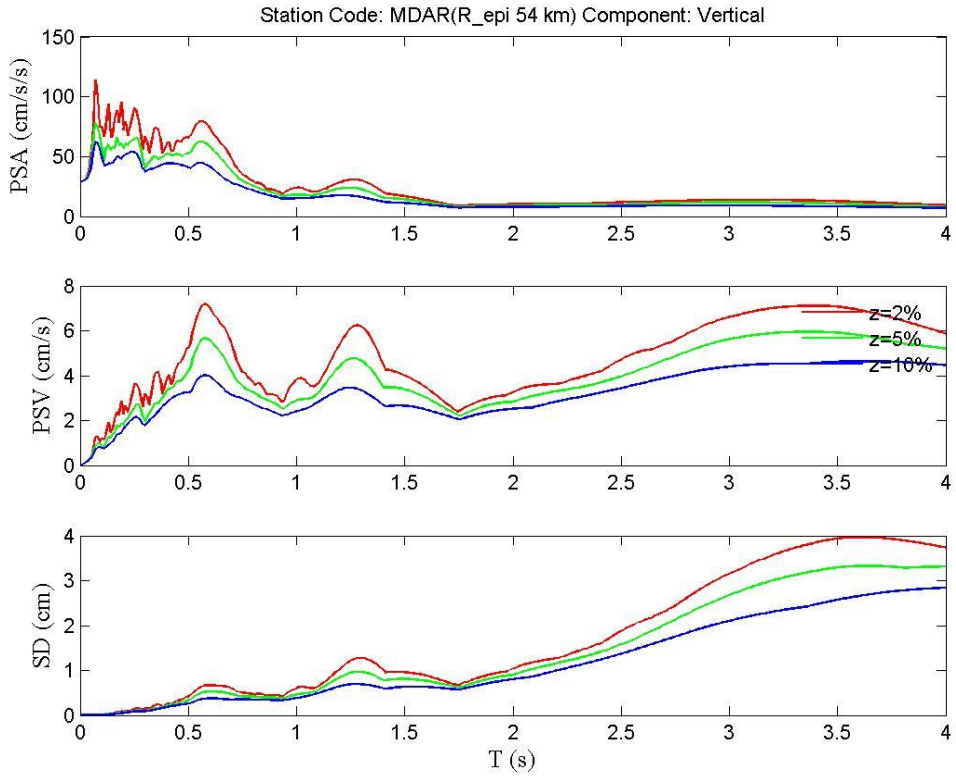
Station Code: MDAR(R_epi 54 km) Component: Vertical
PSA (cm/s/s)
PSV (cm/s)
SD (cm)
z=2%
z=5%
z=10%
T (s)

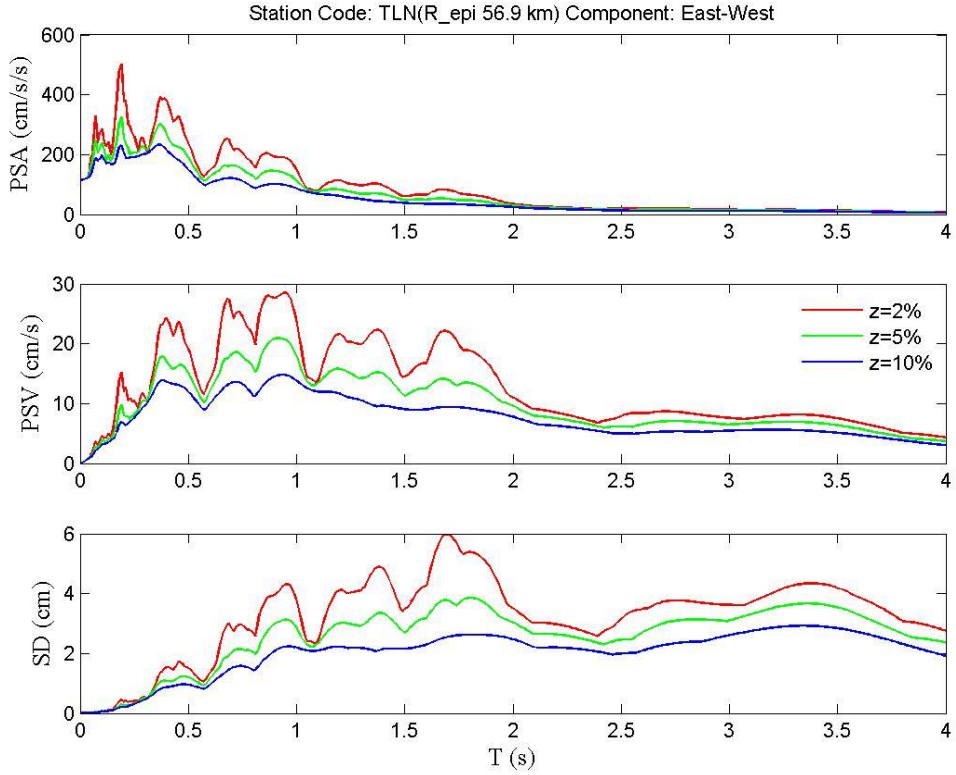
Station Code: TLN(R_epi 56.9 km) Component: East-West
PSA (cm/s/s)
PSV (cm/s)
SD (cm)
T (s)
z=2%
z=5%
z=10%

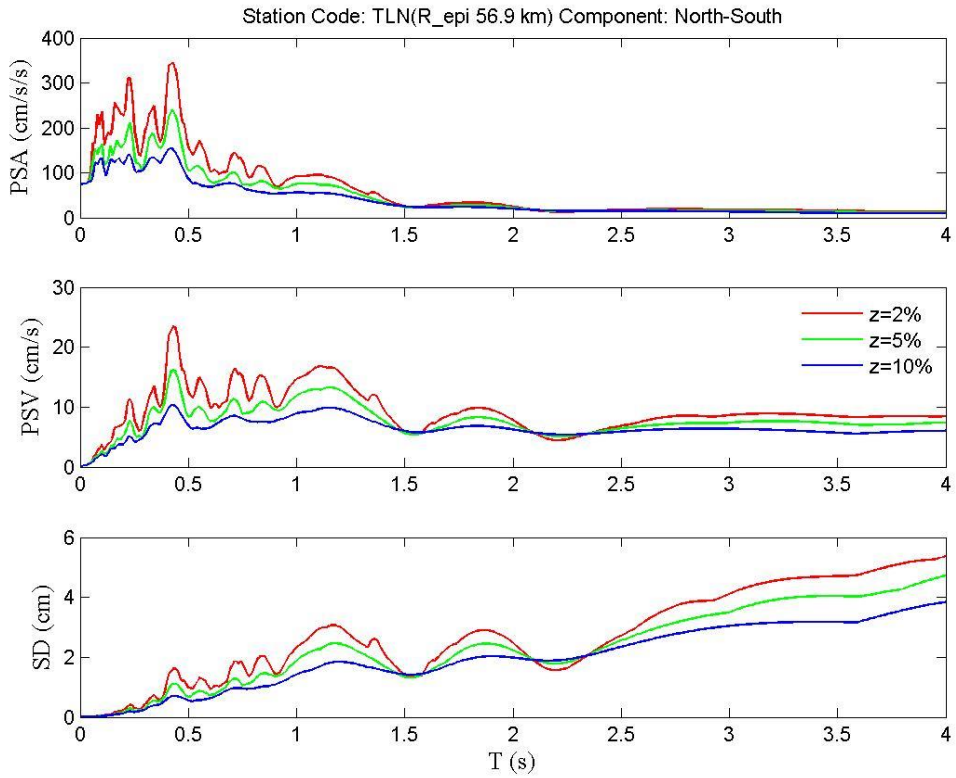
Station Code: TLN(R_epi 56.9 km) Component: North-South
PSA (cm/s/s)
PSV (cm/s)
SD (cm)
T (s)
z=2%
z=5%
z=10%

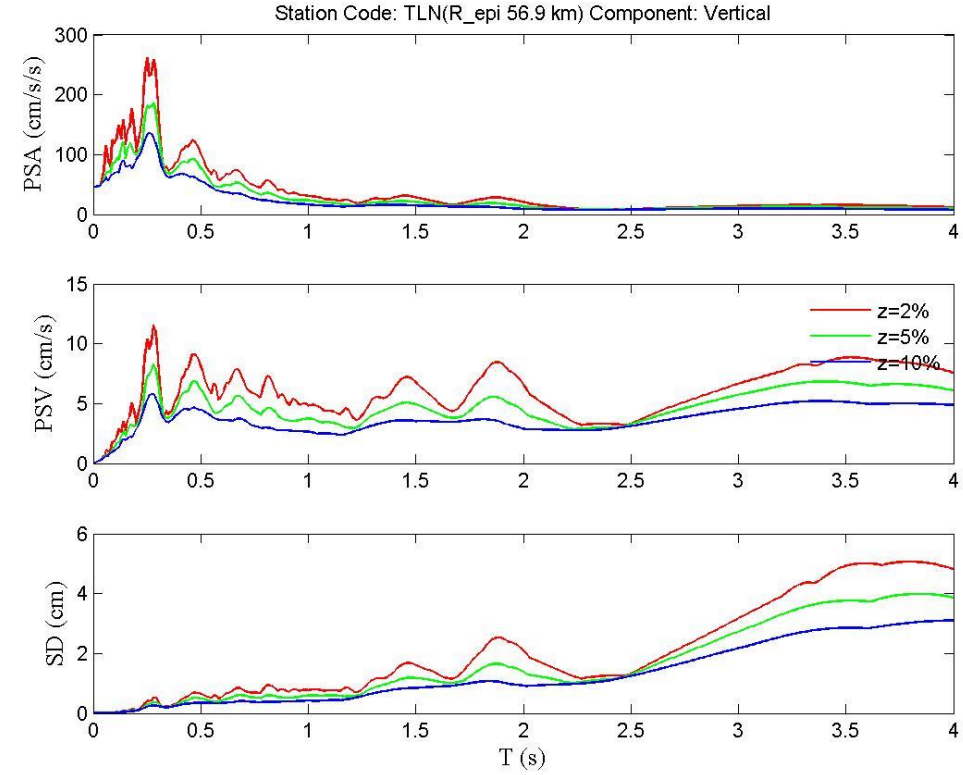
Station Code: TLN(R_epi 56.9 km) Component: Vertical
PSA (cm/s/s)
PSV (cm/s)
SD (cm)
z=2%
z=5%
z=10%
T (s)

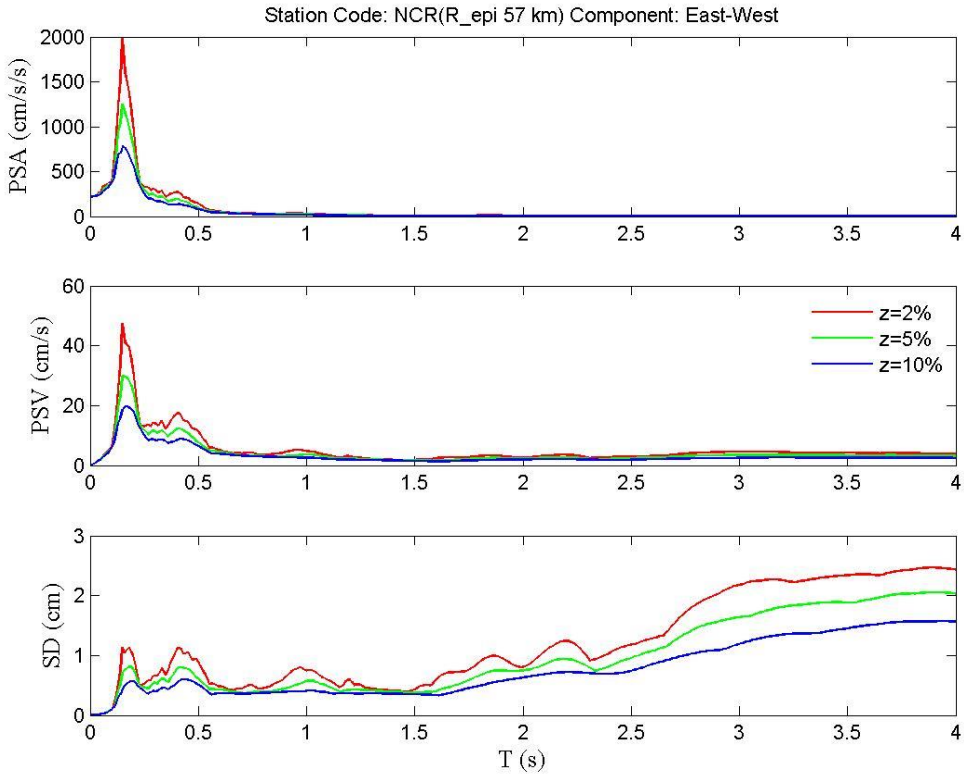
Station Code: NCR(R_epi 57 km) Component: East-West
PSA (cm/s/s)
PSV (cm/s)
SD (cm)
z=2%
z=5%
z=10%
T (s)

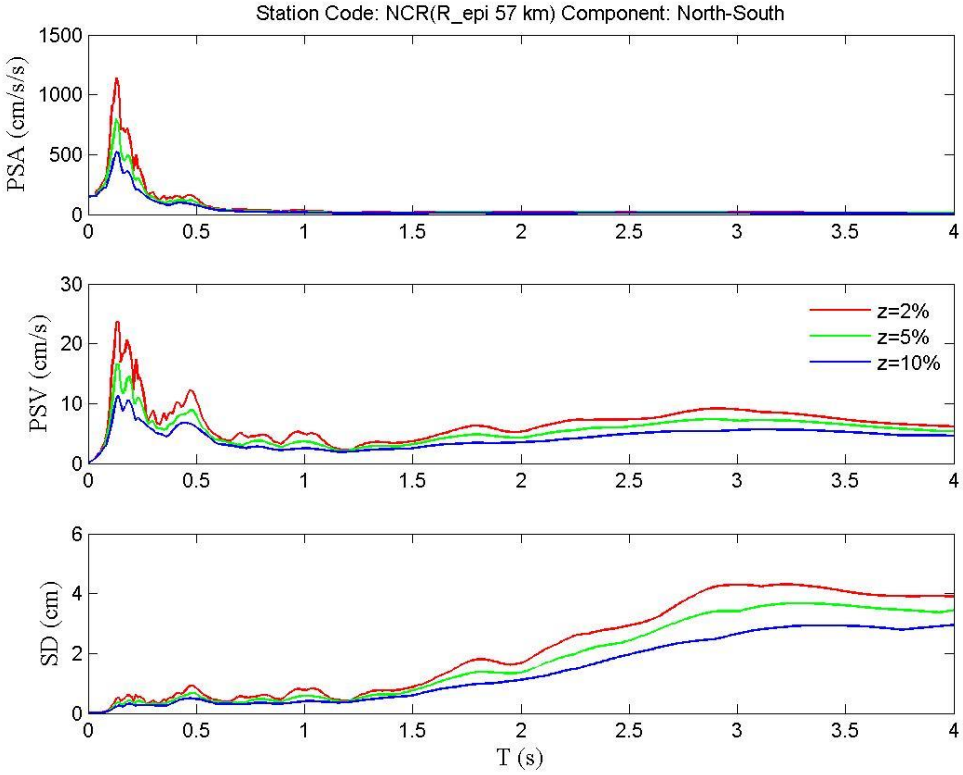
Station Code: NCR(R_epi 57 km) Component: North-South
PSA (cm/s/s)
PSV (cm/s)
SD (cm)
z=2%
z=5%
z=10%
T (s)

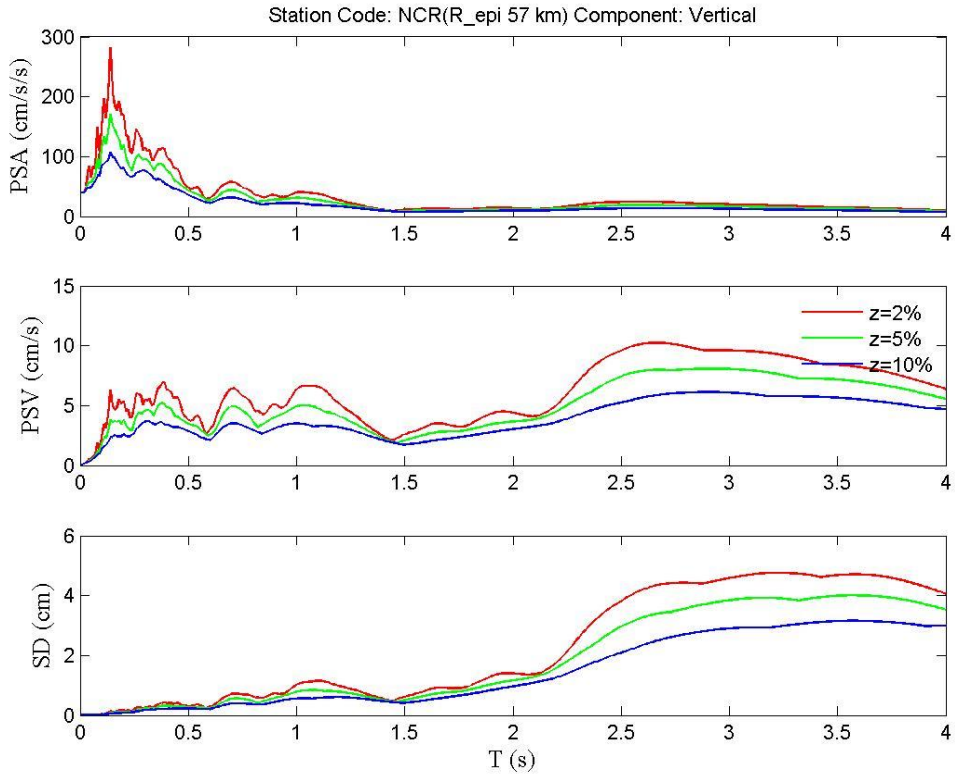
Station Code: NCR(R_epi 57 km) Component: Vertical
PSA (cm/s/s)
PSV (cm/s)
SD (cm)
z=2%
z=5%
z=10%
T (s)

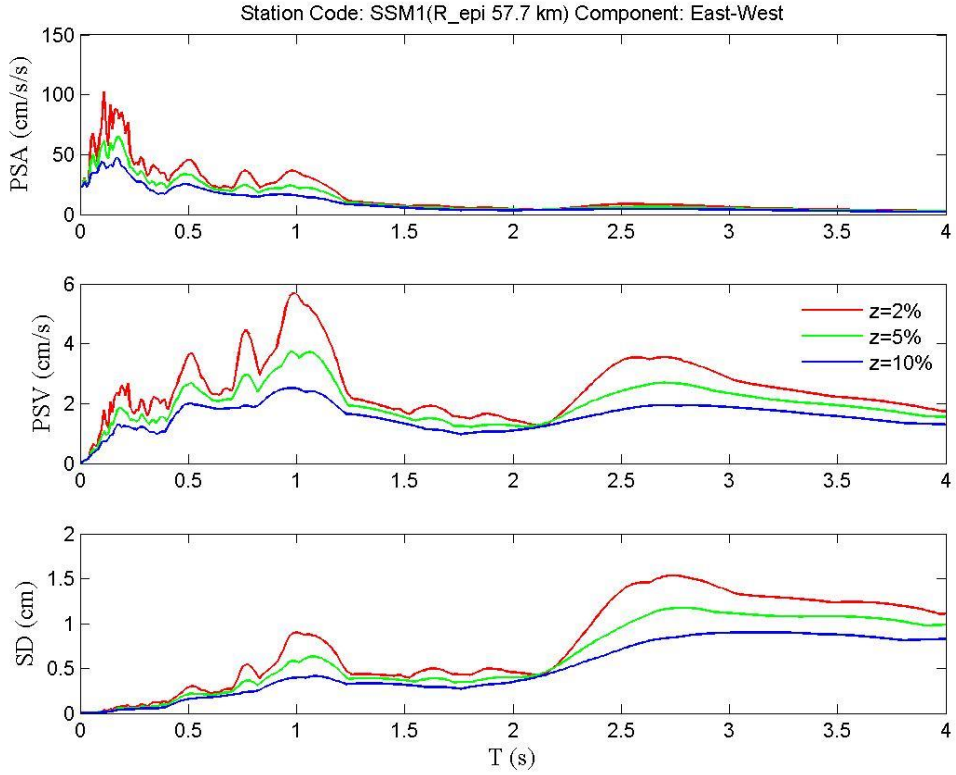
Station Code: SSM1(R_epi 57.7 km) Component: East-West
PSA (cm/s/s)
PSV (cm/s)
SD (cm)
z=2%
z=5%
z=10%
T (s)

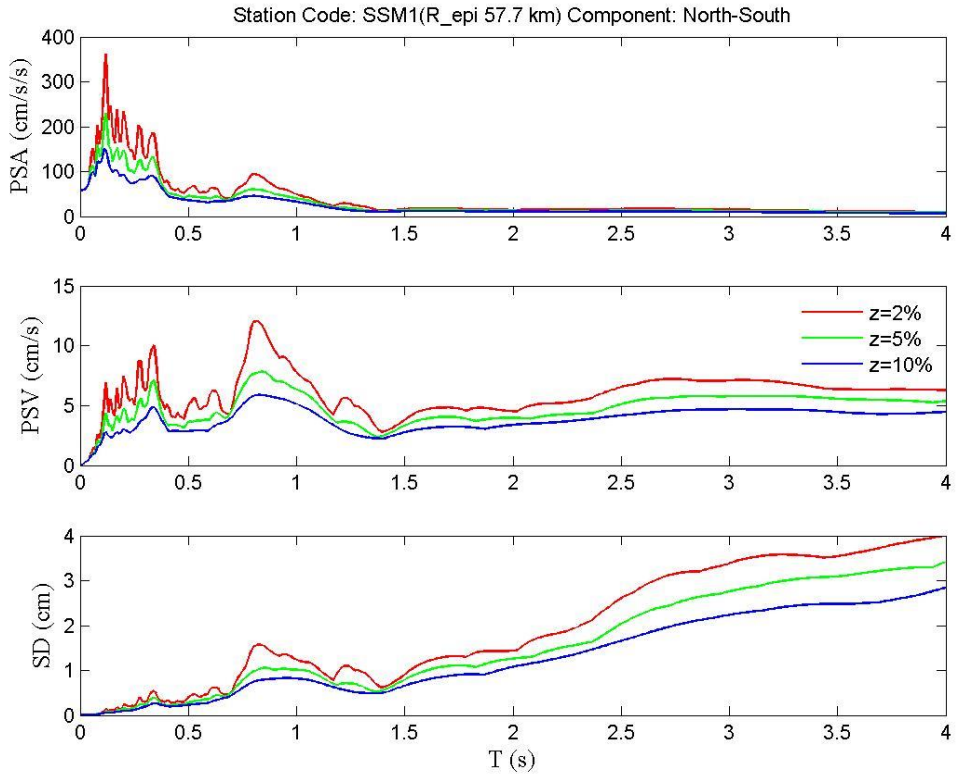
Station Code: SSM1(R_epi 57.7 km) Component: North-South
PSA (cm/s/s)
PSV (cm/s)
SD (cm)
z=2%
z=5%
z=10%
T (s)

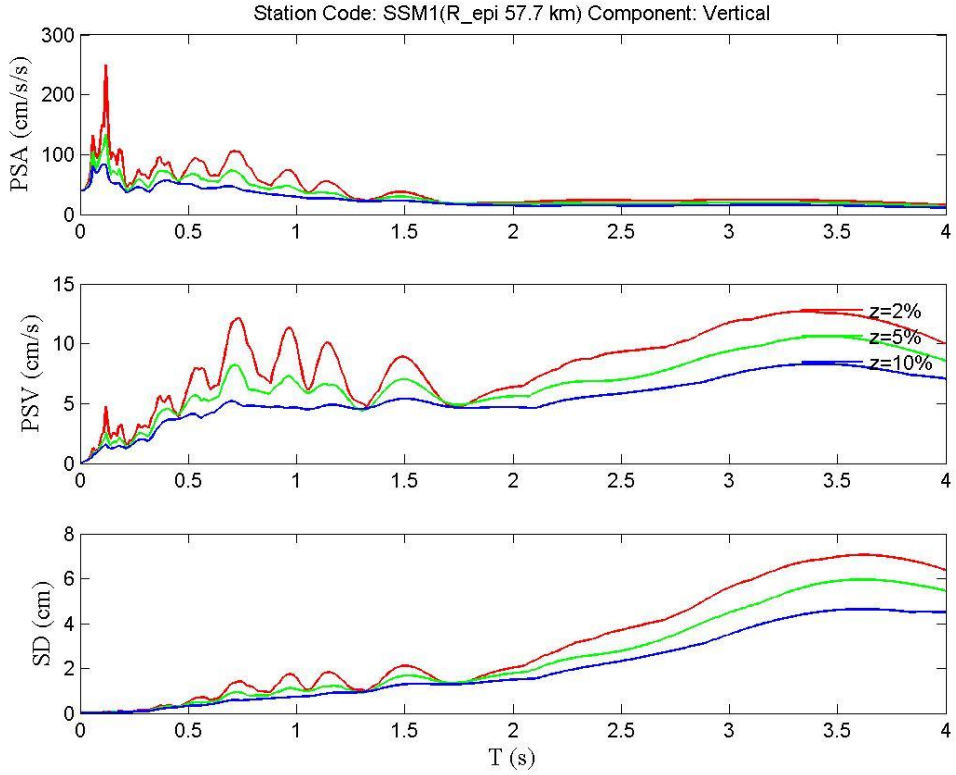
Station Code: SSM1(R_epi 57.7 km) Component: Vertical
PSA (cm/s/s)
PSV (cm/s)
SD (cm)
z=2%
z=5%
z=10%
T (s)

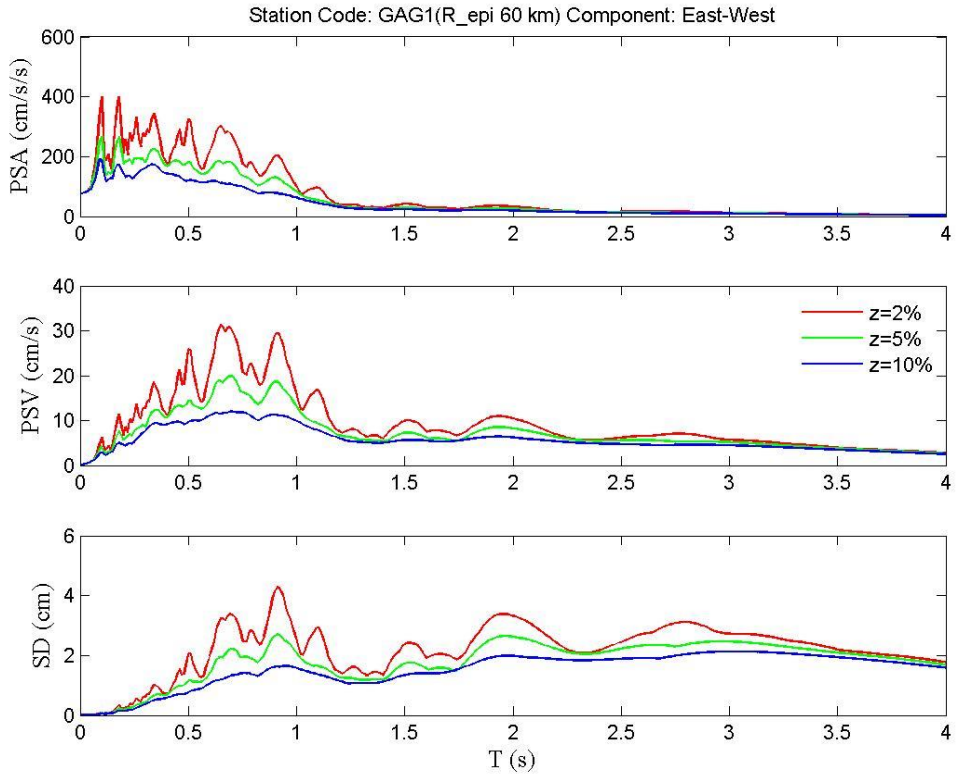
Station Code: GAG1(R_epi 60 km) Component: East-West
PSA (cm/s/s)
PSV (cm/s)
SD (cm)
z=2%
z=5%
z=10%
T (s)

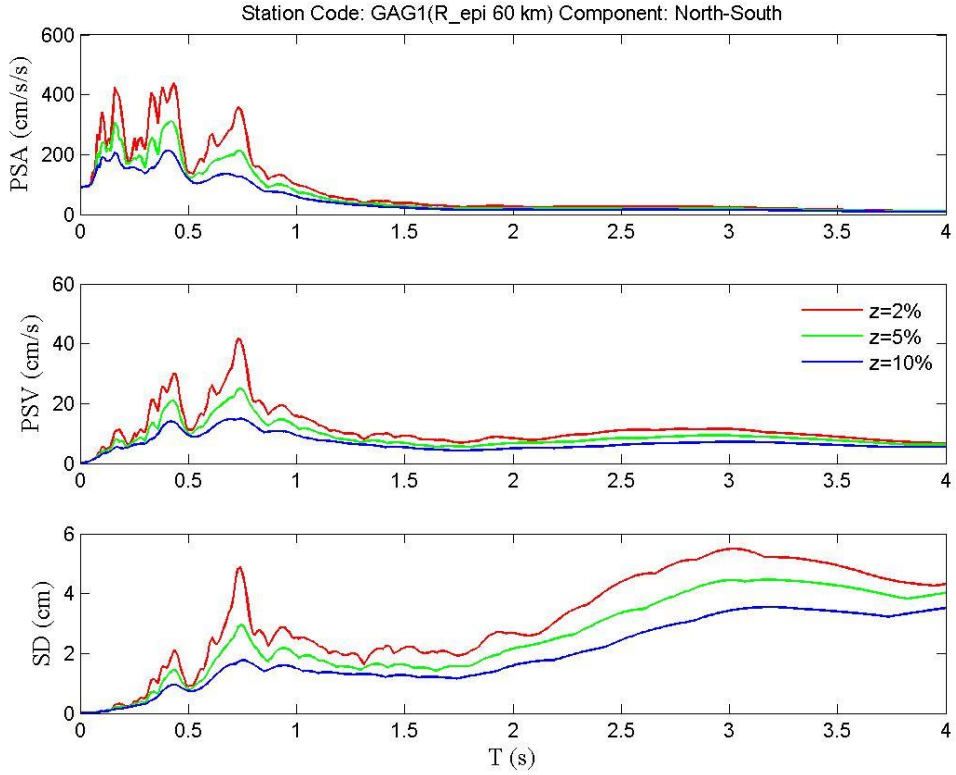
Station Code: GAG1(R_epi 60 km) Component: North-South
PSA (cm/s/s)
PSV (cm/s)
SD (cm)
z=2%
z=5%
z=10%
T (s)

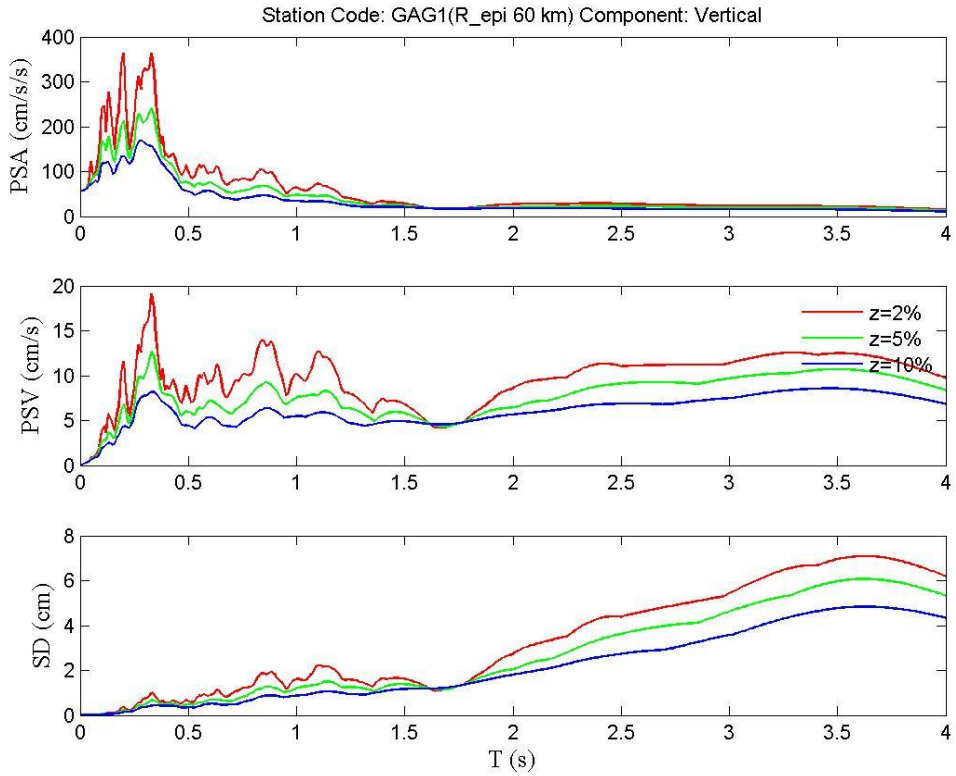
Station Code: GAG1(R_epi 60 km) Component: Vertical
PSA (cm/s/s)
PSV (cm/s)
SD (cm)
z=2%
z=5%
z=10%
T (s)

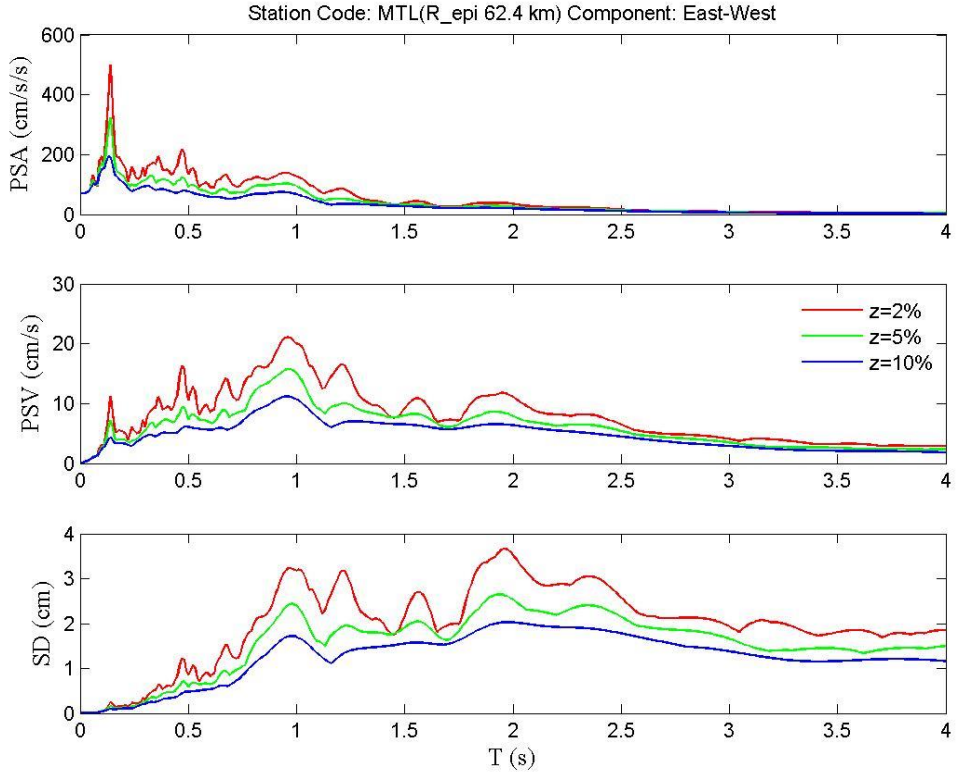
Station Code: MTL(R_epi 62.4 km) Component: East-West
PSA (cm/s/s)
PSV (cm/s)
SD (cm)
z=2%
z=5%
z=10%
T (s)

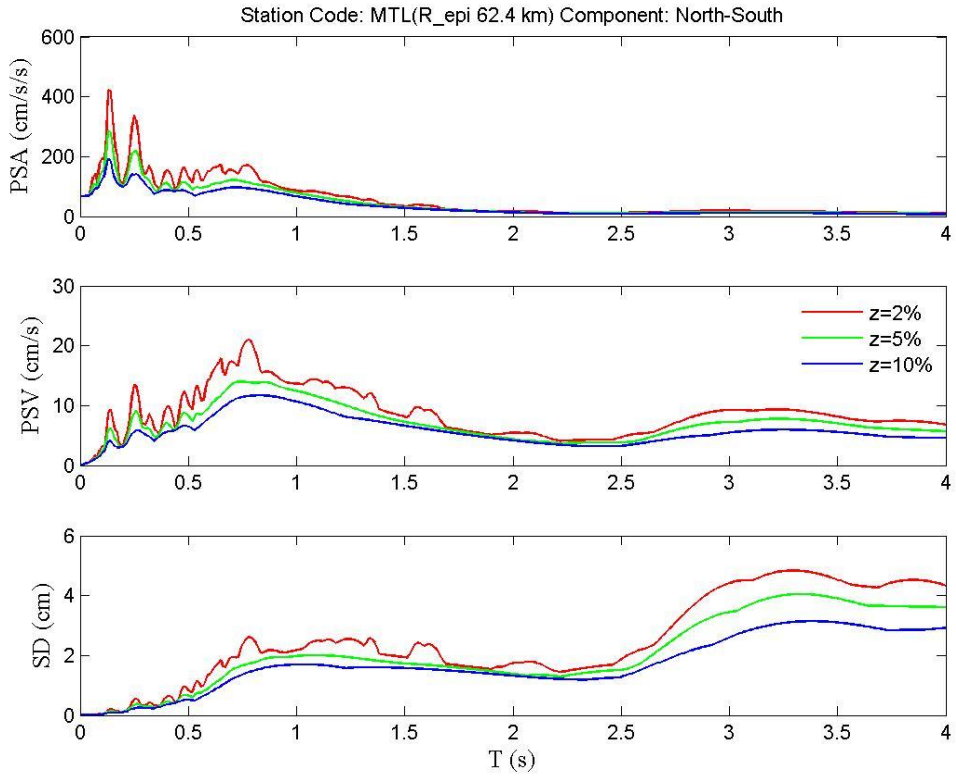
Station Code: MTL(R_epi 62.4 km) Component: North-South
PSA (cm/s/s)
PSV (cm/s)
SD (cm)
z=2%
z=5%
z=10%
T (s)

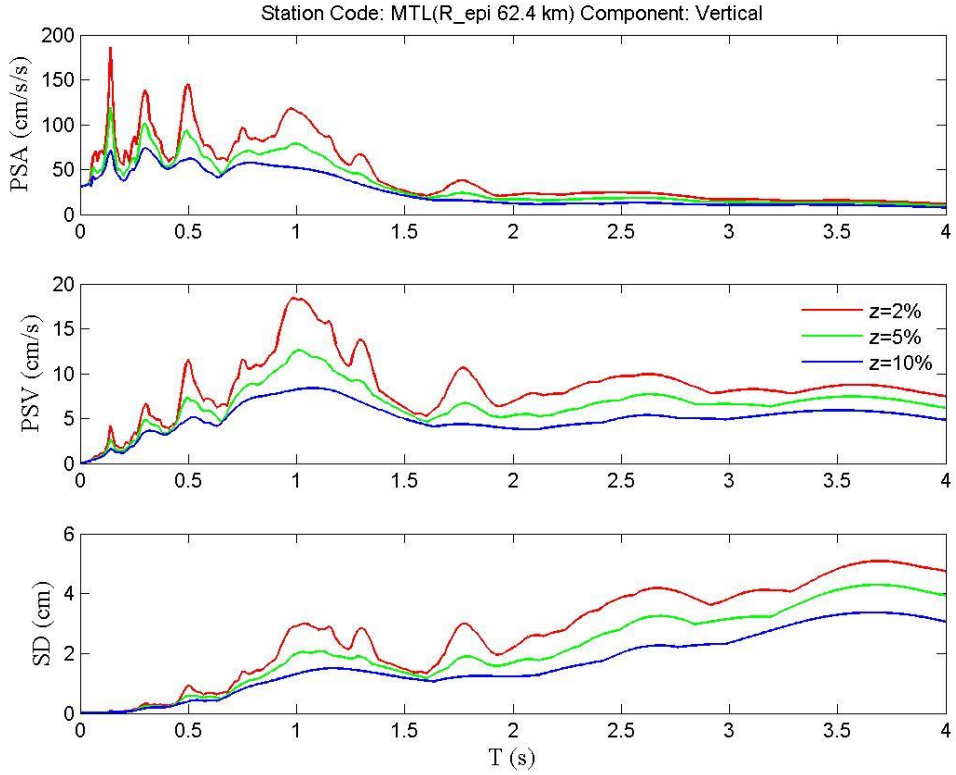
Station Code: MTL(R_epi 62.4 km) Component: Vertical
PSA (cm/s/s)
PSV (cm/s)
SD (cm)
z=2%
z=5%
z=10%
T (s)

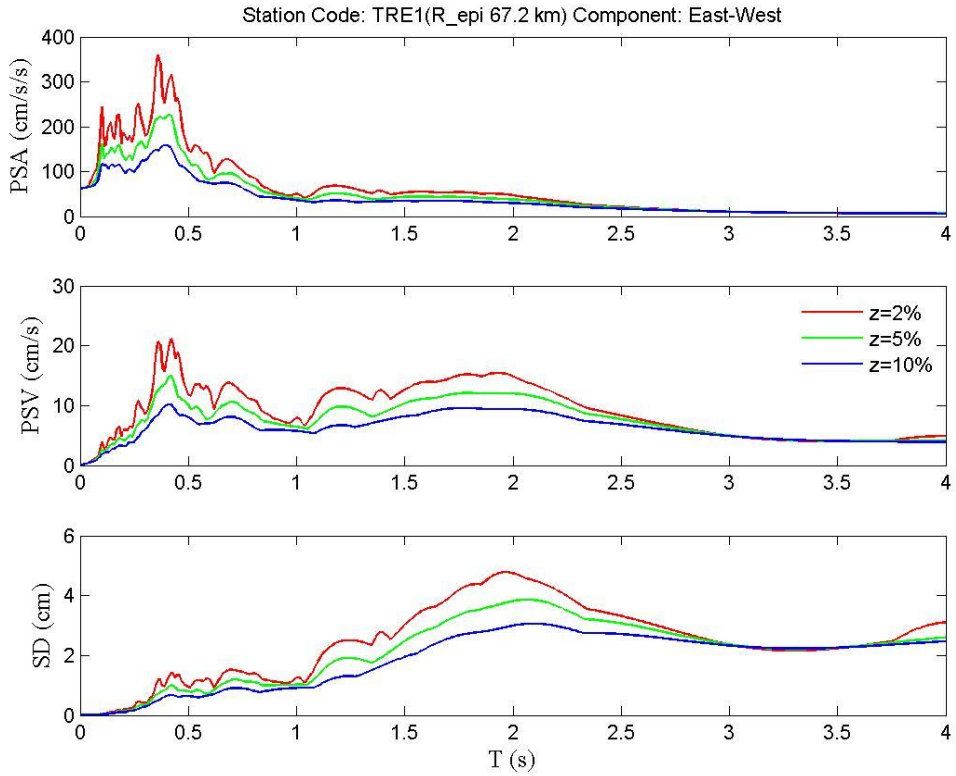
Station Code: TRE1(R_epi 67.2 km) Component: East-West
PSA (cm/s/s)
PSV (cm/s)
SD (cm)
z=2%
z=5%
z=10%
T (s)

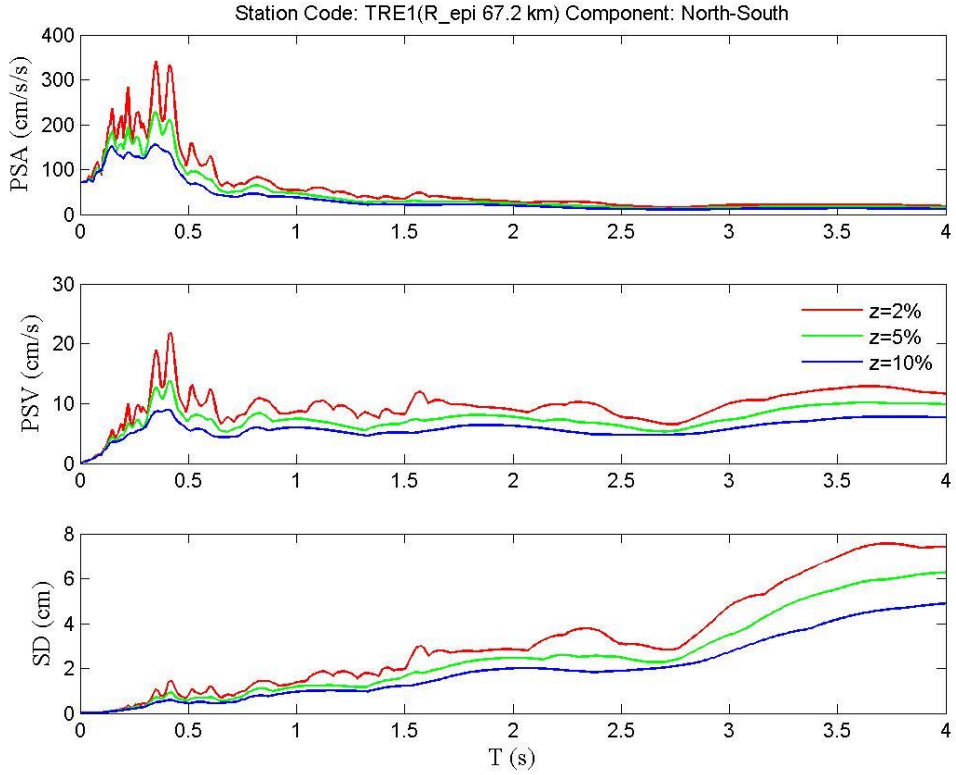
Station Code: TRE1(R_epi 67.2 km) Component: North-South
PSA (cm/s/s)
PSV (cm/s)
SD (cm)
z=2%
z=5%
z=10%
T (s)

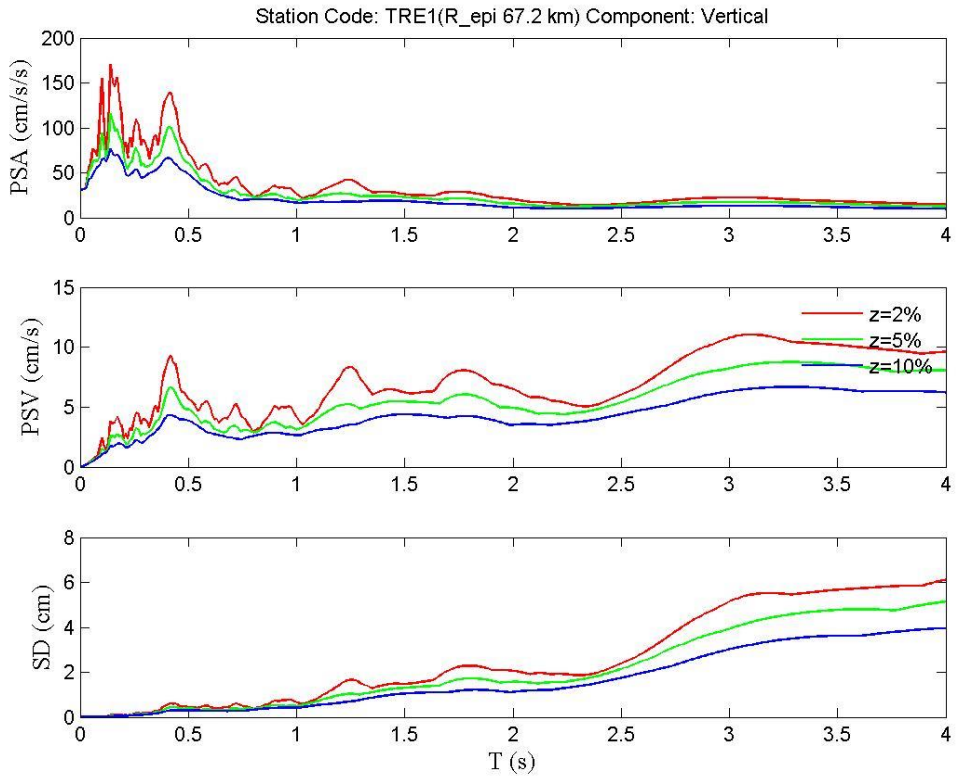
Station Code: TRE1(R_epi 67.2 km) Component: Vertical
PSA (cm/s/s)
PSV (cm/s)
SD (cm)
z=2%
z=5%
z=10%
T (s)

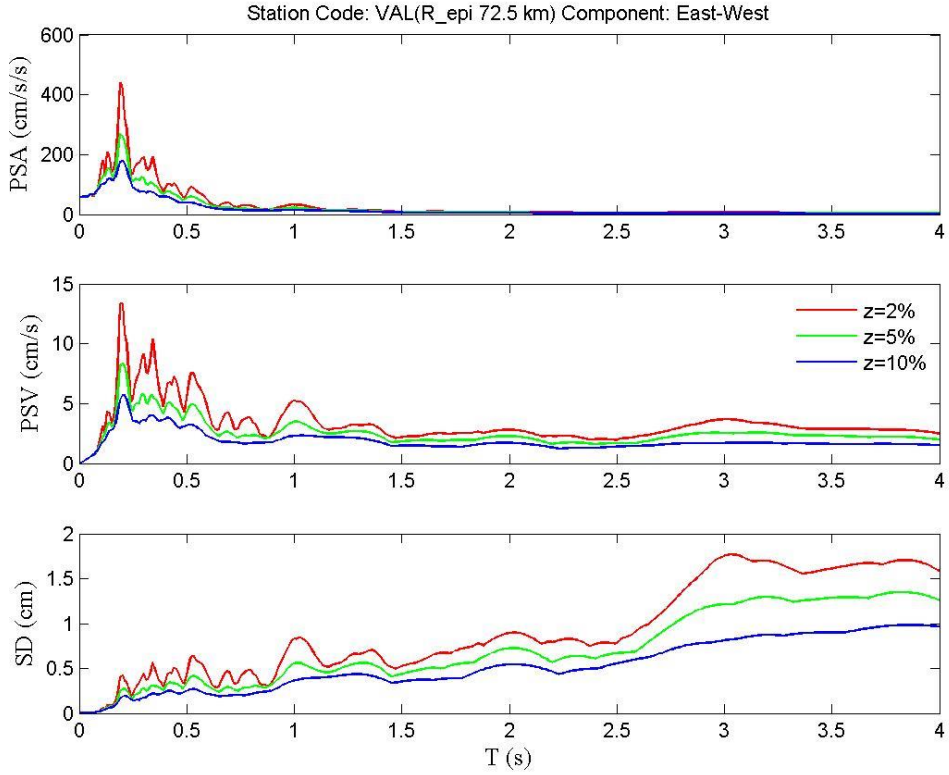
Station Code: VAL(R_epi 72.5 km) Component: East-West
PSA (cm/s/s)
PSV (cm/s)
SD (cm)
z=2%
z=5%
z=10%
T (s)

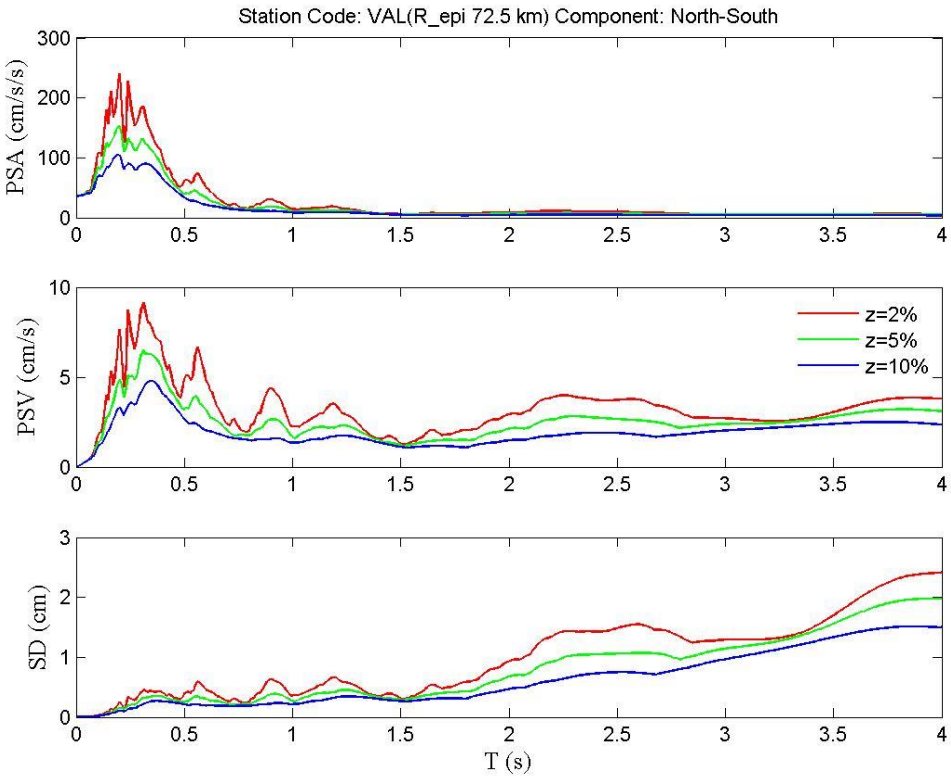
Station Code: VAL(R_epi 72.5 km) Component: North-South
PSA (cm/s/s)
PSV (cm/s)
SD (cm)
z=2%
z=5%
z=10%
T (s)

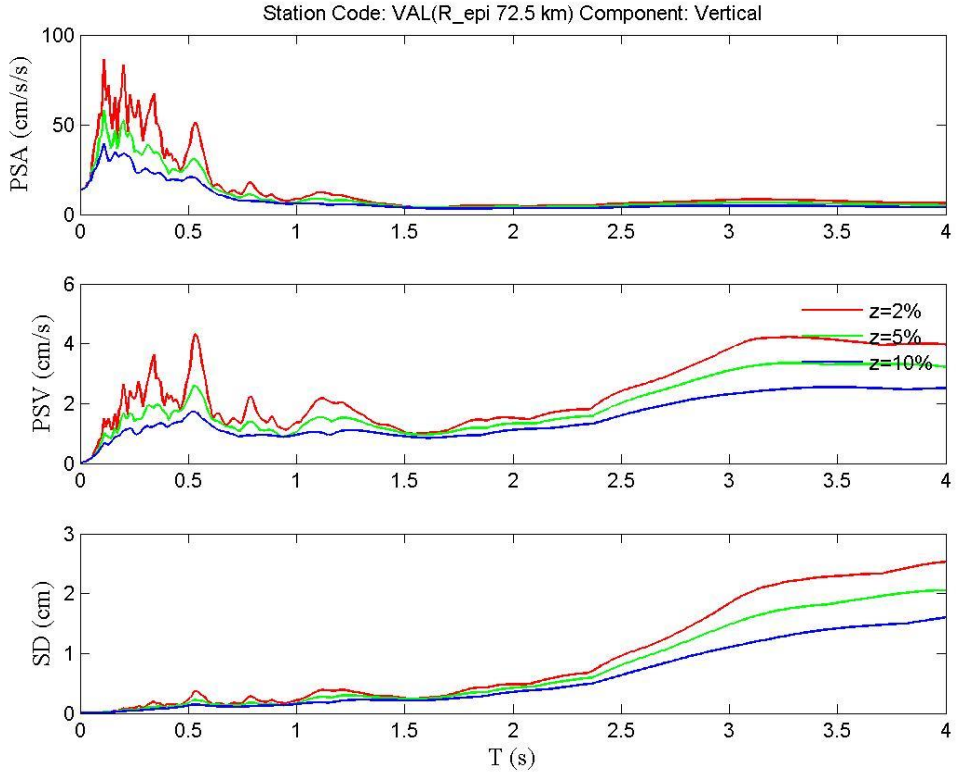
Station Code: VAL(R_epi 72.5 km) Component: Vertical
PSA (cm/s/s)
PSV (cm/s)
SD (cm)
z=2%
z=5%
z=10%
T (s)

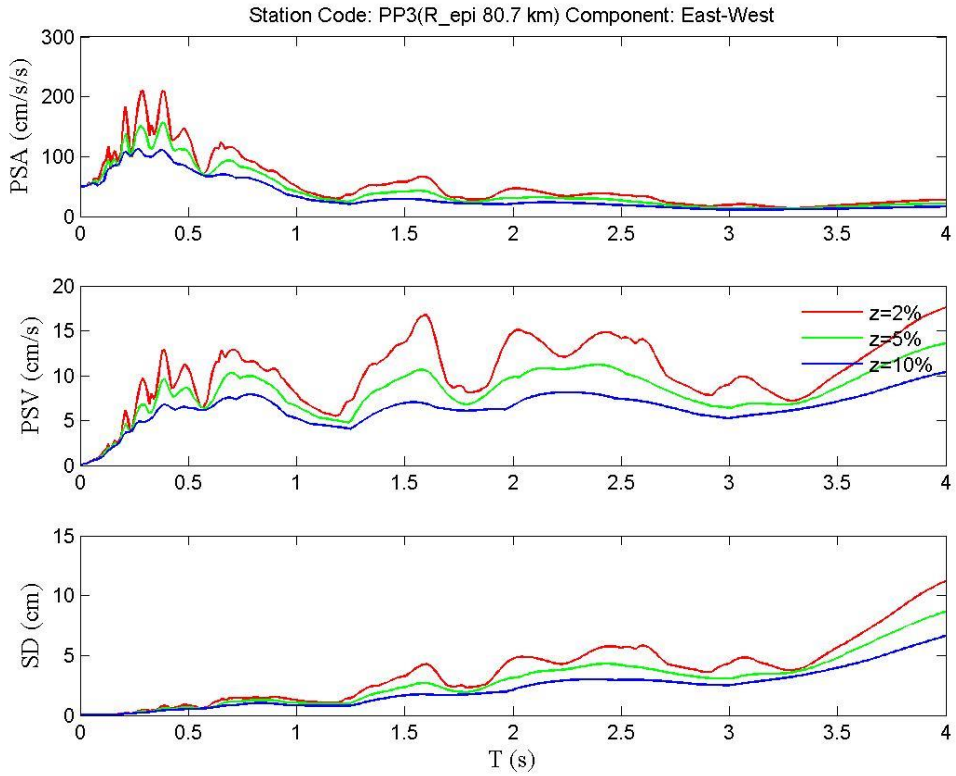
Station Code: PP3(R_epi 80.7 km) Component: East-West
PSA (cm/s/s)
PSV (cm/s)
SD (cm)
z=2%
z=5%
z=10%
T (s)

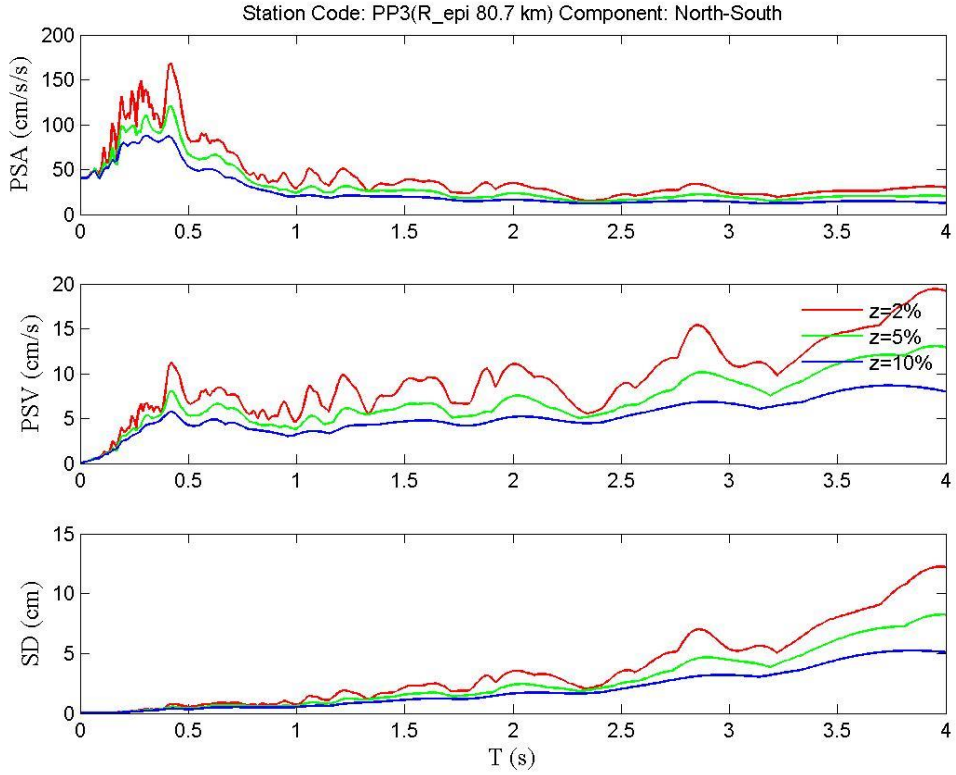
Station Code: PP3(R_epi 80.7 km) Component: North-South
PSA (cm/s/s)
PSV (cm/s)
SD (cm)
z=2%
z=5%
z=10%
T (s)

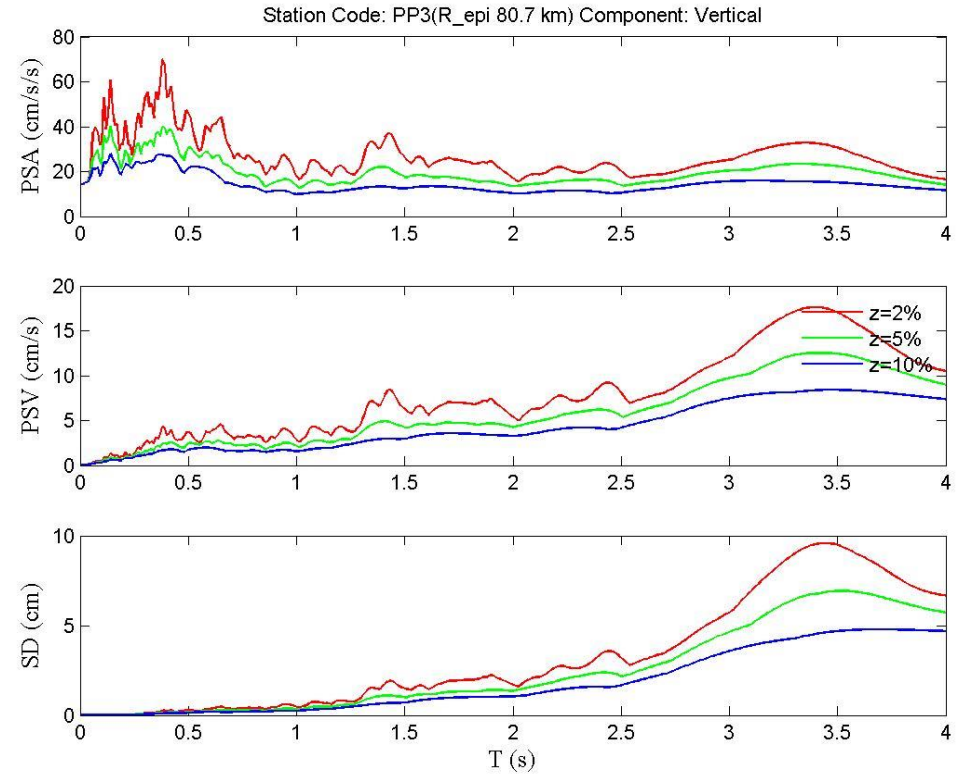
Station Code: PP3(R_epi 80.7 km) Component: Vertical
PSA (cm/s/s)
PSV (cm/s)
SD (cm)
z=2%
z=5%
z=10%
T (s)

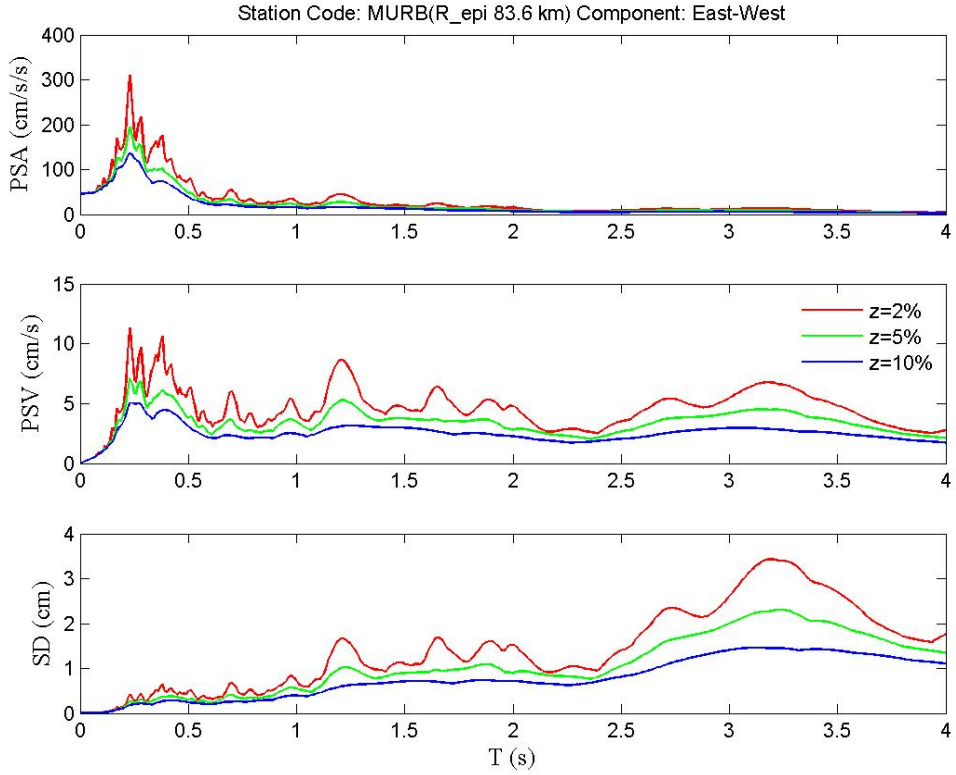
Station Code: MURB(R_epi 83.6 km) Component: East-West
PSA (cm/s/s)
PSV (cm/s)
SD (cm)
T (s)
z=2%
z=5%
z=10%

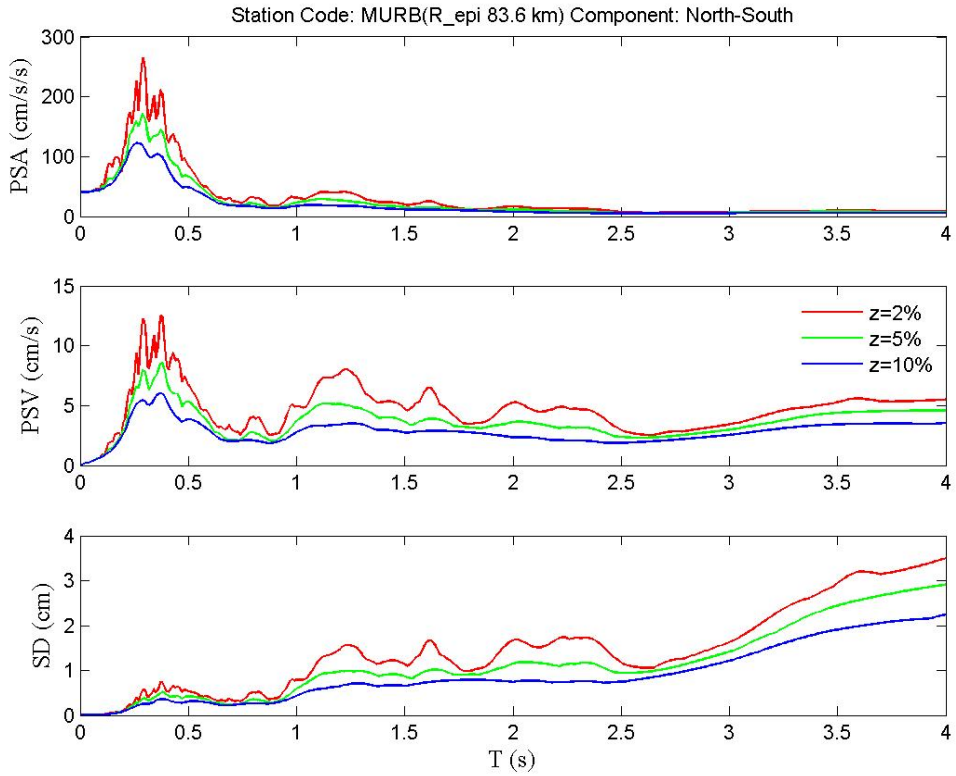
Station Code: MURB(R_epi 83.6 km) Component: North-South
PSA (cm/s/s)
PSV (cm/s)
SD (cm)
T (s)
z=2%
z=5%
z=10%

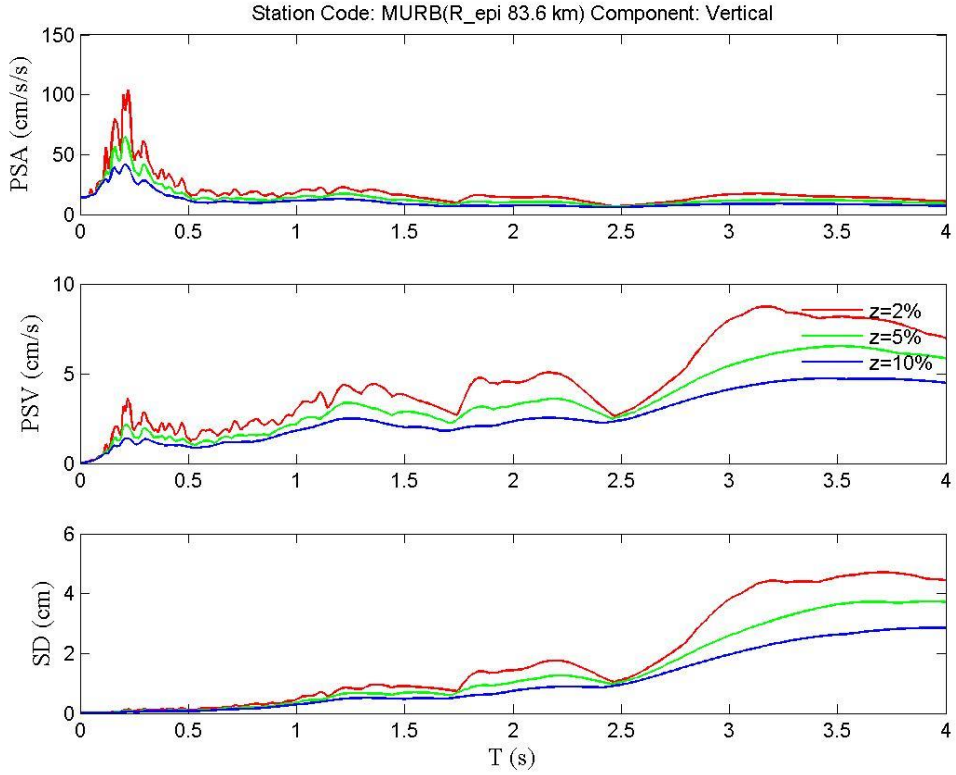
Station Code: MURB(R_epi 83.6 km) Component: Vertical
PSA (cm/s/s)
PSV (cm/s)
SD (cm)
z=2%
z=5%
z=10%
T (s)

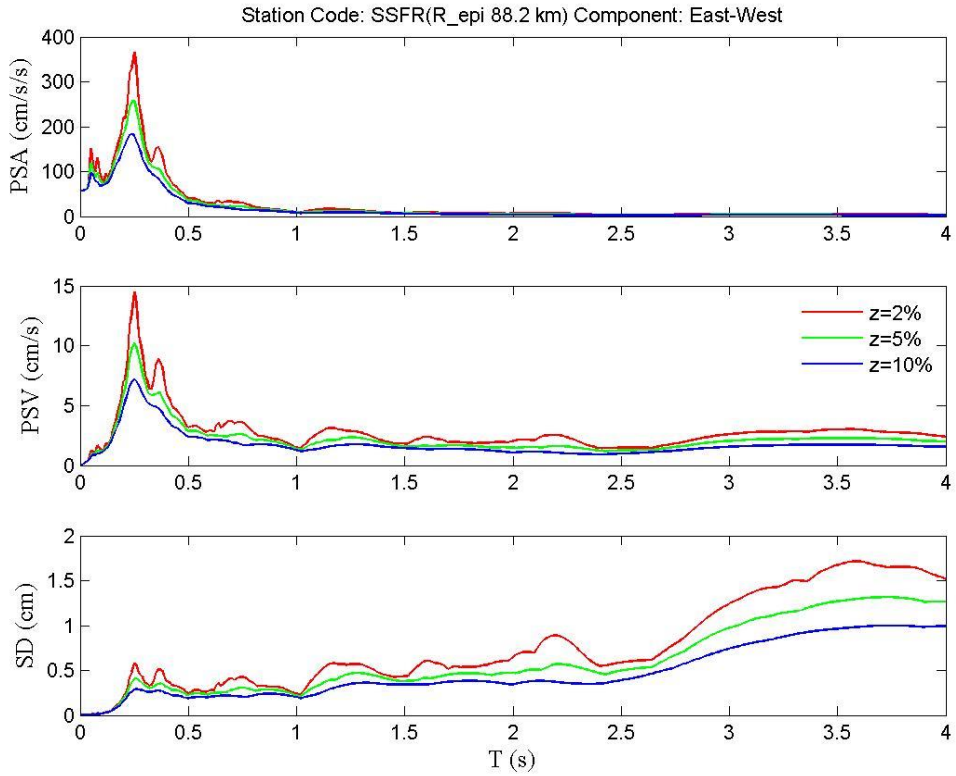
Station Code: SSFR(R_epi 88.2 km) Component: East-West
PSA (cm/s/s)
PSV (cm/s)
SD (cm)
z=2%
z=5%
z=10%
T (s)

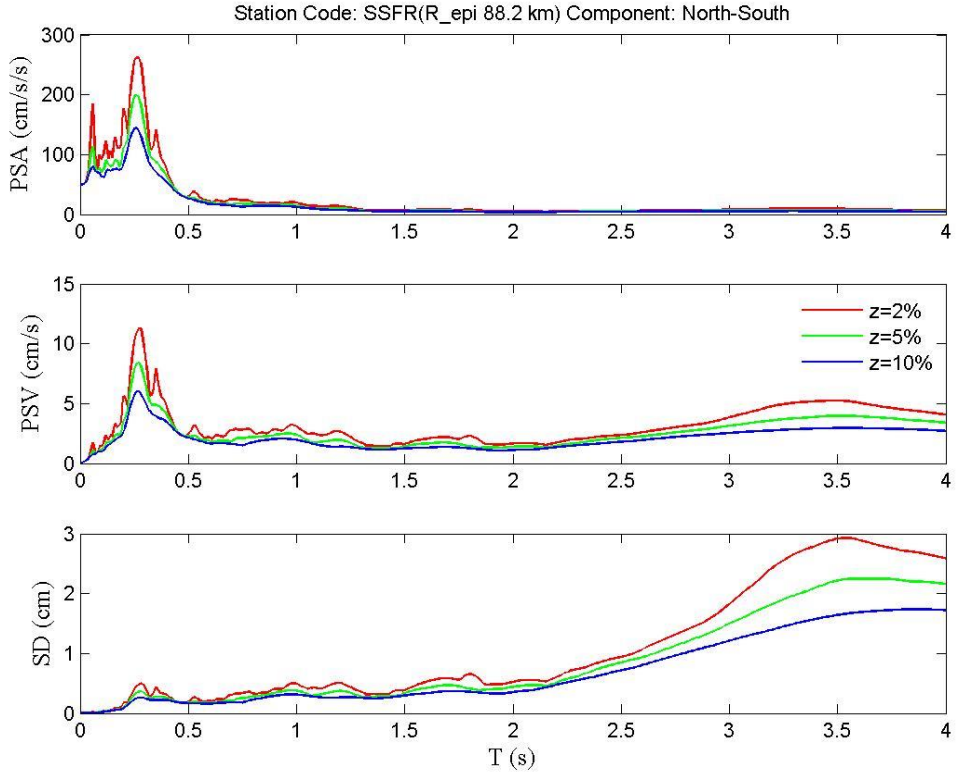
Station Code: SSFR(R_epi 88.2 km) Component: North-South
PSA (cm/s/s)
PSV (cm/s)
SD (cm)
z=2%
z=5%
z=10%
T (s)

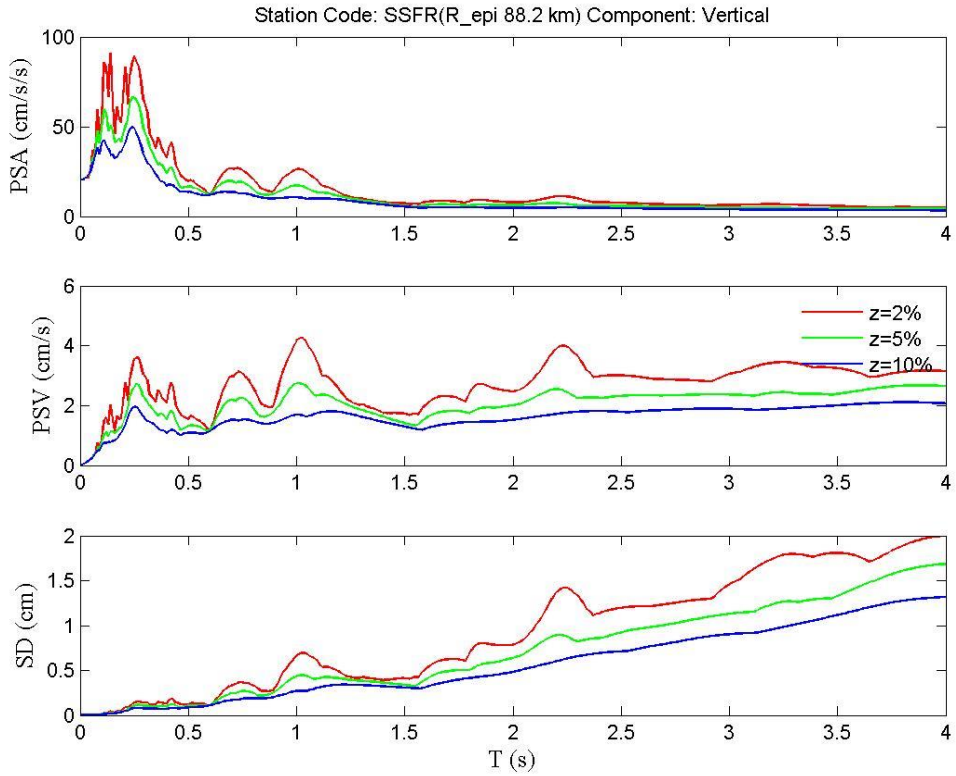
Station Code: SSFR(R_epi 88.2 km) Component: Vertical
PSA (cm/s/s)
PSV (cm/s)
SD (cm)
z=2%
z=5%
z=10%
T (s)

# 7. Comparison with the Italian seismic code

The pseudo-acceleration response spectra associated to the horizontal ground motions recorded by the four stations with lowest epicentral distance (AMT, NRC, RM33 and SPD) are compared with the elastic spectra provided by the Italian seismic code (NTC2008) at the corresponding sites for soil class provided in Appedix 1 and four different return periods ($T_R$): 50, 475, 975 and 2475 years. Note that comparison of individual earthquake recordings with probabilistic hazard is a delicate issue and no direct conclusions can be drawn (see Iervolino, 2013)

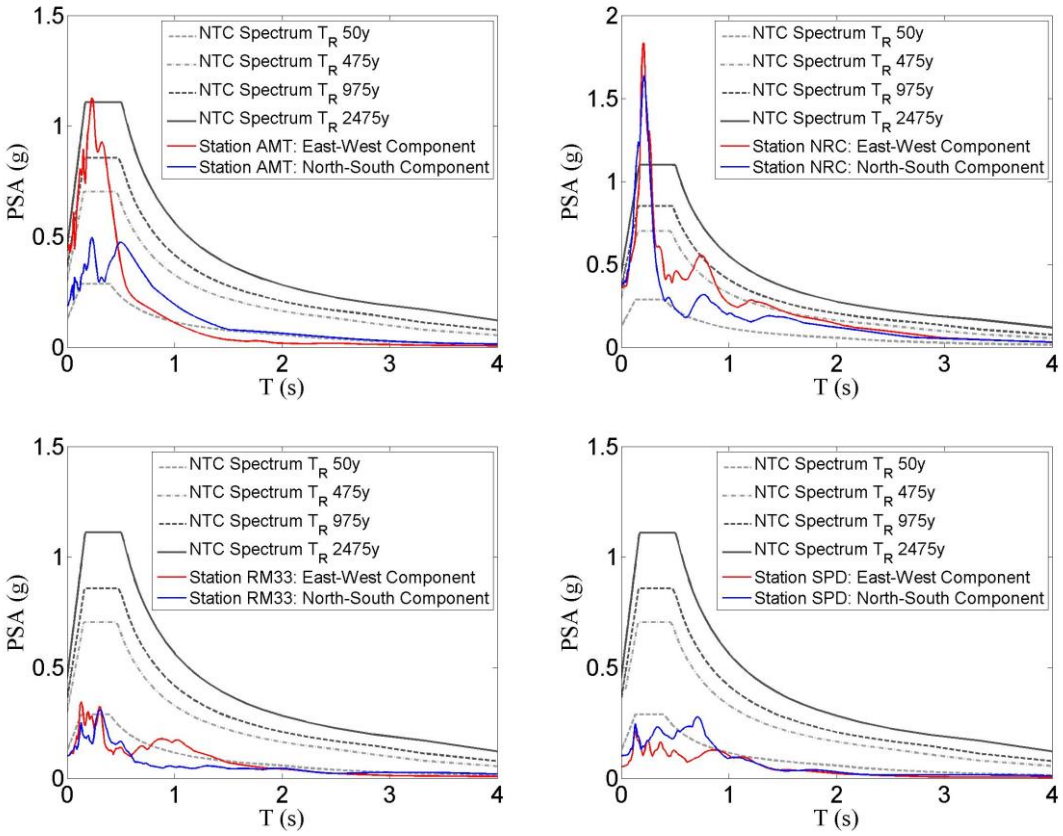


# References


Bindi, D., F. Pacor, L. Luzi, R. Puglia, M. Massa, G. Ameri, and R. Paolucci (2011). Ground motion prediction equations derived from the Italian strong motion database, Bull. Earthq. Eng. 9, 1899–1920.

Iervolino I. (2013) Probabilities and fallacies: why hazard maps cannot be validated by individual earthquakes. Earthquake Spectra, 29(3): 1125–1136.

Paolucci, R., F. Pacor, R. Puglia, G. Ameri, C. Cauzzi, and M. Massa (2011). Record processing in ITACA, the new Italian strong motion database, in Earthquake Data in Engineering Seismology, Geotech- nical, Geological and Earthquake Engineering Series, S. Akkar, P. Gulkan, and T. Van Eck (Editors), Vol. 14(8), 99–113.

# Appendix 1

Stations highlighted in gray are not used in the analysis

| net_code | station_code | ec8_code | st_latitude | st_longitude |
|---|---|---|---|---|
| BA | PZUN | B* | 40.6458 | 15.807 |
| FR | SMPL | A* | 42.094 | 9.285 |
| IT | 0CAN | | 43.4723 | 12.6308 |
| IT | AMT | B* | 42.63246 | 13.28618 |
| IT | ANB | B* | 43.59229 | 13.50741 |
| IT | ANT | A* | 42.41811 | 13.0786 |
| IT | AQF | B* | 42.38054 | 13.35474 |
| IT | AQK | B | 42.34497 | 13.40095 |
| IT | AQV | B | 42.37722 | 13.34389 |
| IT | ASP | C* | 42.848 | 13.6479 |
| IT | ATN | A* | 41.62032 | 13.80115 |
| IT | AVL | C* | 40.92283 | 14.78704 |
| IT | AVZ | C | 42.02746 | 13.42593 |
| IT | BCN | C* | 40.63435 | 15.38238 |
| IT | BGR | B* | 43.88951 | 11.99129 |
| IT | BNE | C* | 41.12756 | 14.78488 |
| IT | BRS | A* | 42.32427 | 13.59007 |
| IT | BSS | B* | 42.19173 | 13.84527 |
| IT | BTT2 | D | 41.99833 | 13.54306 |
| IT | BVG | C | 42.93237 | 12.61107 |
| IT | BZZ | B | 42.33703 | 13.46858 |
| IT | CCT | C* | 43.3683 | 12.2346 |
| IT | CER | B* | 41.2595 | 15.9102 |
| IT | CLF | D | 43.03671 | 12.92043 |
| IT | CLN | B* | 42.08522 | 13.52072 |
| IT | CMB | B* | 41.5628 | 14.6523 |
| IT | CME | A* | 43.9543 | 10.3012 |
| IT | CPS | B | 42.27162 | 13.7583 |
| IT | CRP | C* | 44.7823 | 10.8703 |
| IT | CSA | C* | 43.00802 | 12.5906 |
| IT | CSD | B | 42.75405 | 12.00354 |
| IT | CSN | B | 44.13701 | 12.24141 |
| IT | CSO1 | B* | 42.10093 | 13.08804 |
| IT | CSS | B | 41.48579 | 13.82309 |
| IT | CTD | B* | 42.38837 | 12.9477 |
| IT | CTS | C* | 43.49199 | 12.2234 |
| IT | CVM | A* | 42.99409 | 11.28231 |
| IT | DUR | B* | 41.6611 | 14.4565 |
| IT | FAZ | C | 44.29802 | 11.89075 |
| IT | FBR | C* | 43.3436 | 12.9119 |
| IT | FIE | B* | 43.80725 | 11.29439 |
| IT | FMG | A* | 42.26803 | 13.11722 |
| IT | FOC | C* | 43.0263 | 12.89651 |
| IT | FOS | B* | 43.01459 | 12.83513 |
| IT | FRT | | 41.6926 | 13.255 |
| IT | FSS | C* | 43.69048 | 12.81007 |
| IT | GBB | B* | 43.35697 | 12.59725 |
| IT | GBP | C | 43.31381 | 12.58949 |
| IT | GNU | A* | 42.80382 | 12.57015 |
| IT | GRN | A* | 41.81346 | 13.31699 |

| | | | | |
|---|---|---|---|---|
| IT | GSA | B | 42.42069 | 13.51936 |
| IT | LSS | A | 42.55824 | 12.96889 |
| IT | MCR | C* | 43.79989 | 12.44751 |
| IT | MCS | B* | 43.99437 | 12.10744 |
| IT | MLF | B | 40.9944 | 15.6527 |
| IT | MMP1 | B* | 42.24923 | 12.74832 |
| IT | MNF | A* | 43.05968 | 13.18447 |
| IT | MNG | A* | 41.70354 | 15.95803 |
| IT | MNT | A* | 43.1397 | 11.18279 |
| IT | MTL | B | 43.24944 | 13.00834 |
| IT | NAP | C* | 40.79926 | 14.17961 |
| IT | NCR | E | 43.11158 | 12.78467 |
| IT | NRC | B | 42.79254 | 13.09648 |
| IT | NRN | A* | 42.51556 | 12.51944 |
| IT | ORP | B | 41.27923 | 15.26506 |
| IT | PAN | B* | 43.00581 | 12.14362 |
| IT | PGG | B* | 42.32287 | 13.53945 |
| IT | PNC | B* | 42.84745 | 11.6936 |
| IT | PNN | C | 43.81816 | 12.26285 |
| IT | PSC | A | 41.81204 | 13.7892 |
| IT | PTI | B* | 43.06657 | 13.65708 |
| IT | PTL | B* | 43.42733 | 12.4486 |
| IT | PVF | B* | 44.3331 | 10.82523 |
| IT | PZI1 | B* | 42.4356 | 13.3262 |
| IT | RDG | A* | 41.9264 | 15.8792 |
| IT | RQT | B* | 42.81309 | 13.31103 |
| IT | RTI | D | 42.43028 | 12.8291 |
| IT | SAG | A* | 40.93156 | 15.18763 |
| IT | SBC | A | 41.91316 | 13.10552 |
| IT | SCF | B* | 42.26512 | 13.99849 |
| IT | SDM | A* | 42.28971 | 13.55765 |
| IT | SGMA | B* | 41.6845 | 14.9644 |
| IT | SGPA | B | 41.6876 | 14.9629 |
| IT | SGPA | B | 41.6876 | 14.9629 |
| IT | SGSC | B* | 41.6892 | 14.9581 |
| IT | SGSC | B* | 41.6892 | 14.9581 |
| IT | SIG | C* | 43.3308 | 12.7408 |
| IT | SNG | C | 43.68558 | 13.22616 |
| IT | SNI | B* | 42.632 | 12.5536 |
| IT | SNM | B* | 43.93433 | 12.44929 |
| IT | SNS1 | C* | 43.5735 | 12.1312 |
| IT | SOR | | 41.7203 | 13.6136 |
| IT | SPD | B* | 42.51514 | 13.37104 |
| IT | SPM | A* | 42.72324 | 12.75127 |
| IT | SPO1 | | 42.7344 | 12.7363 |
| IT | SSC | E | 42.87473 | 11.87679 |
| IT | SSG | B* | 43.56986 | 12.14632 |
| IT | SSO | | 43.5715 | 12.154 |
| IT | STF | B* | 43.90811 | 11.79446 |
| IT | SUL | A* | 42.089 | 13.934 |
| IT | SULA | C* | 42.0734 | 13.9166 |
| IT | SULC | C* | 42.068 | 13.909 |
| IT | SULP | B* | 42.085 | 13.9274 |
| IT | TLN | B* | 43.2159 | 13.25838 |
| IT | TOD | A* | 42.73817 | 12.38728 |
| IT | TRE | C* | 42.8765 | 12.7358 |
| IT | TRL | A* | 42.46131 | 12.93231 |
| IT | TRN1 | D* | 42.5582 | 12.6461 |

| | | | | |
|---|---|---|---|---|
| IT | TRV | B* | 41.78294 | 14.55071 |
| IT | TSC | A* | 42.42261 | 11.8696 |
| IT | TVL | B* | 41.89302 | 12.77322 |
| IT | UMB | B* | 43.25444 | 12.2556 |
| IT | VAL | B* | 43.1593 | 12.6017 |
| IT | VLL | B* | 41.67047 | 12.77267 |
| IT | VLN | C* | 43.14273 | 11.89472 |
| IT | VNF1 | C* | 41.4805 | 14.0501 |
| IT | VSE | B* | 42.12218 | 14.70719 |
| IV | ACER | B* | 40.7867 | 15.9427 |
| IV | APEC | B* | 43.55846 | 12.41991 |
| IV | APRC | | 41.75738 | 15.54308 |
| IV | ASOL | A* | 45.8003 | 11.9023 |
| IV | ATCC | B* | 43.18514 | 12.63994 |
| IV | ATFO | B* | 43.3666 | 12.5715 |
| IV | ATLO | B* | 43.3152 | 12.4073 |
| IV | ATPC | B* | 43.4807 | 12.457 |
| IV | ATTE | A* | 43.1979 | 12.3536 |
| IV | ATVO | B* | 43.38211 | 12.40663 |
| IV | BDI | B* | 44.0624 | 10.597 |
| IV | BIOG | B* | 41.1999 | 15.13263 |
| IV | BOB | B* | 44.7679 | 9.4478 |
| IV | BRIS | B* | 44.2245 | 11.7666 |
| IV | BSSO | A* | 41.5461 | 14.5938 |
| IV | CADA | B* | 43.1942 | 13.7614 |
| IV | CAFE | A* | 41.028 | 15.2366 |
| IV | CDCA | C* | 43.4584 | 12.2336 |
| IV | CERA | A* | 41.5978 | 14.0183 |
| IV | CIMA | B* | 43.3053 | 13.67009 |
| IV | CMPO | C* | 44.5808 | 11.8056 |
| IV | COR1 | B* | 43.6318 | 13.0003 |
| IV | CPGN | B* | 43.8011 | 12.3205 |
| IV | CRMI | B* | 43.7956 | 10.9795 |
| IV | CRND | C* | 45.8361 | 12.0131 |
| IV | CTL8 | C* | 45.2755 | 9.7621 |
| IV | FAEN | C* | 44.2895 | 11.877 |
| IV | FERS | C | 44.9035 | 11.5406 |
| IV | FIU1 | B* | 43.18856 | 12.9316 |
| IV | FOSV | B* | 43.29483 | 12.76117 |
| IV | FRE8 | A* | 46.015 | 12.3552 |
| IV | GAG1 | B* | 43.2381 | 13.0674 |
| IV | GATE | B* | 41.51315 | 14.9102 |
| IV | GUMA | B* | 43.0627 | 13.3352 |
| IV | IMOL | C* | 44.35955 | 11.74248 |
| IV | LEOD | C* | 45.4582 | 10.1234 |
| IV | MCEL | A* | 40.3249 | 15.8019 |
| IV | MDAR | B* | 43.1927 | 13.1427 |
| IV | MELA | A* | 41.7059 | 15.127 |
| IV | MGAB | A* | 42.91263 | 12.11214 |
| IV | MGR | B* | 40.1376 | 15.5535 |
| IV | MNTV | C* | 45.1495 | 10.7897 |
| IV | MOCO | B* | 41.37 | 15.158 |
| IV | MODE | C* | 44.6297 | 10.9492 |
| IV | MRB1 | B* | 41.1227 | 14.96815 |
| IV | MRLC | B* | 40.7564 | 15.48892 |
| IV | MSAG | A* | 41.712 | 15.9096 |
| IV | MTRZ | B* | 44.3128 | 11.4248 |
| IV | MURB | B* | 43.263 | 12.5246 |

| | | | | |
|---|---|---|---|---|
| IV | NDIM | C* | 44.8873 | 10.8987 |
| IV | NEVI | B* | 44.5834 | 10.3163 |
| IV | NRCA | B* | 42.83355 | 13.11427 |
| IV | OPPE | C* | 45.3082 | 11.1724 |
| IV | ORZI | C* | 45.4056 | 9.9307 |
| IV | OSSC | B* | 43.5236 | 11.2458 |
| IV | PAOL | A* | 41.03121 | 14.56749 |
| IV | PCRO | B* | 43.6077 | 13.5323 |
| IV | PIEI | A* | 43.53567 | 12.535 |
| IV | PIGN | A* | 41.2 | 14.17989 |
| IV | POFI | A* | 41.71743 | 13.71202 |
| IV | PP3 | C* | 43.3778 | 13.6095 |
| IV | PTRJ | A* | 41.3641 | 14.529 |
| IV | RM33 | B* | 42.509 | 13.2145 |
| IV | RNI2 | A* | 41.70328 | 14.1524 |
| IV | ROM9 | B* | 41.82842 | 12.51553 |
| IV | ROVR | A* | 45.6468 | 11.0721 |
| IV | SACS | B* | 42.84906 | 11.90967 |
| IV | SALO | A* | 45.6183 | 10.5243 |
| IV | SANR | C* | 45.64 | 11.6099 |
| IV | SBPO | C* | 45.0511 | 10.9199 |
| IV | SERM | C* | 45.01 | 11.2958 |
| IV | SGG | A* | 41.38667 | 14.37917 |
| IV | SGTA | B* | 41.135 | 15.365 |
| IV | SIRI | B* | 40.1821 | 15.8675 |
| IV | SNAL | A* | 40.9254 | 15.2091 |
| IV | SNTG | A* | 43.255 | 12.9406 |
| IV | SSFR | A* | 43.4363 | 12.7822 |
| IV | SSM1 | B* | 43.22878 | 13.17696 |
| IV | STAL | B* | 46.2601 | 12.7104 |
| IV | TERO | B* | 42.62279 | 13.60393 |
| IV | TRE1 | B* | 43.3112 | 13.31285 |
| IV | TREG | C* | 45.523 | 11.1606 |
| IV | TRIV | B* | 41.7666 | 14.5502 |
| IV | VAGA | A* | 41.4154 | 14.2342 |
| IV | VENL | D* | 45.4167 | 12.3765 |
| IV | VITU | A* | 41.18326 | 14.63015 |
| IV | VOBA | C* | 45.6429 | 10.504 |
| IV | VULT | B* | 40.9549 | 15.6163 |
| IV | ZCCA | B* | 44.35085 | 10.9765 |
| IV | ZEN8 | A* | 45.6378 | 10.7319 |
| IV | ZOVE | B* | 45.4536 | 11.4876 |
| MN | AQU | B* | 42.35388 | 13.40193 |
| MN | BLY | | 44.7488 | 17.1839 |
| MN | CUC | A* | 39.9938 | 15.8155 |
| MN | VLC | A* | 44.1594 | 10.3864 |
| OX | ACOM | | 46.548 | 13.5137 |
| OX | AGOR | | 46.2329 | 12.0472 |
| OX | CGRP | | 45.8806 | 11.8047 |
| OX | CIMO | | 46.3116 | 12.4448 |
| OX | CLUD | | 46.4569 | 12.8814 |
| OX | MPRI | | 46.2408 | 12.9877 |
| OX | SABO | B* | 45.9875 | 13.6336 |
| OX | VARN | | 45.9922 | 12.1051 |
| OX | ZOU2 | | 46.5584 | 12.9729 |
| ST | DOSS | | 45.8808 | 11.1884 |
| ST | VARA | A* | 45.826 | 10.8965 |